

UNIVERSITÀ DEGLI STUDI DI NAPOLI "FEDERICO II"

POLO DELLE SCIENZE E DELLE TECNOLOGIE

DIPARTIMENTO DI SCIENZE DELLA TERRA, DELL'AMBIENTE E DELLE RISORSE



XXVII Ciclo di Dottorato

Dinamica Interna dei Sistemi Vulcanici e Rischi Idrogeologico-Ambientali

PhD Thesis

The Somma-Vesuvius medieval eruptive activity: A study of its impact on the heavily inhabited south-western sector of the volcano.

Coordinator: Professor Benedetto De Vivo

Tutor: Professor Giuseppe Rolandi

Co-Tutor: Dr. Claudia Principe

Phd Student: Dr. Annarita Paolillo

A.A. 2015/2016



ACKNOWLEDGEMENTS

These PhD years were intense and rich of unexpected obstacles, but also moments of satisfaction and victory.

Many were the people I met along the way... each with its own contribution was essential to the achievement of this important goal.

Therefore, I would like to say “Thank you!” to all those who have helped and supported me, hoping not to forget anyone...

My PhD Advisors, Professor Giuseppe Rolandi and Dr. Claudia Principe fostered my professional growth, lending me their knowledge, their patience and leading me to challenging field work.

The PhD Coordinator, Professor Benedetto De Vivo, never missed an opportunity to give me life lesson and chances to grow professionally. He’s a grumpy old man of course, but his reproaches were always constructive and indeed helped!

I am deeply grateful to Dr. Claudia Cannatelli for her support, advices and availability.

Professor Christopher Kilburn of the University College in London and Professor Robert Bodnar and Professor Robert Tracy of Virginia Tech in Blacksburg, welcomed me in their labs, offered their expertise and advices me on my work. Their generosity is greatly appreciated. They also allowed me access to the analytical facilities available in their institutions. Dr. Esteban Gazel of Virginia Tech also welcomed me in his research group, giving me the opportunity to interact with his students.

Dr. Monica Capodanno, Dr. Sonia La Felice and Dr. Luca Fedele trained me in the usage of analytical equipment, on laboratory methodologies, and sedimentological and chemical analysis.

Dr. Marina Bisson, always available to explaining me how to deal with G.I.S.

A huge **THANKS** to all of YOU !!!

TABLE OF CONTENTS

Chapter 1: Introduction	1
Chapter 2: Regional Geology	4
Chapter 3: The Somma-Vesuvius volcano	7
3.1. Geological setting	7
3.2. Eruptive history	8
Chapter 4: Synthematic map of the south-western sector of the Vesuvius volcano, Italy	11
Abstract	11
4.1. Introduction	12
4.2. Geological outlines	12
4.3. Mapping methodology	13
4.3.1. Unconformity Bounded Stratigraphic Units (UBSU)	14
4.3.2. Archaeological and Historical criteria	15
4.4. Stratigraphy/Legend	19
Unconformity bounded units	19
4.4.1. Present-Vesuvius Synthem	19
4.4.2. Medieval-Vesuvius Synthem	22
4.4.3. Ancient-Vesuvius Synthem	23
4.4.4. Proto-Vesuvius Synthem	24
4.4.5. Prehistoric-Vesuvius Synthem	24
4.5. Petrographic features	25
4.6. Morphological and volcano-tectonic elements	26
4.7. Discussion and Conclusions	28
Software	29
Supplementary Material	29

Chapter 5: Study on the medieval eruptive activity of the Somma-Vesuvius volcano based on the analysis of tephra fallout deposits	31
Abstract	31
5.1. Introduction	31
5.2. Medieval History of Vesuvius: From VI to XVII century	32
5.2.1. VI century	33
5.2.2. VII century	33
5.2.3. VIII century	34
5.2.4. X-XI century	34
5.2.5. XII century	34
5.3. Samples studied and Analytical Methods	35
5.3.1. Tephra fallout deposits	35
5.3.2. Vesuvian Tephra fallout samples	36
5.3.3. Electron Microprobe Analysis (EMPA)	37
5.4. Discussion and conclusions	38
Chapter 6: Volcaniclastic Debris-Flows in densely inhabited areas: the case of the Somma-Vesuvius municipalities (Southern Italy)	40
Abstract	40
6.1. Introduction	41
6.2. Recent Historical activity of Somma-Vesuvius	43
6.3. Materials and Methods	45
6.4. Spatial and temporal analysis of historical events during the 20 th century	47
6.5. Morphological considerations	50
6.6. Volcaniclastic historical flows recorded in <i>Torre del Greco</i> municipality	57
6.7. Discussion and Conclusions	58
Chapter 7: Summary & Conclusions	59
References	i-viii



CHAPTER 1

1. Introduction

Our planet undergoes continuous transformations due to the influence of natural phenomena and of the inconsiderate man-made alterations of the territory.

The concept of total risk was born due to the interactions among man and the environment. It is based on the combination of natural and socio-economic factors, and it is quantified using the following relation (Allen et al., 1980):

$$\mathbf{RISK = f(hazard, vulnerability, and value of exposed)}$$

To each hypothetical natural event will be attributed a value of risk, and, consequently, an expected damage, defined as “*the probability of economic loss for the occurrence of a natural event*”. The fundamental assumption is: “*future events will occur in an area with the same mode (style and size) and with the same average frequency with which they occurred in the past*”. Hence the paramount importance of investigating and reconstructing in detail the behaviour of the natural phenomenon that occurred in a given area.

The Italian territory is affected by a multiplicity of natural phenomena, each one with an associated degree of risk. We can define two types of risk: *i*) tectonic and volcanic; *ii*) hydrogeological (which can be further subdivided in hydraulic and geomorphological).

In volcanic areas, in addition to the risk of eruptive events, it is very common the occurrence of volcanic-related mud flows (Pareschi et al., 2000b), which can be sin-eruptive and inter-eruptive (Capra et al., 2004), the latter occurring when intense and/or persistent rains remobilize loose pyroclastic deposits (Zanchetta et al., 2004b).

Under the implicit assumption that “*past activity is the key for understanding the future*”, a detailed reconstruction of the eruptive history is of the utmost importance in order to produce a realistic model of an active volcano. Furthermore, the results stemming from an historical analysis of the eruptive history must be integrated and connected with data regarding the current geodynamic situation of the area.

The whole dataset consents, then, to generate an updated cartography by means of G.I.S, which allows to render the hazard readily visible through thematic maps. A zonation map, which can be used to construct a possible hazard map, can be constructed combining the morphological characteristics of the area with the concavity and the form factor of the basin, the distribution of gradients derived using an

accurate Digital Elevation Model (DEM), the study of its hydrology, and the thickness of the pyroclastic deposits (from fall, surge and flow; [Bisson et al., 2010](#)).

The huge demographic and urban growth of the towns located on the slopes of Vesuvius, and the high risk associated with the probability of the event, and the expected eruptive scenery, are the main reason why this volcano has become one of the most studied and monitored in the world.

Vesuvius is located in the *graben* structure of the Campanian Plain, which formed during the opening of the Tyrrhenian Basin in the Plio-Pleistocene, and that was followed by volcanic activity in its late stage. Somma-Vesuvius is a composite stratovolcano, made up of the ancient Somma caldera and of a recent central cone, Vesuvius. Its history is filled with events displaying different types of eruptive styles, and, of course, the volcano is widely known for its paroxysmal Plinian eruptions, of which the best known is the *Pompei* Eruption of AD 79, described by the letters of Pliny the Younger to Tacitus.

A large body of literature was produced in the last few decades, in order to understand the deep structure of the volcano, its internal mechanisms, and to distinguish the different cycles of its eruptive history. Petrologic and isotopic studies identify one of the Vesuvius magma chambers at a depth range of 3-6 km ([Civetta and Santacroce, 1992](#); [Barberi et al., 1981](#)). Fluid inclusions based studies suggest the presence of pockets of magma at a depth between 2 and 12 km ([Belkin et al., 1998, 1993, 1985](#)). Structural-tectonic studies indicate that Vesuvius developed in a graben formed at the intersection of two fault systems with the direction, respectively, NE-SW and NW-SE ([Vilardo et al., 1996](#); [Finetti and Morelli, 1974](#)). [Nunziata et al. \(2006\)](#), using one- and two-dimensional VP models obtained by TomoVes experiment, identified a magma chamber at a depth of about 8-10 km.

The pyroclastic deposits, emplaced as the result of the largest and oldest explosive eruptions, can be identified in the distal areas of the volcano, where they are generally preserved in colluvial deposits, with a few interbedded in the alluvial fan sequences ([Zanchetta et al., 2004a](#); [Di Vito et al., 1998](#)).

At least four of the major Plinian events occurred over the past 18,000 years, and were separated by periods of quiescence of variable length or by minor activities (“inter-Plinian” stage). A detailed knowledge of the behaviour of the volcano in these stages is of primary importance for the prediction of its possible future eruptions ([Andronico and Cioni, 2002](#)).

The collection of historical documents, such as chronicles, iconographies, paints etc., combined with the reconstruction of the historical toponomastic, and the usage of maps to connect all the available data, proved to be an invaluable multidisciplinary tool to determine the evolution of the town of *Torre del Greco* and to develop a reliable assessment of the volcanic hazard in the study area.

The morphology of the municipality of *Torre del Greco* is the result of a combination of constructive and destructive events, and, while it is still possible to identify the location and the characteristics of many outcrops, the intense urbanization has obliterated several important ones, making the reconstruction much more challenging.

The territory of *Torre del Greco* is also affected by frequent events such as landslides (i.e. debris-flows), floods and erosion, which contribute to increase the hazard conditions. These events are associated to the presence of loose volcanic deposits and are triggered by heavy rainfalls that tend to remobilize them. These are historically recurring events, as shown by the attempt of the *Borbone* to control water flow in the Vesuvian area by the way of building the *Regi Lagni*. The highly chaotic urbanization of the Vesuvian area turned many riverbeds, originally natural outflow paths for rainwater, in streets (riverbeds-roads), totally altering the function of the original drainage network. Our morphological analysis highlights the present hydrogeological condition and defines the likely paths of lava flows and, above all, of mud flows, both of great importance for the definition of the hazard.

The focus of this PhD thesis is the assessment of the hazards related to the presence of pyroclastic deposits in the densely populated Vesuvian area, evaluating, in particular, the hydrogeological and the volcanic hazard.

This work improved the understanding of the Vesuvius eruptive behaviour and contributed significant data for the generation of more reliable models for the evaluation of the volcanic hazard for the population that lives on the flanks and in the surroundings of this volcano.

Particular attention was paid to the largest of the Vesuvian towns, *Torre del Greco*, because its territory is the most affected by these two typologies of hazard, due to its natural morphology originated by the historical Vesuvian eruptive activity and to the anthropological alterations of its area.

The PhD project is divided in three parts: (i) a detailed mapping of the south-western sector of Vesuvius, integrating stratigraphic and petrologic data with archaeological and historical information; (ii) a study of the medieval eruptive activity of the Somma-Vesuvius volcano, an important period of the Vesuvius activity, which has been, definitely, under-researched, in which we focused on the tephra fallout deposits, integrating newly collected data with those already available in literature; (iii) the assessment of the hazard connected to the Volcaniclastic Flows.

For the volcanological map of Vesuvius and the assessment of the connected volcanic hazard, we carried out a detailed and accurate study of the eruptive history of Vesuvius, followed by field surveys. For each eruption, we created a classification database according to the following criteria: the eruptive period, the eruptive typology, the VEI, the eruptive deposits typology, the chemical composition. We located all the relevant faults, localized the vents, rebuilt paths of lava flows and determined the distribution of the tephra. All maps were realized using ArcGis™ software.

For studying the medieval eruptive activity, samples of tephra collected during the field surveys were analysed through stratigraphic analysis (grain analysis) and petrologic analysis (Scanning Electron Microprobe, Electron Microprobe Analysis and Laser Ablation).

For the hazard connected to the Volcaniclastic Flow, we located source areas, expansion areas, collected historical data on rainfall and determined the evolution of the morphological and urban settings.

CHAPTER 2

2. Regional Geology

The structure of a volcano is the result of the interaction of three main factors: *i*) regional tectonic which controls the emplacement of the volcano, possibly the deep magma supply rate (Ellis and King, 1991), and the distribution of eruptive fractures; *ii*) the stresses induced by the dynamics of a shallow magma chamber (inflation phenomena; caldera collapses; Martí et al., 1994); *iii*) the loading of the volcanic edifice (flank collapses; Chevallier, 1986). The regional stress field configuration is dependent on the large-scale tectonic regime (normal, strike-slip, reverse; Guiraud et al., 1989).

The Mediterranean area is one of the most complex geodynamic regions on Earth, and major processes such as spreading of the oceans, subduction, orogeny, and volcanism act concurrently to shape it and determine its evolution.

The present geological configuration of the central-western Mediterranean area is the result of the collision between Eurasian and African tectonic plates, started in Cretaceous times and still going on at present (Doglioni et al., 1998; Figure 2.1).

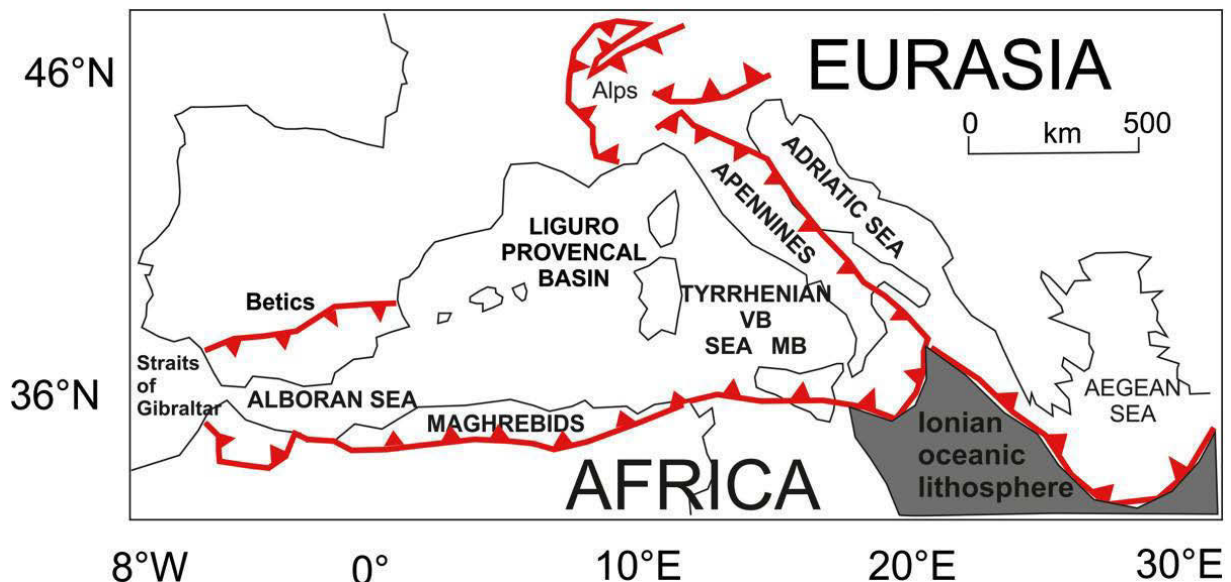


Fig. 2.1: Outline schematically showing the main thrust fronts (barbed line) that bound Neogene fold and thrust belts of the Mediterranean region. The general context of convergence in the region is expressed by the slow convergence of the African and Eurasian plates, schematically identified.

The two sub-basins of the Tyrrhenian Sea (in light shading; VB, *Vavilov* basin; and MB, *Marsili* basin), bounded by the Apennine/Maghrebid chain, are small ocean-floored back arc basins generated by the subduction and rollback of the Ionian slab, a portion of the remnant oceanic lithosphere (Marani and Trua, 2002).

In more than 60 million years, this process produced the deformation of the lithosphere and the formation of two main orogenic phases, the Alpine and the Apennine orogeny. In the last 10 million years, the opening of the Tyrrhenian basin, associated with an anticlockwise rotational motion of the Italian peninsula, was the prevalent geodynamic activity.

Italian volcanism developed within this geodynamic context, and can be divided into three main geographical regions: *i*) the Roman province extending from *Monte Amiata* to *Colli Albani*; *ii*) the Campanian province, which includes the *Roccamonfina*, Phlegraean Fields and Vesuvius volcanic complexes and lies along a crude east-west alignment from *Vulture* to *Ponza*; *iii*) the Aeolian Islands and the *Etna* volcanic complexes, together with scattered offshore volcanoes and the *Pantelleria complex*, located south-west of Sicily.

The Tyrrhenian basin is characterized by a tensile tectonic and subsea volcanism (*Marsili* and *Vavilov* volcanoes). This led the reduced crustal thickness allowing the underlying mantle to rise to shallower depths. The combination of mantle uplift and eastward crustal motion produced a three-path zone of crustal fracture (about to the north, east and south-west), centred about 100 km west of the present Campanian coast.

[Luongo \(1988\)](#) elaborated a model for explaining the complex dynamic of the Southern Tyrrhenian (slab in subduction for the collision between the convergence between Africa-Europe, the opening of the Tyrrhenian basin and plume in rise, spreading of the Tyrrhenian and bending of the Apennine Arc, Maghrebain Chain, inversion of the subduction process) ([Figure 2.2](#)).

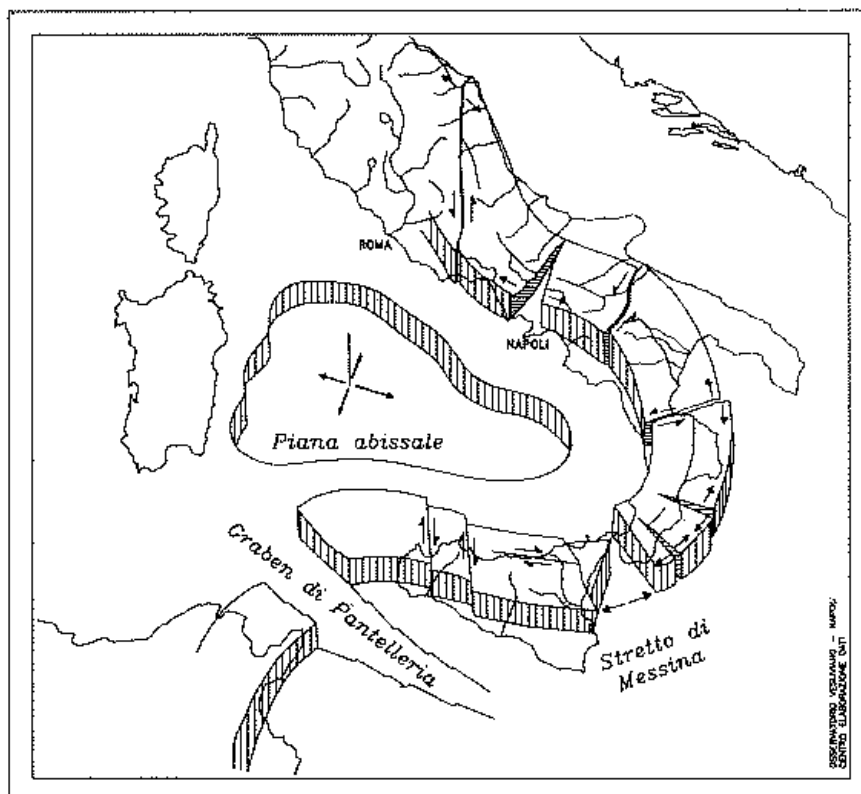


Fig. 2.2: Spread of the Tyrrhenian basin and *bending* of the Italian peninsula ([Luongo, 1988](#)).

The genesis of the Campanian volcanism was interpreted by [Luongo et al. \(1991\)](#) in the same way. The mantle rises towards the lithosphere producing a stress field. This causes fractures to 120° along the three main directions, which are the preferential path of rise of magma feeding the active volcanoes in this area (Somma-Vesuvius, Ischia, Phlegraean Fields; [Figure 2.3](#)).

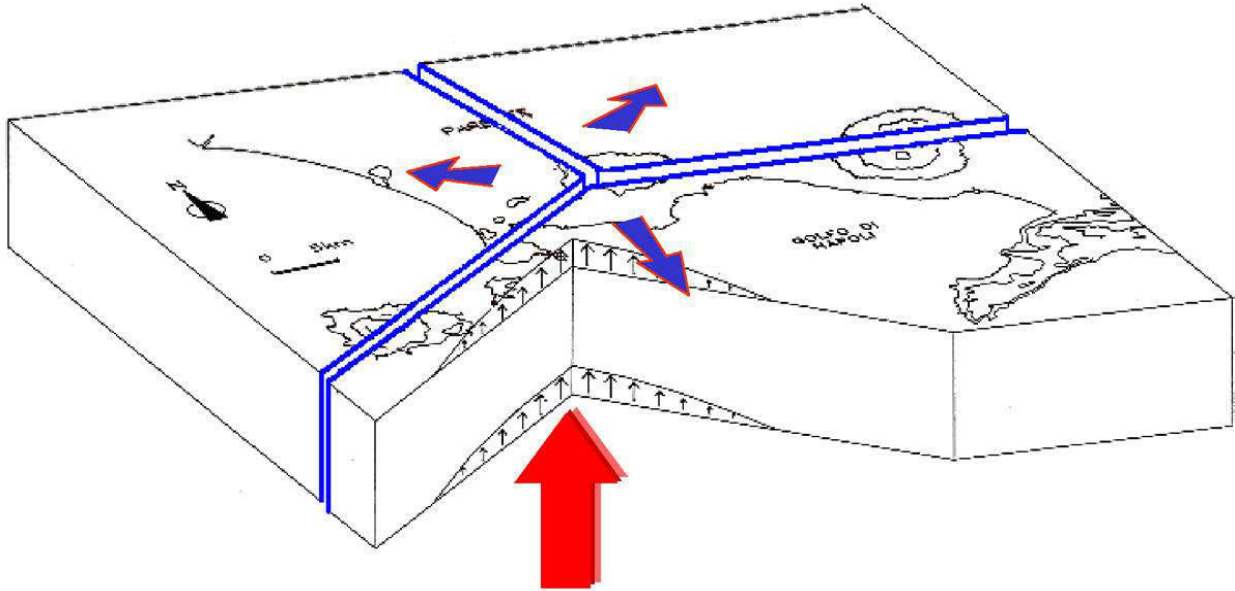


Fig. 2.3: Interpretation of the origin of the Campanian Volcanism. ([Luongo et al., 1991](#)).

In this area, there is the Campanian Plain, a structural depression of Plio-Quaternary age, located between the eastern side of the Tyrrhenian Sea and the Southern Apennines chain. Its tectonic structure consists of NW-SE/NNW-SSE- and NNE-SSW/NE-SW-trending faults ([Hyppolite et al., 1994](#); [Oldow et al., 1993](#); [Bigi et al., 1990](#)), which produce the uplift of the Mesozoic carbonates bordering the plain. An ENE-WSW- trending crustal discontinuity separates the Somma-Vesuvius sector (crustal thickness of 35 km) from the Phlegraean Fields-*Procida-Ischia* sector (crustal thickness of 25 km; [Ferrucci et al., 1989](#); [Locardi and Nicolich, 1988](#)). It represents the Tyrrhenian '41st parallel line' strike-slip faults system ([Spadini and Wezel, 1995](#); [Lavecchia, 1988](#)).

CHAPTER 3

3. The Somma-Vesuvius volcano

3.1. Geological setting

The Somma-Vesuvius volcanic complex is one of the most famous and studied in the world. As a matter of fact, it is the place where volcanology was born, due to the famous description of the AD 79 eruption by Pliny the Younger and being the location of the first Volcanological Observatory (Osservatorio Reale Vesuviano), built in 1841 by the will of the King of the two Sicilies, *Ferdinando di Borbone*.

It is a moderate-size (1281 m a.s.l.) stratovolcano, consisting of an older poly-phased edifice of Monte Somma ([Principe et al., 1999](#)) and a recent cone, Vesuvius or *Gran Cono* ([Arnò et al., 1987](#)), which developed within the caldera after the AD 472 eruption ([Rolandi et al., 1998](#)) ([Figure 3.1](#)).



Fig. 3.1: The Somma-Vesuvius volcano, satellite photo.

It is situated along the western side of the Campanian Plain and is associated to both the regional and local stress fields, at the crossing point of two regional Quaternary sets of fault heading NW-SE and NE-SW ([Bruno and Rapolla, 1999](#); [Bruno et al., 1998](#); [Bianco et al., 1998](#); [Vilardo et al., 1996](#)).

Its peculiarity is the marked morphologic contrast between the large and irregular arched reef of Monte Somma and the regular cone of Vesuvius.

The Somma edifice consists of lava flows and minor scoria fall/flow deposits, whereas the Vesuvius products also include pyroclastics related to both Plinian and sub-Plinian eruptions. The Somma caldera consists of ring-faults formed during Plinian and/or sub-Plinian eruptions. The caldera has an elliptic shape with the major axis roughly oriented in E-W direction. The caldera rims are well developed in the northern sector of the edifice, where the walls are sub-vertical and reach a maximum height of about 280 m. In the southern and western sectors of the volcano, the caldera rims are covered by the products of the post-1631 activity (Rosi et al., 1987).

Volcanic activity that occurred after the AD 79 *Pompei* Eruption (the last Plinian event), was concentrated in the Somma caldera and in the south-western sector of the volcano, located 600 m below than the northern one.

3.2. Eruptive History

The late Pleistocene activity of the Neapolitan volcanoes is poor known. In fact, in proximal areas, there are no outcrops of ancient deposits because they are covered by the younger one.

It is possible to find the pyroclastic deposits of the biggest ancient explosive eruptions inside the colluvial deposits or interbedded in the successions of alluvial fan, in the distal areas (Zanchetta et al., 2004b; Di Vito et al., 1998).

The volcanism in the Vesuvian area can be dated at about 4000 ky BP (Brocchini et al., 2001; Santacroce, 1987).

The growth of Monte Somma post-dates the Campanian Ignimbrite products erupted from Phlegraean Fields 39,000 years ago (De Vivo et al., 2001), and the caldera is the result of collapses, related to major explosive eruptions in the last 22,000 years. During these eruptions, effusive and explosive volcanic activity alternated with periods of quiescence (Cioni et al., 1999). The past explosive activity of Somma-Vesuvius has been characterized by many eruptions largely variable in magnitude, intensity and composition of the involved products, which led to the dispersion of pyroclastic deposits over large areas (Cioni et al., 2008).

The Plinian eruption of the Basal Pumice, about 18 ky BP, determined the beginning of the mainly explosive activity (Bertagnini et al., 1998; Andronico et al., 1995; Arnò et al., 1987), the origin of the volcanic-tectonic collapse of the Monte Somma's large cone and the formation of the caldera (Cioni et al., 1999).

After this strong eruption, the activity of the volcano was characterized by some effusive phases and the beginning of the long period of quiescence, which ended with the sub-Plinian eruption of the Greenish Pumice, about 16 ky BP (Arnò et al., 1987).

The successive activity of the volcano is marked by three Plinian eruptions: the “*Mercato Pumice*”, about 8 ky BP (or *Ottaviano*’s Eruption; [Rolandi et al., 1993a](#)); the “*Avellino Pumice*”, about 1995±10 cal BC ([Sevink et al., 2011](#); [Sulpizio et al., 2010a and b](#); [Rolandi et al., 1993b](#)); and the eruption of the AD 79 of *Pompei*, called “*Pompei Pumice*” ([Cioni et al., 1999](#); [Lirer et al., 1997, 1973](#); [Arnò et al., 1987](#); [Sigurdsson et al., 1985](#)). These eruptions are spaced out by many sub-Plinian eruptions and phases of low energy activity, with Strombolian eruptions and effusive activity.

After the *Mercato* eruption, Vesuvius had a long period of rest. Interbedded the *Mercato* and *Avellino* eruptions, it is possible to identify the fallout deposit of *Agnano Monte-Spina* Pumice, coming from Phlegraean Fields.

In the span time between the *Avellino* and *Pompei* eruptions, [Andronico and Cioni \(2002\)](#) recognize six major eruptions (AP1-AP6), interbedded by some smaller events. AP1 and AP2 are considered weak sub-Plinian eruptions and AP3 until AP6 are considered strong Strombolian eruptions. [Rolandi et al. \(1998\)](#) and [Somma et al. \(2001\)](#), called this period “Protohistoric” and identify it in three Strombolian-Volcanian events, interbedded by paleosoils.

The eruptive activity of Vesuvius, between AD 79 and AD 1631, is little well-known because its historical sources are scarce and fragmented if compared with the wide documentation about the last activity period between AD 1631 and 1944 ([Cerbai and Principe, 1996](#)).

Probably, the *Pompei* eruption left the system open. The following centuries were characterized by a number of explosive eruptions ([Andronico et al., 1996a and b](#)), effusive and mixed eruptions ([Principe et al., 2004](#)), and the initial construction of a central cone within the caldera depression ([Cioni et al., 1999](#)). An explosive eruption, presumably, took place in AD 203 and a fairly long period of rest preceded the AD 472 *Pollena* eruption ([Sulpizio et al., 2007, 2005](#); [Rolandi et al., 2004](#); [Arnò et al., 1987](#); [Rosi and Santacroce, 1983](#); [Delibrias et al., 1979](#)). After that last one, a number of eruptions (many with lava flows) were often issued by eccentric vents and reached the sea at several points, drawing the actual morphology of the coast ([Principe et al., 2004](#)).

In particular, the Vesuvian effusive activity was concentrated in a relatively short time, between AD 787 and AD 1139, followed by five centuries rest period, until the explosive eruption of the AD 1631.

Vesuvian activity between AD 79 and AD 1631 can be distinguished in a late antique phase, from AD 79 to AD 472, and a medieval phase, from AD 472 to AD 1631, including the fall of the Roman Empire and the beginning of the Middle Ages (respectively, AD 476-1492) ([Rolandi et al., 1998](#)).

The recent volcanic history of Somma-Vesuvius begins with the AD 1631 eruption, which left the conduit open, and ends with the 1944 event ([Cioni et al., 2008](#); [Santacroce et al., 2008](#); [Arrighi et al., 2001](#); [Arnò et al., 1987](#)). It includes three century-long periods of semi-persistent activity, alternating effusive eruptions and mild/violent Strombolian explosions, often accompanied by the issue of low level of lava and the presence of short rest periods (never exceeding 7 years) ([Arrighi et al., 2001](#)).

Due to the presence of morphological barrier of Monte Somma, lava flowed along the southern sector of the volcano, while the pyroclastic fallout was distributed towards E-SE, in accordance with the direction of prevailing winds.

The activities in that period took place both at the central crater and intra-calderic vents, positioned inside the Somma caldera (the 1855 lava flows; 1858; 1867; 1872; 1891-94 *Colle Margherita*; 1895-99 *Colle Umberto*), which filled the circular depression in the caldera of Monte Somma and Vesuvius.

In a very few cases (in 1861, 1794 and 1760 eruptions), eccentric vents opened at low altitudes and outside the caldera wall.

Actually, Vesuvius is in a quiescent phase, which started after the 1944 eruption.



CHAPTER 4

SYNTHETIC MAP OF THE SOUTH-WESTERN SECTOR OF THE VESUVIUS VOLCANO, ITALY

(Submitted to *Journal of Maps*)

Abstract

Through the field surveys, it was possible to produce a new and detailed volcanological map of the south-western sector of Vesuvius, at the 1:10,000 scale. We considered the last 4000 years of eruptive activity of Vesuvius. The mapping work was done integrating stratigraphic and petrologic data with archaeological and historical information, showing interaction between volcanological, morphological and human aspects of this very densely populated sector of the volcano. Here, all the historical lava paths and tephra deposits were accurately and correctly identified and reported, mapped using the subdivision of stratigraphic/cartographic elements in Synthetic units, which greatly helped the description of the volcanic behaviour. Archaeological and historical data were used in support of the cartography of the lava flows emitted during the last 2000 yrs.

Oldest volcanic deposits outcropping in the mapped area are the huge pyroclastic covers of the two great Plinian eruptions of *Pompei* (AD 79) and *Avellino* (4000 BP). During medieval time only few tens of lava flows were emplaced in this area. They were, mainly, outpoured from lateral vents recognized and mapped, instead than directly from the central Vesuvius crater. These eccentric vents are positioned very near to the present coastline.

Keywords

Vesuvius, UBSU, cartography

4.1. Introduction

The geological maps of Vesuvius, available in the literature, give a detailed cartography restricted only to the most recent lava flows (Santacroce and Sbrana, 2003; Rosi et al., 1987; Johnston-Lavis, 1891; Le Hon, 1866). However, the work of Principe et al. (2004) clearly shows the existence of a number of lava flows emitted during the volcanic activity of the medieval period, which are still well visible on Vesuvius shoreline and that were generated, mainly, by eccentric vents positioned at the foot of the main volcanic cone. Beforehand, these lava flows were thought to belong to the AD 1631 small-scale Plinian eruption (Le Hon, 1866). This new detailed volcanological map of the south-western sector of Vesuvius (Supplementary Material) correctly identifies all the medieval lava flows outcropping in this area of the volcano and their relationships with the pyroclastic deposits emitted during the *Avellino*, *Pompei* and AD 1631 eruptions.

4.2. Geological outlines

Somma-Vesuvius volcano complex is situated in the Campanian Plain (Figure 4.1) on the coast of the Gulf of Naples (Southern Italy), at the intersection of a NW-SE and a NE-SW oriented fault system (Bigi et al., 1990; Cassano and La Torre, 1987; La Torre et al., 1983; Finetti and Morelli, 1974).

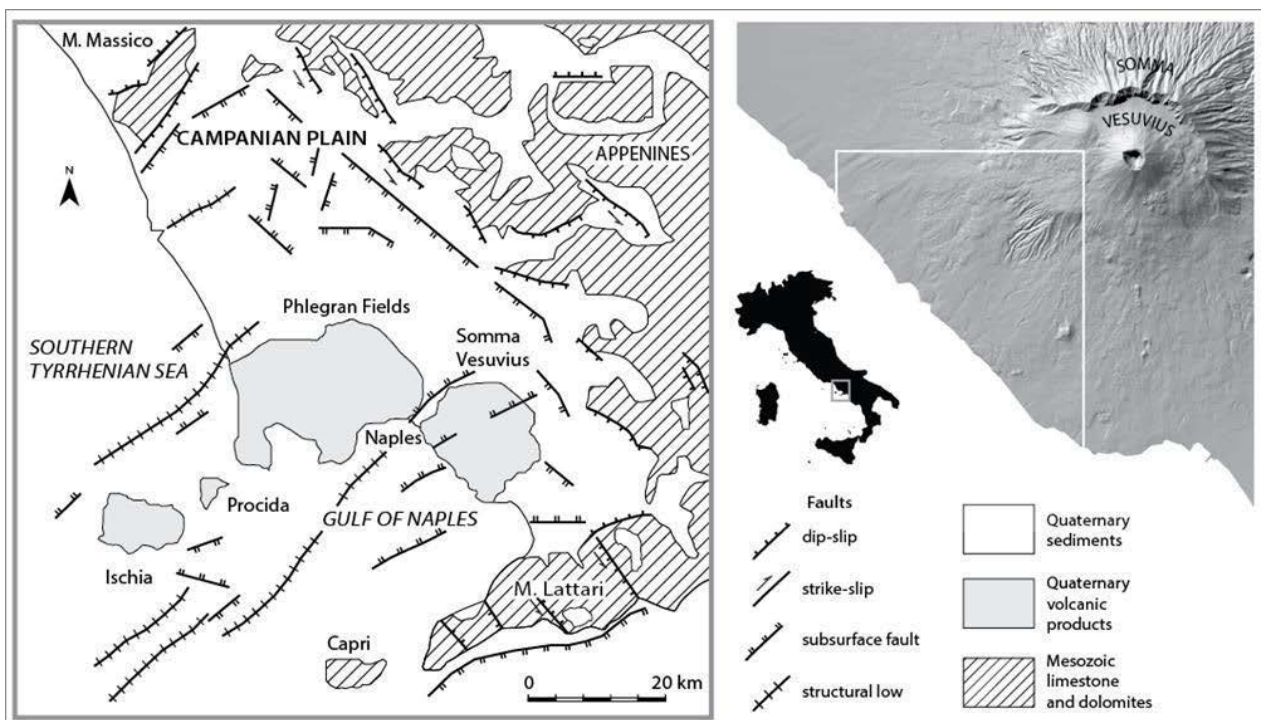


Fig. 4.1: (a) Geological sketch map of Campanian Plain (modified from: Bigi et al., 1990; Cassano and La Torre, 1987; La Torre et al., 1983; Finetti and Morelli, 1974).
(b) Somma-Vesuvius volcano with the delimitation of the mapped area (white line).

It is a composite volcano formed by the poly-phased edifice of Monte Somma (Principe et al., 1999) interested by multiple collapses (Cioni et al., 1999), and surrounding a younger cone (Vesuvius) (Arnò et

al., 1987). The activity of the Somma-Vesuvius complex starts, approximately, after the Phlegraean Field Campanian Ignimbrite super-eruption, occurred about 39 kyrs ago (De Vivo et al., 2001), while the last eruption happened in 1944 (Arnò et al., 1987). During the last 4000 years of activity Vesuvius experienced few main explosive events: the small-scale Plinian eruption of AD 1631 (Rosi et al., 1993), the sub-Plinian AD 472 eruption (Sulpizio et al., 2007, 2005; Rolandi et al., 2004; Arnò et al., 1987; Rosi and Santacroce, 1983) and the two large Plinian eruptions, at AD 79 (*Pompei* eruption; Sigurdsson et al., 1985) and 1995 ± 10 cal BC (*Avellino* eruption; Sevink et al., 2011; Sulpizio et al., 2010a and b; Rolandi et al., 1993b). Mild explosive activity (from Strombolian and violent Strombolian to sub-Plinian) took place during intra-Plinian periods (Cioni et al., 2013; D’Oriano et al., 2011; Di Renzo et al., 2007; Andronico and Cioni, 2002; Arrighi et al., 2001). A number of lava flows have outpoured from central crater (*‘Gran Cratere’*) or from fissures opened on the main Vesuvius cone (*‘Gran Cono’*) (Principe et al., 2004, 1987). Before the work of Principe et al. (2004), the understanding of eccentric activity, with vents opening foothill of the main Vesuvius cone, was limited to a few lava flows, principally emitted in modern times (e.g. 1861, 1794, 1760 eruptions) (Principe et al., 1987).

4.3. Mapping methodology

Field Mapping was realized using the topography at the 1:5,000 scale, produced by *Cassa del Mezzogiorno* (Southern Italy Development Agency) in 1978 (Plates 448132, 448133, 466011, 466012, 466014), and, then, digitized using the *Cartografia Tecnica Numerica Provinciale della Regione Campania* (Technical Digital Cartography of the Campanian Regional Authority), at the same scale (1:5,000, produced in 2004 and 2005), based on aerial photographs taken during the years 1998-99.

The digital map, geocoded into WGS84 UTM 33N reference cartographic system, was subsequently super-imposed to the Shaded Relief derived from a Digital Elevation Model (DEM) with a spatial resolution of 10 m. The DEM was obtained by interpolating 3D vector data from two different cartographic sources: IGM (Military Geographical Institute) raster maps at a scale of 1:25,000 (updated to 1980; Bisson et al., 2007a) and vector cartography at a scale of 1:2,000 (1987). Contour lines and spot heights obtained by digitizing the IGM raster data have a height precision of 1-7 m, whereas the contour lines and spot heights of the 1:2,000 cartography have a planimetric and altimetric precision of 1.2 and 0.6-0.9 m, respectively (Tarquini et al., 2007). All vector data were first interpolated to build a Triangular Irregular Network (TIN) by using the DEST (Determination of Earth Surface Structures) algorithm, a variation of the Delaunay method that solves the problem of false flat morphological features introduced by the Delaunay triangulation (Favalli and Pareschi, 2004).

Based on the outcropping areas, field, historical, archaeological and morphological data sets, the volcanological map reported into **Supplementary Material** was produced. The intense urbanization of the

peri-Vesuvian area has deleted the major part of outcrops, relegating them only in correspondence of roads cuts, quarried areas and construction sites.

4.3.1. *Unconformity Bounded Stratigraphic Units (UBSU)*

In our cartography ([Supplementary Material](#)) we used lithostratigraphic units as mappable objects in the field; hence the smallest formal lithostratigraphic units ([NACSN, 1983](#)) in the map are beds (essentially lapilli beds) and flows (essentially lava flows or pyroclastic flows). The basic lithostratigraphic unit (i.e. the formation) was not used in this case, because our map represents only a portion of a wider geological body (i.e. the Vesuvius volcano).

The mapped lithostratigraphic units were grouped in Unconformity Bounded Stratigraphic Units (UBSU) ([Figure 4.2](#)).

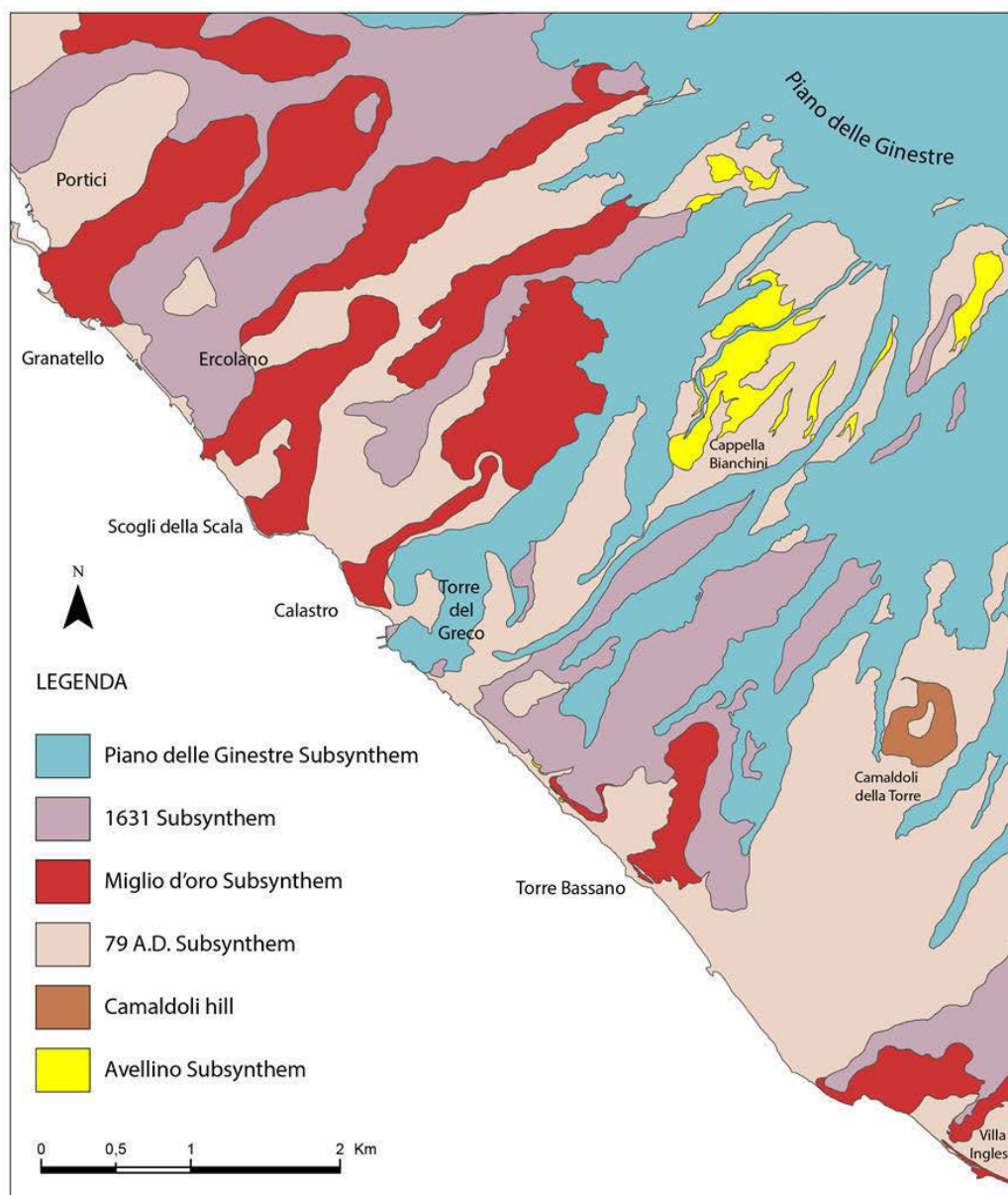


Fig. 4.2: Volcanological sketch Map of the south-western sector of Vesuvius. The mapped units are grouped into Synthematic units.

Chang (1975), Salvador (1994, 1987) and Murphy and Salvador (1999) proposed the use of Synthems to represent cartographic units bounded by discontinuities. An unconformity-bounded unit is defined as ‘*a body of rocks bounded above and below by specifically designated, significant, and demonstrable discontinuities inside the stratigraphic succession (angular unconformities, disconformities, etc.), preferably of regional or interregional extent*’ (Salvador, 1987). In the same context, unconformity is defined as a surface of erosion and/or non-deposition between rock bodies, representing a significant hiatus or gap in the stratigraphic succession, caused by the interruption of deposition for a significant span of time (Salvador, 1987). Finally, these discontinuity surfaces must be recognizable on the field (Bonomo and Ricci, 2010).

In respect to other types of units often used in volcanological maps (such as lithotypes or eruptive units), the use of UBSU represents a clearer and more pragmatic approach to stratigraphic analyses, in order to achieve a better, more descriptive, and more lucid interpretation of the whole geologic history of the area in which the volcanic districts insist (Salvador, 1987). It is an objective manner to synthesize the volcanic evolution and to distinguish major phases on the basis of reproducible field characteristics, while also taking into account the geological (in the sense of not-volcanological) events occurred inside and/or at the limit of a given volcanic district (Groppelli and Viereck-Goette, 2010; Principe and Giannandrea, 2008).

In volcanic areas unconformities can be due to a number of causes that are specific of volcanic activity, such as a period of quiescence, an erosional phase, a shifting of the feeding system, an abrupt change in eruptive style, or a volcano-tectonic event like the formation of a caldera or of a sector collapse. The rank of an unconformity depends on its geographic extension, the duration of an associated hiatus, or its volcano-structural significance.

The application of the unconformity-bounded units concept to volcanic areas can face problems of scale (temporal and spatial), as usually hiatuses are of short duration, because of the sometimes-limited areal extent of units. We paid particular attention to this topic when working on this map, since it represents only a portion in time and space of a larger and older volcanic edifice. In truth, the very fact that this map represents a part of a volcano points to the need to use very objective and replicable cartographic criteria.

4.3.2. *Archaeological and Historical criteria*

Early maps of Vesuvius which date back to the XVIII century (La Vega, 1797; Morghen, 1794; Carafa, 1775; Figure 4.3a, b and c) have been an important source of information for the present work, and allowed us to reconstruct changes of toponymy and topography in an area that has been recurrently disrupted by volcanic activity. In addition to these maps, the Johnston-Lavis (1891) map produced during 1888-89 (Figure 4.3d) (based on the topographical plan in six sheets, at the same scale 1:10,000,

produced by the IGM of Florence from 1871 to 1876) has been instrumental for mapping lava flows, especially those of the XIX century.

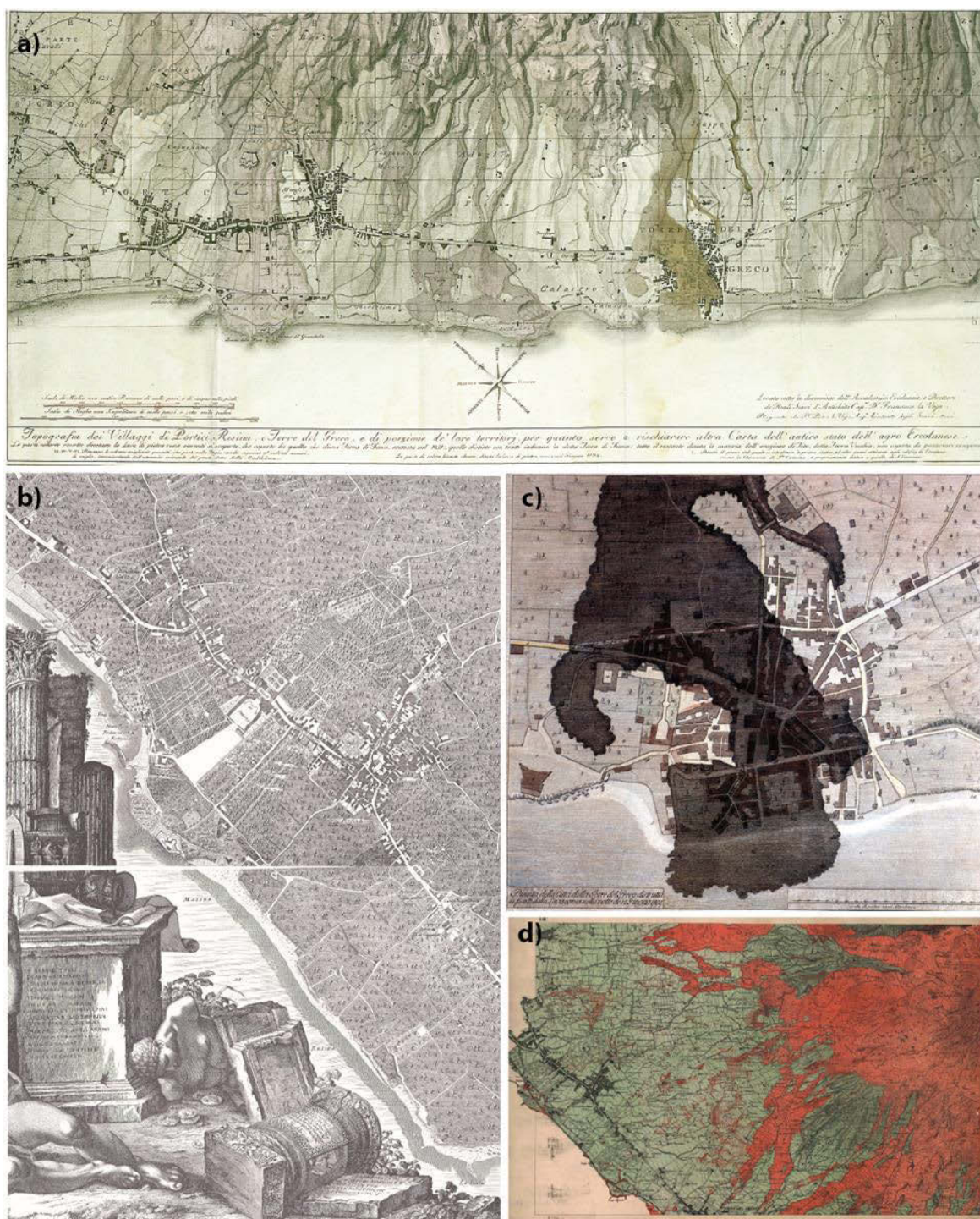


Fig. 4.3: Historical maps of the Vesuvius south-western sector.

(a) In the map of [La Vega \(1797\)](#) are reported the better exposed lava flows before and after the AD 1631 eruption in this sector of the volcano, the 1631 nuées ardentes deposits ('*Terra di Fuoco*', literally 'fiery soil'), and the deposits of the Pompei eruption ('*Terra Vecchia*', literally 'old soil'), not covered by other eruptions. Pompei eruption is named 'Tito' eruption, because that eruption dates AD 79 at the time of the Roman emperor *Titus Flavius Caesar Vespasianus Augustus* (from AD 79 to AD 81).

(b) Portion of the topographic map printed by [Giovanni Carafa Duca di Noja](#) in 1775. This map represents the most accurate description of the Vesuvian area into XVIII century.

(c) The accurate cartography of the front of the 1794 lava flow that destroyed *Torre del Greco*, in the plate of [Antonio Ciofi \(1774\)](#) engraved by [Raffaello Morghen](#).

(d) PLATE III (Locality *Granatello-La Scala*) of the Mt. Vesuvius' geological map, compiled by [Henry James Johnston-Lavis \(1891\)](#) and drawn in six sheets at the scale of 1:10,000 on the topography realized by the students of the Military Topography Institute of Florence in 1875-86.

The *Pompei* eruption in AD 79 sealed all the southern sector of Vesuvius with tens of meter of loose lapilli and ashes, *nuèes ardentes* and lahar's deposits. While undoubtedly destructive, the event preserved much of the Roman presence in the territory, first of all *Ercolano*, *Pompei* and *Oplontis* villages, and today Roman ruins punctuate as archaeological sites the lowermost slopes of Vesuvius. The Roman sites inside the mapped area were used during fieldwork as a stratigraphic marker.

Another useful tool for the control of lava flow patterns was the census of information regarding building age and the transformation of a large number of churches, chapels, and historical edifices (mansions and rural villas) built from XVI to XX century at the foots of the volcano, especially along the old road called *Strada Regia delle Calabrie* (De Seta et al., 1980), nowadays *Via Nazionale*, running near the coast, from the city of Naples to *Torre del Greco* and *Torre Annunziata* towns to the south.

The large number of witness's reports of eruptive events still preserved in the main specialized Italian and European libraries (Principe, 1997), helped in reconstructing eruptive phenomenology, deposits typologies, and deposits distribution of eruptions and eruptive periods. Despite the fact that these reports carry the reputation of being fictional and imprecise, an appropriated selection of chronicles and treatises based on historiographical criteria effectively supported our field and cartographic work (Principe, 1998).

The extraordinarily of the historical record for the Vesuvius area is due to the long history of human presence in a land that has a pleasant climate, fertility of the soil, connection facilities by sea (due to the presence of the Gulf of Naples), and overland (even before the construction of the Roman consular roads). A great impulse to land development, after Roman times, can be attributed to the establishment of Naples (15 km away from the Vesuvius summit) as the capital of the Kingdom of the Two Sicilies (1266), and few centuries later (1738) by the construction, due to *Carlo III Borbone*, of the *Royal Palace of Portici*.

This volcanological map reproduces the original pattern of each lava flow using all the available information. The resulting cartography takes into account the flow directions of each lava flow and its relationships with the pre-existing morphology.

Geological mapping carried out in heavily developed areas is by necessity a compromise between the real location of outcropping stratigraphic units and the *strata* of asphalt and concrete that cover them. In the Vesuvius area the intense and long-lasting mining activity of lava flows and lapilli covers ('*pozzolana*') magnify this problem. All the villages around Vesuvius are completely built with these volcanic products, as well as most of the city of Naples. The original pattern of lava flows was partially erased by excavations and covered by a carpet of buildings (Figure 4.4). On the other hand lava flows and '*pozzolana*' quarries, when present, have been very useful in stratigraphic reconstruction as well as the presence of road cut and construction sites facilitates to locate outcrops. Finally, in the northern portion of the map, the lower slopes of the Vesuvius cone areas are part of the Vesuvius National Park, which made it easier to map the lava flows that date to the XIX century.

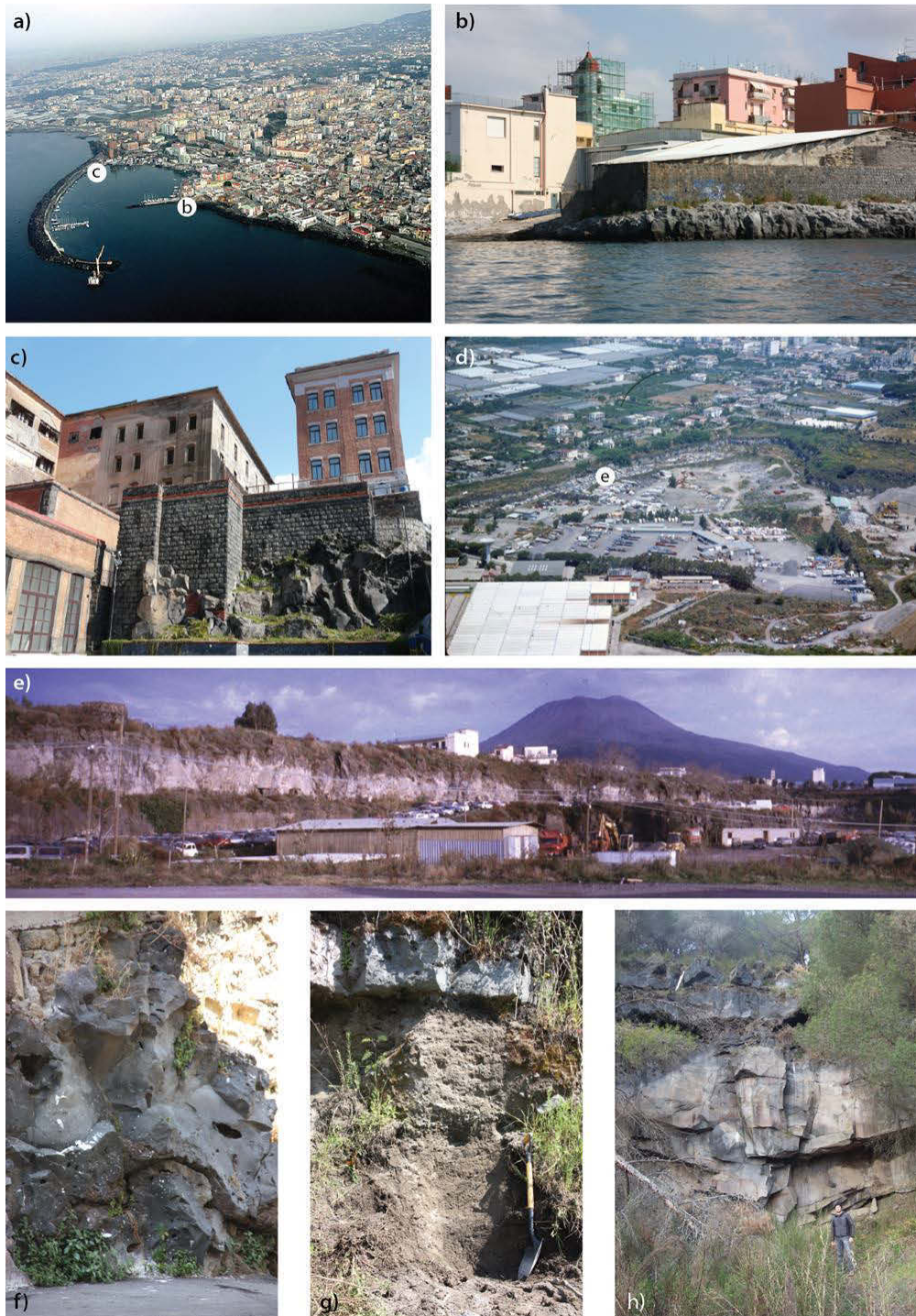


Fig. 4.4: (a) Aerial photo of *Torre del Greco* with its many buildings. (b) The front of the 1794 lava flow, still outcropping along the coast of *Torre del Greco*. In the background the bell tower of the church of *Portosalvo*. (c) The *Calastro* lava flow ('cal' in the volcanological map) outcropping along the coast of *Torre del Greco*, underneath the old *Molini Marzoli* edifices. (d) Aerial photo of *Villa Inglese* quarried area. This ancient quarry take is name from the villa of the English gentlemen Sir William Hamilton. (e) Interior of *Villa Inglese* Quarry with the '*Il Villa Inglese*' lava flow ('vin1' in the volcanological map) extensively outcropping. The Vesuvius main cone in the background. (f) Particular of a vesiculated lava flow ('tir' in the volcanological map). (g) Deposit of Concentrated Piroclastic Density Current (CPDC), emplaced during the AD 1631 small-scale Plinian eruption. The lava flow on top of the CPDC is one of the thin lava flow emitted from the main Vesuvius crater during the 1806 eruption. (h) Inside an abandoned quarry, North of the *Camaldoli della Torre* Hill, the 1804-05-06 thin lava flows overlap the huge medieval flow named '*Il Villa Inglese*'. The name of this characteristic lava flow is due to the fact that it was extensively quarried, since the eighteenth century in *Villa Inglese* locality along the coast, due to its poor vesiculation and porphyricity in respect to most Vesuvius lavas.

4.4. Stratigraphy/Legend

Unconformity bounded units

The stratigraphy of the last 4000 yrs of Vesuvius activity has been subdivided in five Synthem (Figure 4.5). The unconformities that separate these Synthem are angular unconformities, erosional surfaces, disconformities (i.e. irregular or uneven erosion surfaces or indications of weathering in essentially parallel bedding), and soils, corresponding to a significant depositional hiatus in the stratigraphic succession. Lithostratigraphic units were distinguished during fieldwork on the basis of their lithologic characteristics and stratigraphic position (NASCN, 1983). In the map (Supplementary Material) lithofacies symbols have been super-imposed on the colours indicating each bed or flow unit. This allows the immediate identification of different lithologies such as lapilli covers or pyroclastic flows deposits.

The 36 lithostratigraphic mapped units are grouped in Synthem and Subsynthem as follows (Figure 4.5):

4.4.1. *Present-Vesuvius Synthem*

It comprises the *Piano delle Ginestre* and *AD 1631* Subsynthem. The top surface of the *Piano delle Ginestre* Subsynthem is represented by the present-day morphology, while the base, which separated it from the *AD 1631* Subsynthem, is represented by the collapse surface of the Vesuvius cone after the AD 1631 small-scale Plinian eruption (Rosi et al., 1993). The unconformity at the base of the *AD 1631* Subsynthem is a soil deposit developed during five centuries of volcanic rest before the AD 1631 eruption (Principe and Marini, 2008; Rosi et al., 1993). It separates the *Present-Vesuvius* Synthem from the *Medieval-Vesuvius* Synthem (Figure 4.5).

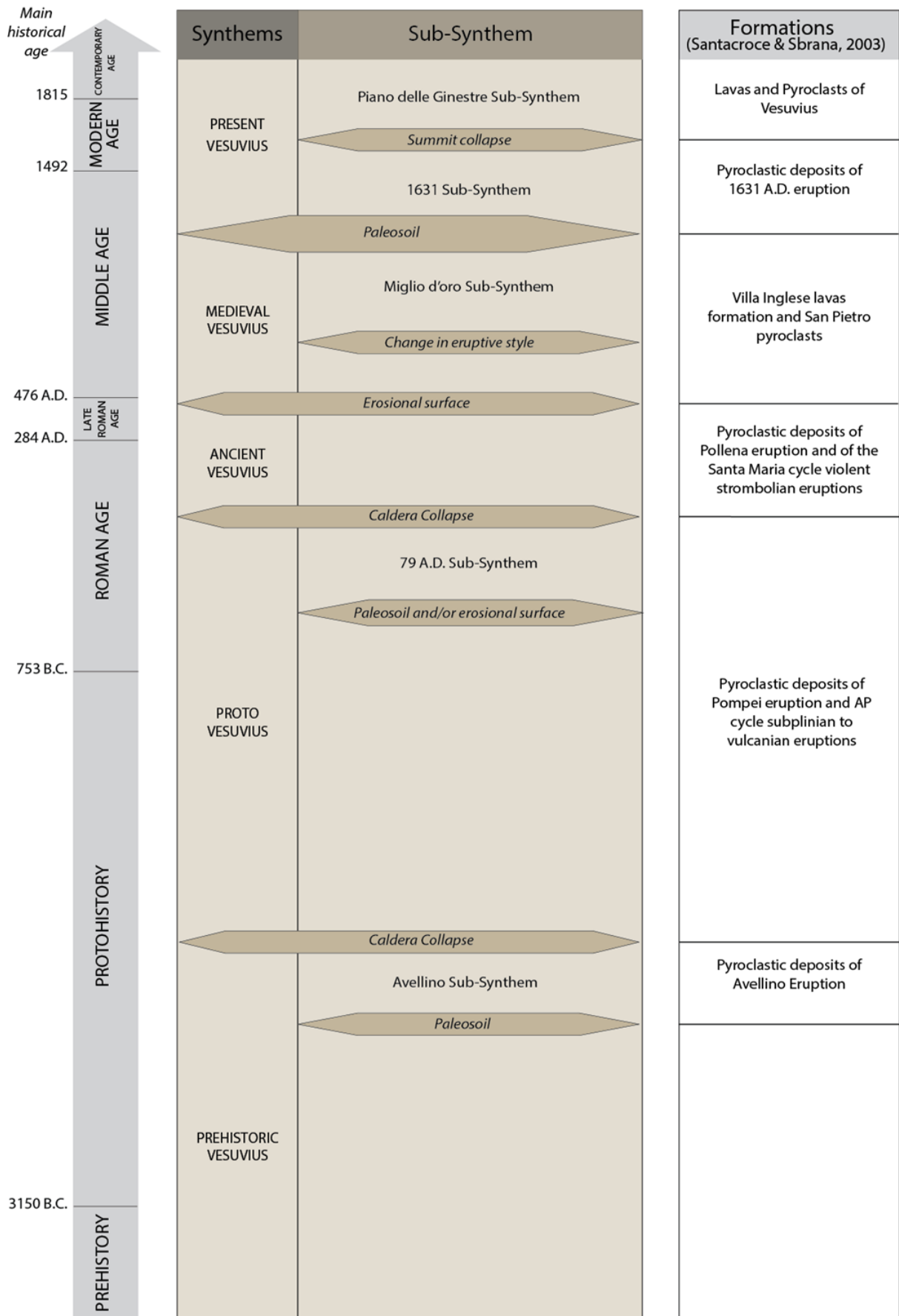


Fig. 4.5: Synthematic subdivision and related unconformities.

The *Piano delle Ginestre* Subsynthem consists of 19 lava flows units and a bed of lapilli tephra, emitted during the whole period from post-1631 activity to 1944. The majorities of the lava flows have limited thickness (from 1 to 5 m), and were emitted either from the main crater or from vents opened at the Vesuvius main cone foots (Principe et al., 1987) and did not reach the shoreline. There are only three exceptions to this general behaviour, which are: *i*) the main lava flow of the 1794 eruption which entered the sea with a thick and steep front and destroyed 4/5 of the ancient city of *Torre del Greco* (Figure 4.3a and c); *ii*) the 1858 eruption that continued in *iii*) the 1861 fissure lava flows, with the formation inside the *Canteroni* and *Piano delle Ginestre* area of a number of lava domes and *coulées* with rope structure. As a whole, the lava flows and pyroclasts emitted during the post-1631-1944 period have phono-tephritic composition (Figure 4.6). The minerals assemblage comprises clinopyroxene, leucite, plagioclase, olivine, biotite, and Fe-Ti oxides in various proportions (Arrighi et al., 2001; Belkin et al., 1993).

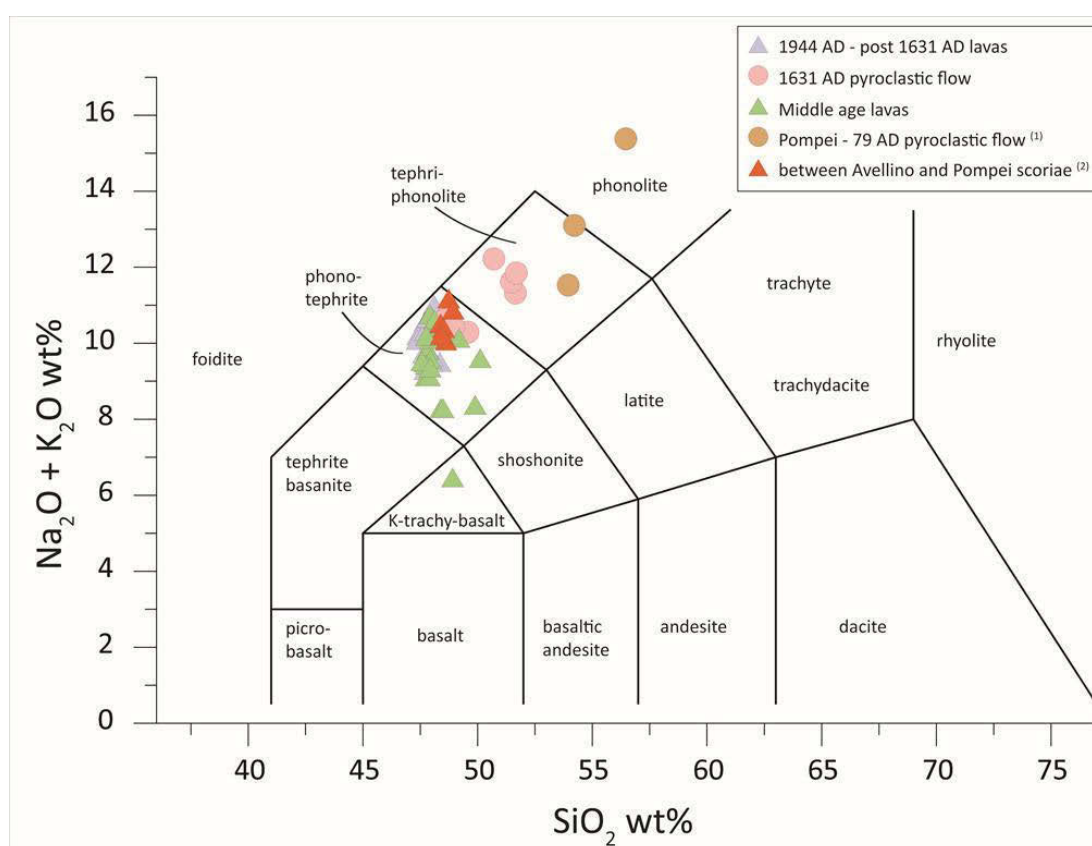


Fig. 4.6: Total Alkali Silica chemical classification diagram (Le Maitre, 2002).
 (1) Data from Cioni et al. (1995); (2) data from Di Renzo et al. (2007).

Deposits emplaced during the AD 1631 eruption represent the *AD 1631* Subsynthem. Here the mapped area shows outcrops of Concentrated Pyroclastic Density Currents deposits (CPDC). The 1631 CDPC are mainly unconsolidated, gravity controlled, and extremely rich of old lava blocks, skarn fragments and cumulate. The magmatic fraction is made of dark-green scoriae with clinopyroxene and euhedral leucite phenocrystals as most evident phases (Rosi et al., 1993). Chemical classification of the flows juvenile fraction ranges from phono-tephrite to tephri-phonolite (Figure 4.6). This eruption marked the end of a rest period that lasted at least 5 centuries (Principe and Marini, 2008).

4.4.2. Medieval-Vesuvius Synthem

The *Medieval-Vesuvius* Synthem contains the *Miglio d'Oro* Subsynthem that separates the mainly effusive period of activity from IX to XII century from few explosive events occurred close to the AD 472 large eruption (D'Oriano et al., 2011; Santacroce and Sbrana 2003; Rolandi et al., 1998). The *Medieval-Vesuvius* Synthem is separated from the *Ancient-Vesuvius* Synthem by an erosional surface with drainage patterns super-imposed on the pre-existing morphology produced by the *Pompei* eruption deposits. In other areas of the volcano this surface setup on the AD 472 eruption deposits (Figure 4.7 and 4.8).

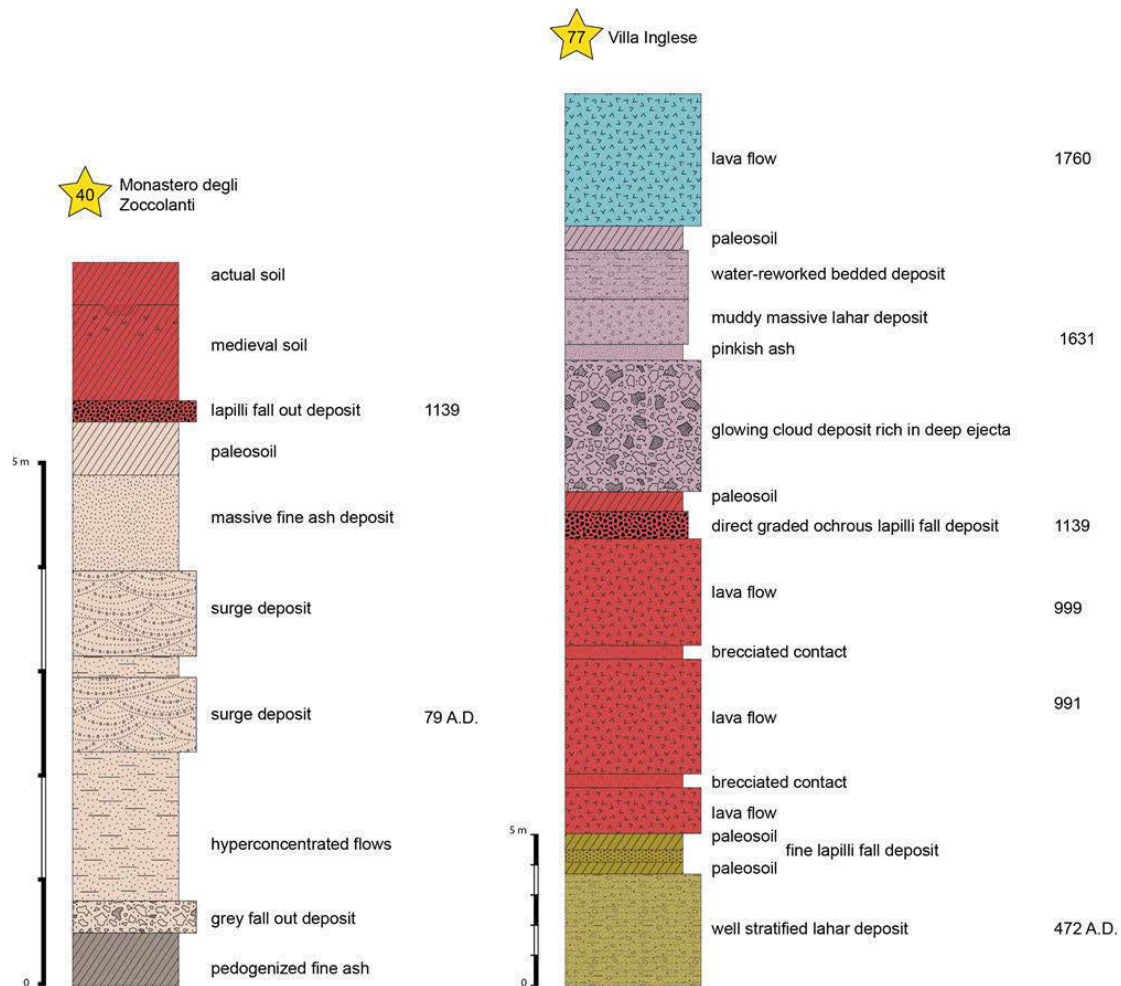


Fig. 4.7: Stratigraphic sections:
(a) inside excavation works of *Convento degli Zoccolanti* in *Torre del Greco* town;
(b) at *Villa Inglese* quarry (modified from Principe et al., 1987).

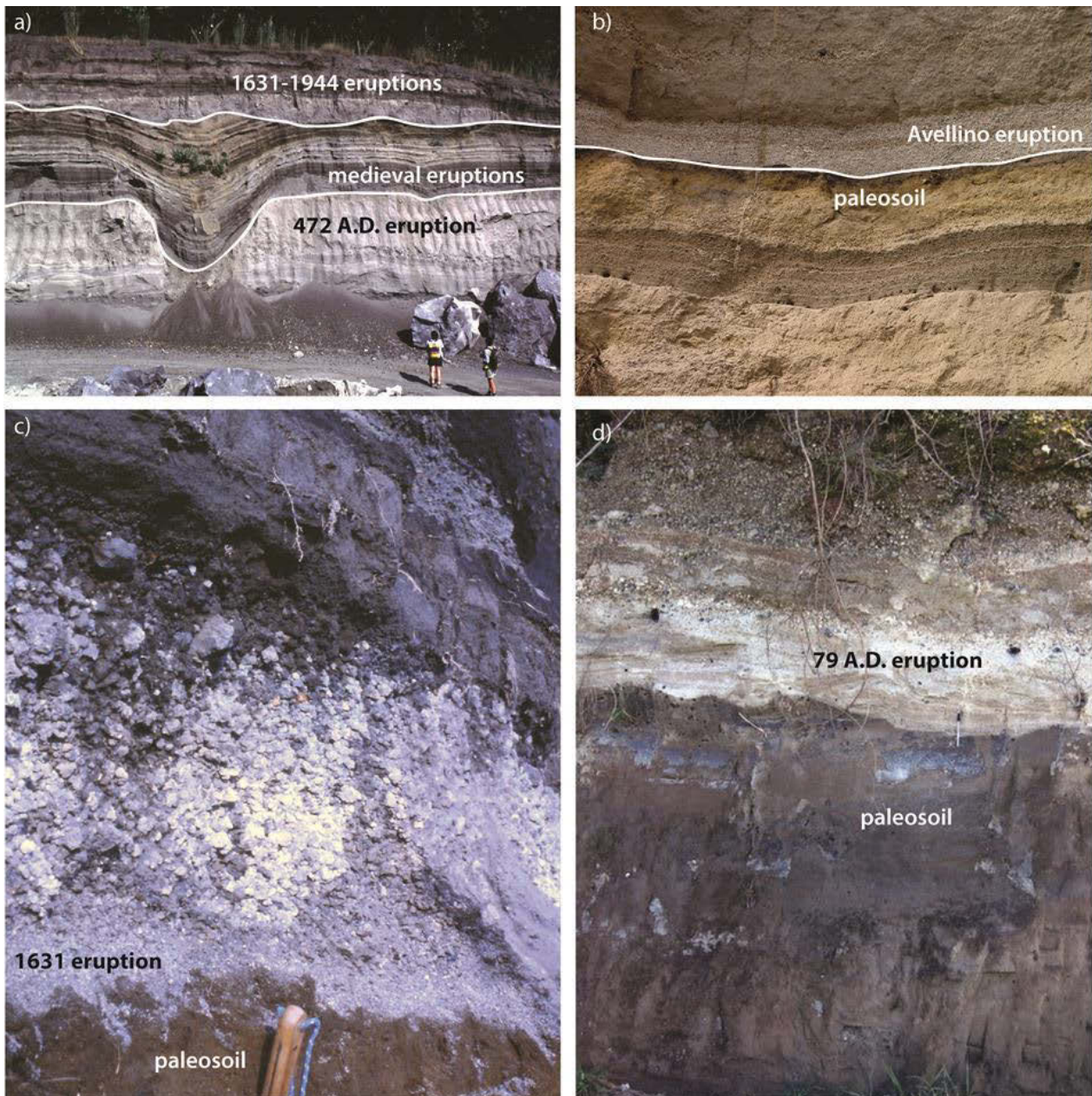


Fig. 4.8: Unconformities inside the pyroclastic sequence of the last 4000 years.

(a) In *Pozzelle* quarry (south-east of the Vesuvius cone) the Medieval and Modern tephra deposits are over imposed to a curved morphology formed because of the setting of a new hydrography on the AD 472 sub-Plinian eruption deposits (from Principe and Tanguy, 2009).

(b) The Orange-brown paleosoil underlying the *Avellino* Plinian fallout in the quarry of *Trapolino* (north of the Vesuvius cone) (from Principe and Tanguy, 2009).

(c) The 5 centuries of rest-related paleosoil at the base of the deposits of the AD 1631 small-scale Plinian eruption outcropping in the type section at *San Leonardo* (north-east of the Vesuvius cone; modified from Rosi et al., 1993).

(d) *Pompei* eruption deposits outcropping at *Case Sarciniello* (north-west of the 1794 eruption lowermost vents), overlapped to a paleosoil with traces of cultivation.

4.4.3. *Ancient-Vesuvius Synthem*

The *Ancient-Vesuvius Synthem* comprises the AD 472 eruption deposits. The boundary between the *Ancient Vesuvius Synthem* and the *Proto-Vesuvius Synthem* is the unconformity generated by the AD 79 eruption-related caldera collapse (Cioni et al., 1999). As well as in the case of the explosive eruption close to the 472, the AD 472 eruption deposits do not outcrop in the mapped area.

4.4.4. *Proto-Vesuvius Synthem*

The deposits of the *Pompei* eruption, occurred in AD 79 (Sigurdsson et al., 1985), are diffusely present in the south-western sector of Vesuvius. The deposits emitted during this eruption were found as a thick cover (tens of meters in the more proximal sites) all over the mapped area, filling old valleys and cancelling the previous hydrography. The lower limit of the *AD 79* Subsynthem is represented by a thick paleosoil found on top of the *Avellino* eruption ashes, and that in some places shows traces of cultivation (Figure 4.8). Other eruptive episodes occurred inside the time span between *Avellino* and *Pompei* eruptions (Arnò et al., 1987). This is the case of the *Camaldoli della Torre* scoria cone (Di Renzo et al., 2007; Figure 4.9). In deep cuts of *Cappella Bianchini* area tephra related to the mild explosive eruptions named AP by Andronico and Cioni (2002) are also present. The top of AD 79 deposits in large areas of the map still represents the present-day morphology, where they have been reworked, eroded and carved by a new hydrography ('nn' in the map). Chemical composition of *Pompei* pumices ranges from tephri-phonolite to phonolite (Figure 4.6).



Fig. 4.9: The *Camaldoli della Torre* scoria cone in the foreground and the Vesuvius main cone in the background.

4.4.5. *Prehistoric-Vesuvius Synthem*

The *Avellino* Plinian eruption (1995±10 BC; Sevink et al., 2011) extensively outcrops at the base of the reconstructed stratigraphic sequence. The *Avellino* eruption-related caldera collapse (Cioni et al., 1999; Sulpizio et al., 2010a and b) or sector collapse (Milia et al., 2009, 2008 and 2007; Rolandi et al., 2004) and the tuff-ring morphology formed in the last phase of this eruption (Cioni et al., 1999), define the boundary between the *Proto-Vesuvius* Synthem and the *Prehistoric-Vesuvius* Synthem. The base of the *Avellino* eruptive sequence is poorly visible inside the mapped area. The *Avellino* deposits can be

defined as a subsynthetic unit due to the underlying presence of a marked paleosoil characterized by a distinctive dark-brown colour and indicative of a climatic and paleo-environmental change (Zanchetta et al., 2013; Figure 4.8).

4.5. Petrographic features

The chemical composition of each unit was determined on representative samples (Figure 4.6) and it is in agreement with the geochemical data presented in literature for lava flows (Belkin et al., 1993) and tephra (Di Renzo et al., 2007; Sulpizio et al., 2005; Arrighi et al., 2001; Cioni et al., 1995; Rosi et al., 1993). The main petrographic characteristics, mineral assemblages of phenocrysts and microlites, vesicularity, and rock colour of all lithostratigraphic units, were reported on Figure 4.10.

Units	clinopyroxene	leucite	plagioclase	olivine	biotite	Fe-Ti oxides	vesicles	rock color *
1944	○ f	● f	○ f	○ f	○ m	● m	○	N6 medium light gray
1895-99	○ f	● m	○ f		○ f	● m	●	N5 medium gray
1872	○ f	● m	● m		○ f	○ f ● m	○	N4 medium dark gray
1867	● f	● m	○ m		○ f	● m	●	N6 medium light gray
1861	○ f ● m	○ f ● m	● m	○ m	○ f ○ m	● m	○	N4 medium dark gray
1858	○ f	● f	● f	○ f		○ m	○	N3 dark gray
1847	○ f	○ f ● m	● m		○ f	● m	○	N4 medium dark gray
1822	● f	○ f ● m	● m		● f	● m	○	N5 medium gray
1806	○ f ● m	○ f ● m	● m	○ m		● m	○	N5 medium gray
1805	○ f ● m	○ f ● m	● m	○ m		● m	●	N5 medium gray
1804	○ f ● m	○ f ● m	● m	○ m	○ f ● m	● m	○	N5 medium gray
1794	○ f	○ f ● m	● m	○ f	○ f	○ m	○	N4 medium dark gray
1767	○ f	○ f ● m	● m		○ f	○ m	○	N5 medium gray
1737	● f	○ m	● m	○ f	○ f	● m	●	N5 medium gray
1717	● f	○ f ○ m	● m	○ f		● m	○	N5 medium gray
1698	○ f ● m	○ f ● m	● m	○ f ○ m		● m	○	N5 medium gray
1697	● f	○ f ● m	● m		○ f	● m	●	N5 medium gray
1694	○ f	○ f ● m	● m	○ f		● m	●	N4 medium dark gray
mpg	● f	○ f ● m	● m	○ f ○ m	○ f ○ m	● m	○	N5 medium gray
cum	○ f ● m	○ f ● m	○ m			● m	●	N4 medium dark gray
tir	○ f ● m	○ f ○ m	● m			○ m	○	N4 medium dark gray
vin 1	○ f ○ m	○ f ● m	○ m	○ f	○ f ● m	● m	○	N4 medium dark gray
vin 2	○ f ○ m	○ f ● m	● m			● m	○	N4 medium dark gray
tbs	○ f ○ m	● f ○ m	○ m	○ f ○ m	● m	● m	○	N6 medium light gray
cal	● f ● m	○ f ● m	● m	○ f ○ m	○ m	● m	○	N5 medium gray
gra	● f ● m	○ f ● m	○ m	○ f	○ f ○ m	● m	○	N4 medium dark gray
bel	○ f ○ m	● m	○ m		○ m	● m	○	N5 medium gray
sca	○ f ● m	○ f ● m	○ m	○ f ○ m		● m	○	N4 medium dark gray
fav	○ f ● m	○ f ● m	○ m	○ m		● m	○	N6 medium light gray
tro	○ f ● m	○ f ● m	● m			● m	●	N6 medium light gray
mor	○ f ○ m	○ f ● m	○ m	○ f ○ m	○ f	● m	●	N4 medium dark gray

abundances: ○ rare ○ poor ● abundant ● very abundant

* codes refer to Munsell rock-color chart (2011)

f = phenocrystals

m = microlites

Fig. 4.10: The mineral assemblage and semi-quantitative occurrence of the mapped lava flows.

4.6. Morphological and volcano-tectonic elements

Morphological elements (such as alignments of eruptive vents, drainage irregularities, fault steps, shoreline morphology) were collected in the field and used as kinematic indicators of structural pattern inside the mapped area. Eccentric vents opened during the Modern-Vesuvius period (1858, 1861, 1794) are related to a N070° and a N040°-N050° fracture trend (Figure 4.11).

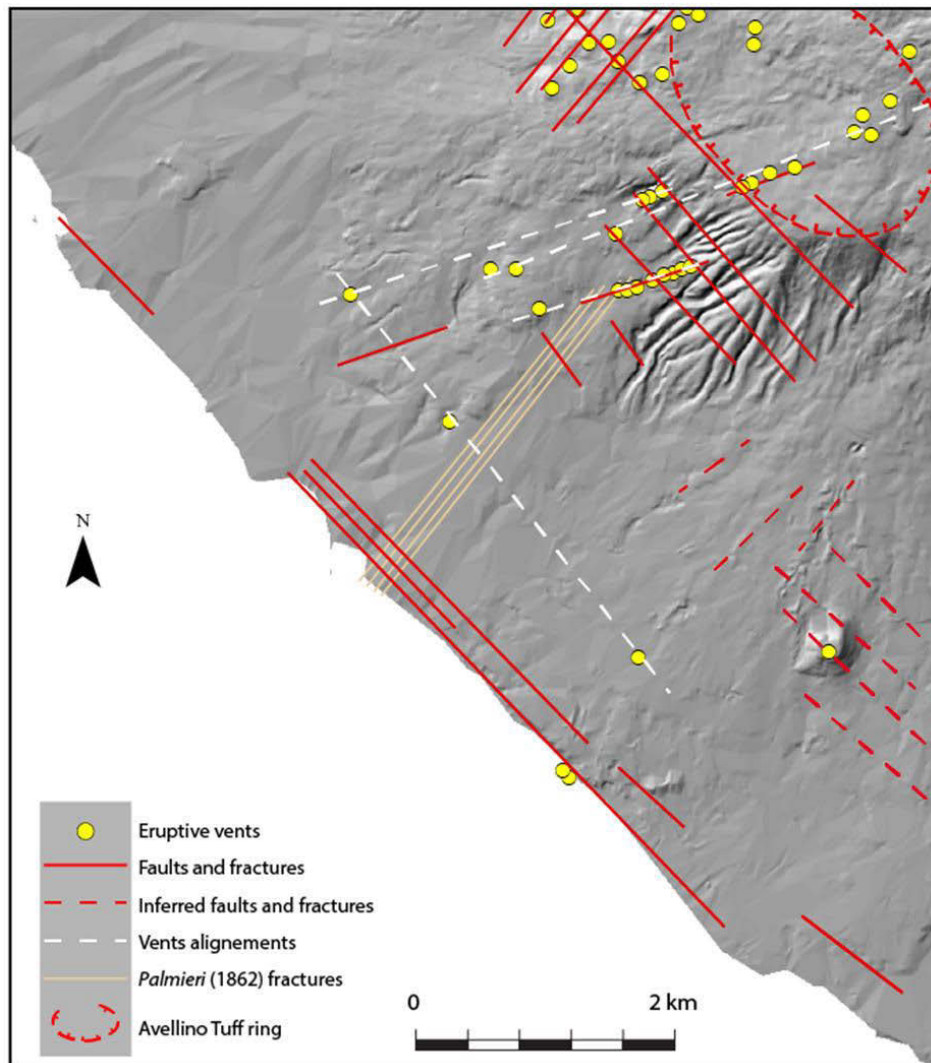


Fig. 4.11: Volcano Tectonic Sketch Map (modified from Principe et al., 2010).
The shaded relief of the DTM is inferred from Tarquini et al. (2007).

Eleven vents aligned on the N070° oriented eruptive fissure opened on December 8th, 1861, during the last eccentric eruption occurred in this sector of the volcano. The 1861 lava flow emission was also followed by the opening of an impressive trend of N040°-N050° oriented fractures that start at high elevations and extend into the sea, causing the destruction of the town of *Torre del Greco* (Palmieri, 1862; Figure 4.12). Medieval lava flow vents are instead aligned along a N320° trend (Figure 4.11).



Figure 4.12: (a) Eleven vents aligned on the N070° oriented eruptive fissure opened on December 8th, 1861, giving origin to a short lava flow (photograph from Palmieri, 1862). Nowadays, buildings covered this portion of the territory and most vents structures are no more recognizable in the field. (b) Maps produced by Palmieri (1862) showing the N040°-N050° oriented fractures that in 1861 extended, from the end of the N070° oriented eruptive fracture, into the sea.

4.7. Discussion and Conclusion

Arrighi et al. (2001) is based on a highly integrated approach, using data collected from different sources (archaeological, historical, toponymy) and different methodologies (archaeometric, petrochemical), combined with detailed fieldwork. This *holistic* methodology enabled us to describe the territory in extremely high detail, while maintaining a connection with the old cartography, which can be compared using a large number of control points (churches, buildings, road's crossings, etc.).

Combining the lithostratigraphy and the Unconformity Bounded Stratigraphic Units (UBSU), recognizing unconformity surfaces within the volcanic successions, allowed us to group 36 lithostratigraphic units into just 5 Synthems.

The UBSU subdivision has been compared with the formations listed in Santacroce and Sbrana (2003) map (Figure 4.5). There is a good correspondence between our Synthematic units (Synthems and Subsynthems) and the lithostratigraphic subdivision established by Santacroce and Sbrana (2003) on the basis of the whole Somma-Vesuvius stratigraphy and mapping. This strengthens the validity of our approach and shows that mapping only real and objective units and elements, such as lava and pyroclastic flow units and discontinuities, allows to produce an effective and accurate map, despite the short stratigraphic interval somewhat limited area covered (about 30% of the Somma-Vesuvius volcanic area).

The term lithosome is generally described as applicable to masses of rock of essentially uniform character and having interchanging relationships with adjacent masses of different lithology (Bates and Jackson, 1987). Lithosomes in volcanic environments have been more recently intended as volcanic centres that exhibit some remaining geomorphic expression (Pasquarè et al., 1992). This definition was difficult to apply at the scale of this map in which the only units that can be identified as a lithosomes are the *Camaldoli della Torre* scoria cone (Figure 4.9) and the *Avellino* tuff ring, both not poligenetic volcanic centres *sensu* Pasquarè et al. (1992).

The chemistry of the lava flows of Vesuvius is quite homogeneous (Figure 4.6), nevertheless it is possible to distinguish the different units in the field on the basis of their colour, blistering and abundance of phenocrysts (Figure 4.10). Indeed the paragenesis was often helpful to solve some problems of attribution, even when affected by important variations in the body of the same lava flow like flotation in the conduit (Principe, 1979).

Software

All the data collected during the fieldwork have been imported, managed and processed using ESRI ArcGIS™, compiling a geo-referenced database, based on vector objects organized in shape-files and using raster data as support.

Supplementary Materials

Volcanological map of the south-western sector of the Vesuvius volcano, Italy.



CHAPTER 5

STUDY ON THE MEDIEVAL ERUPTIVE ACTIVITY OF THE SOMMA-VESUVIUS VOLCANO BASED ON THE ANALYSIS OF TEPHRA FALLOUT DEPOSITS

(In progress)

Abstract

The medieval activity of Vesuvius was investigated on the basis of historical chronicles, field surveys, tephrostratigraphic sequences and chemical analyses.

The products of the AD 1139 eruption of Vesuvius have a phono-tephritic composition, which represents a less evolved magma compared to the two small-scale Plinian eruptions of AD 472 and AD 1631.

The interplinian activity can be triggered by regular influxes of new basaltic magma into a shallow system, stopping its differentiation.

Keywords

Somma-Vesuvius, Medieval activity, AD 1139 eruption

5.1. Introduction

The eruptive history of the last 2000 years of Somma-Vesuvius is characterized by a large variation in eruptive styles, with plinian and interplinian activity, the second one developed, mostly, in the last 3500 years and characterized, essentially, by small-scale effusive-explosive eruptions.

The existence of a medieval eruptions cycle was suggested by historical chronicles, but only scantily described in the scientific literature. Only the careful examination of the stratigraphy confirmed the existence of this important phase in the eruptive history of the volcanic complex. The details of the medieval history of the volcano, much less understood due to the scarcity of outcrops often obliterated by

“crazy” urbanization, can be ascertained using historical records, which are indeed highly useful in constraining the timing of the main events, but often too scarce and imprecise to allow determination of all the phases of activity, of their magnitude and to locate all the types of deposits.

The medieval period, characterized by Strombolian eruptions, is bracketed by the two eruptions of AD 472 and AD 1631, called *Piroclastiti di San Pietro* (Santacroce and Sbrana, 2003), which are taken as benchmarks due to their occurrence in all the stratigraphic successions of the Vesuvian area. Their areal dispersion, mineralogical composition and stratigraphy are well described in the literature, allowing comparisons with our field data and precise identification of the largest and final medieval eruption, the AD 1139, stratigraphically located immediately under the AD 1631 small Plinian eruption, in the south-western sector of Vesuvius.

The eastern side of Somma-Vesuvius is covered by poorly studied interplinian pyroclastic successions, made up of tephra products of different eruptions and generally separated by interbedded charcoal-rich paleosoils.

Correlations of sections, reconstruction of dispersion maps, grain-size and component analysis and glass chemical analysis provided important volcanological information regarding this poorly investigated phase of the medieval activity.

5.2. Medieval History of Vesuvius: From VI to XVII century

In European history, the Middle Ages is the time included between the V and the XV century. It begins with the fall of the Western Roman Empire (AD 476) until 1492, year of the America’s discovery. During this lapse of time, two important eruptions occurred in the eruptive history of Vesuvius: AD 472 sub-Plinian eruption (Sulpizio et al., 2007, 2005; Rolandi et al., 2004; Arnò et al., 1987; Rosi and Santacroce, 1983) and AD 1631 small-scale Plinian eruption (Rosi et al., 1993). This period is called Medieval Activity of Vesuvius (Rolandi et al., 1998).

Although the activity of Vesuvius after the AD 1631 eruption is well acknowledged in the literature with a large amount of published documentation, in comparison, its medieval history is much less understood and with chronological contradictions, both effusive and explosive activity, due to the lack and incompleteness of the historical chronicles and sources. Furthermore, also the number of the truly primary sources (contemporary or nearly the happenings) to the described events is smaller. As already noted by Stothers and Rampino (1983), such differences in the number of sources and eruptions are due to second-hand accounts which were uncritically reported in the literature.

Monks and friars were the main chroniclers during this period, however they described only eruptive events relevant to religious hagiography and politic occurrences. Nevertheless they provided useful records and even some details of the type of volcanic activity. A caveat to keep in mind when reviewing their chronicles is that they usually recorded the beginning and end of a particular volcanic event in

correspondence of the particular historical occurrence of their interest, so altering the actual chronology. An accurate work by [Alfano \(1923\)](#), revised by [Moscarella \(1973\)](#), contains a first selection of verified, unverified and incorrectly dated eruptive events. [Principe \(2003\)](#) provided a summary of the medieval activity of Vesuvius between AD 79 and AD 1631, deduced from critical reading of the original sources proposed by historical chronicles.

Following the AD 472 eruption, the Vesuvius was characterized by a semi-persistent explosive and effusive activity, spanning from the VI to the XII century, which began with an intra-calderic Strombolian activity, and was later interspersed with violent Strombolian activity and lateral and central effusive activity, in particular during the X and XI century.

The 1006-1007 and AD 1139 eruptions were, apparently, exclusively explosive, but, since they were described by authors living outside the Vesuvius area, in the absence of great damages to inhabited areas, the emission of lavas during these eruptions remains possible ([Principe, 2003](#)).

Historical accounts describe a number of parasitic cones, which by age and position may represent the vents of some lavas emitted between AD 79 and AD 1631. These include the *Viulo* and *Fossamonaca* cones, which are still well visible today, two cones at *Tironi* and three cones at *I Monticelli* (“little hills”).

On the basis of the available historical reports, it seems probable that from the early 12th century to AD 1631, the volcano was in a state of repose, marked only by intermittent fumarolic activity.

5.2.1. VI century

The AD 512 eruption, named in some documents the “great eruption of AD 512”, constitutes an example of the problems we have to face when examining potentially misleading historical reports. The timing of this eruption was established by [Alfano \(1924\)](#), on the basis of the report of a tax-free year granted to his subjects by the King Teodorico. In reality the report was referring to a royal edict granting relief to royal subjects who were still suffering from the effects of a devastating eruption occurred in AD 472.

Procopio from *Cesarea* (*De Bello Gotico*, Liber II, Cap IV, and Liber IV, Cap XXXV), *Giovanni* from *Efeso* (*Ecclesiastical History*) and other authors in the western Mediterranean reported the darkening of the sky over Constantinople for many months, accompanied by an unusually harsh winter in *Mesopotamia* in the AD 536. So, an explosive eruption must have occurred around this year ([Stothers and Rampino, 1983](#)).

5.2.2. VII century

During the VII century, the AD 685 eruption was well documented by *Paolo Diacono* (*Historia Longobardorum*, Liber VI, Cap IX) and by *Giorgio Agricola* (*De re metallica. De natura eorum quae effluent ex terra*, Liber IV). In the *Liber Pontificalis* (I, pp. 363-364), published one century later by *Paolo Diacono*, the eruption is dated to the time of Benedict II’s papacy (June 684-May 685), before Easter, in that year, fallen on March 26th. So, this eruption occurred between February and March, after earthquakes like

precursor and lasted a few days. It was a strong explosive eruption, characterized by a Plinian column with related fallout, big amounts of ashes and pyroclastic flows due to the collapse of it, until the sea. The popular tradition tells of a lava underlying the old *Palazzo Baronale* of *Torre del Greco*, originated own from this event but not crop out anymore at present. In fact, the analysis of the historical sources does not clarify whether this eruption also involved lavas ([Principe, 2003](#)).

5.2.3. VIII century

Between the autumn and the winter of the AD 787, *Gregorio Monaco*, in his manuscript in greek (University of Messina Library) told a violent Strombolian eruption, with lava fountains and lava flows (or, maybe, pyroclastic flows, it is no clear) “six miles long”.

5.2.4. X-XI centuries

During these centuries, Vesuvius had the most intensive effusive eruptive activity. In fact, many popular histories were born to explain its behaviour.

Damianus Petrus (*Opera Omnia, Opusculum XIX*) told an eruption with lavas into the sea in AD 968.

Pompeo Sarnelli (*Cronologia dei Vescovi et Arcivescovi Sipontini*) described an explosive eruption in AD 991 with earthquake (“... erupting flames and vomiting ashes...”).

The AD 999 eruption was explained by *Damianus Petrus* (*Opera Omnia, Opusculum XIX*) and *Ubaldo Monaco* (*Chronicum Ducum Neapolis*). They told sudden lava fountains and lava emission (“... piceas atque sulphurea repente flammis erumpere...”) and fine ashes.

Ridolfo Glaber (*Historia Francorum*) wrote of least explosive eruption, with many earthquakes and unbreathable gas (sulphur) emissions, vigorous throwing of blocks (3 miles from the crater) and, in 1006 or 1007.

Finally, *Anonymus Cassinensis* (*Chronicon*), *Anonymus Cavensis* and *Romoaldo Salernitano*, described an eruption with lavas into the sea (“... eructavit incendium, ita ut usque ad mare discurreret...”), occurred in January or February, 27th, 1037.

5.2.5. XII century

Several historical sources describe the AD 1139 eruption, reporting details that typically suggest a Strombolian type, with wide lava flows that reached the sea. In his *Chronicon*, the *Anonimus Cassinensis* recounts of an eruption occurred in 1130, which lasted 40 days. Another eruption is reported in the *Chronicon* of *Falcone Beneventano* and *Romualdo Salernitano*, and dated AD 1139 (on May, 29th). *Giulio Cesare Recupito* ([Recupito, 1633](#)) thought that they were a unique eruption, while *Luigi Palmieri* ([Palmieri, 1887](#)) assumed that they were two paroxysmal phases of the same eruption.

Many modern authors consider this event the last of the Vesuvian medieval eruptive period, which started with the AD 472 eruption.

5.3. Samples studied and Analytical Methods

5.3.1. *Tephra fallout deposits*

Volcanic products (lava flows, ash flows, ash layers and tuffs) can be excellent stratigraphic markers and often provide both correlated and direct numerical age constraints for associated deposits. Volcanic eruptions are usually brief events, and volcanic materials produced by such eruptions are commonly emplaced within a short time after eruption, often within a few hours or days.

Volcanic ash layers (also known as tephra layers) may cover large areas and, consequently, are among the most useful of the volcanic materials for chronostratigraphic correlations.

Tephra is the term used for all pyroclastic materials that are erupted from a volcanic vent, and travel at least in part through the air or with the assistance of volcanic gases ([Thorarinsson, 1974](#)).

The ability to recognize tephra from specific eruptions in the stratigraphic record enable correlation of stratigraphic sequences over wide areas, and, in many cases, allows assignment of numerical ages.

Tephra consist of three main components: 1) volcanic glass, which was part of the molten magma but was quenched rapidly into a supercooled liquid during eruption; 2) lithic fragments, or pieces of pre-existing rocks that became incorporated into tephra during eruption, transport or deposition; and 3) mineral crystals or crystal fragments, which formed in the magma prior to the eruption.

Volcanic glass and mineral crystals or crystal fragments are considered to be juvenile, or comagmatic components of the tephra, and provide the essential physical and chemical characteristics by which tephra layers can be identified and distinguished. Lithic fragments and some of the mineral grains are accidental, if they are from older rocks that formed the walls of the magma chamber or the volcanic vent, and detrital if they were incorporated from clastic sources during transport or deposition.

Mineral composition of tephra varies primarily with the composition of the parent magma.

Tephra can be identify analysing together characteristics such as colour, texture, stratigraphic context, comagmatic mineral grains present and glass chemistry.

The field and petrographic characteristics of a tephra deposit are sometimes sufficiently diagnostic to allowed correlation.

5.3.2. Vesuvian Tephra fallout samples

In the post AD 472 stratigraphy, [Andronico et al. \(1996a, 1996b, 1995\)](#) identified six main explosive-component eruptions, in contrast, [Rolandi et al. \(1998\)](#) only four main explosive eruptions. The last of these eruptions is represented by a lapilli fallout deposit, which was attributed to the AD 1139 eruption by [Rolandi et al. \(1998\)](#). The description and stratigraphic position of this deposit correspond to the “ochraceous” lapilli fallout beneath the 1631 pyroclastic flow deposits described by [Principe et al. \(1987\)](#).

Scoria fall deposits ascribed to the AD 1139 eruption were reported by [Rolandi et al. \(1998\)](#), describing the deposits in the type section at *Terzigno* and drawing a cumulative isopach map.

In the recent geological map of Vesuvius ([Santacroce and Sbrana, 2003](#)) the AD 1139 deposits were included in the „*San Pietro* Pyroclastic Formation“.

Glasses from 8 samples outcropped on the *Torre del Greco* territory were analysed ([Table 5.1](#); [Figure 5.1](#)). The main purpose was to recognize chemical compositions useful for stratigraphic correlation. Therefore, they were analysed with the EMPA analytical technique.

Samples	Type of deposits	Locality
Tz 3 D 1	Lapilli fallout of reddish scoria (1st level)	Terzigno - Cava Ranieri (witness quarry)
Tz 3 D 2	Lapilli fallout of reddish scoria (2nd level)	Terzigno - Cava Ranieri (witness quarry)
TG 3 C	Lapilli fallout of dark scoria	Torre del Greco - Cantiere di Viale Campania
TO 63 A	Lapilli fallout of dark scoria	Torre del Greco - Monastero degli Zoccolanti
TO 63 B	Lapilli fallout of dark scoria	Torre del Greco - Monastero degli Zoccolanti
TORRE 44	Lapilli fallout of dark scoria with alteration ochre coating	Torre del Greco - Cappella Bianchini
TORRE 46	Lapilli fallout of dark scoria above the 79 A.D. eruption	Torre del Greco - Villa Sora
VALE 3	Lapilli	Terzigno - Cava Pozzelle

Tab. 5.1: Type and location of the outcrops.



Fig. 5.1: Location map of the outcrops (see [Table 5.1](#)).

5.3.3. Electron Microprobe Analysis (EMPA)

Major element mineral analyses were obtained using a CAMECA SX-50 electron microprobe at Virginia Tech. Quantitative analysis of major elements used a 15 kV accelerating potential with a beam current of 20 nA. Quantitative analyses were performed using a combination of natural and synthetic standards, with ZAF-type matrix corrections performed using the PAP protocol (Pouchou and Pichoir, 1984). Mineral formulae were calculated based on the number of oxygen (anhydrous) per formula unit for each mineral.

The juvenile products are Phono-Tephrites (SiO_2 47.46 main wt% and 47.39-47.70 range wt%; $\text{Na}_2\text{O}+\text{K}_2\text{O}$ 8.94 mean wt% and 8.27-9.65 range wt%) according to the classification of Le Bas et al. (1986) (Table 5.2; Figure 5.2).

1139 A.D. Eruption								
	TG 3C	TO 63 A	TO 63 B	TORRE 44	TORRE 46	Tz 3D 1	Tz 3D 2	VALE 3
SiO ₂	47.48	47.67	47.57	47.56	47.39	47.68	47.70	46.64
TiO ₂	1.24	1.23	1.20	1.21	1.25	1.17	1.16	1.24
Al ₂ O ₃	17.43	17.20	16.64	17.88	17.34	17.20	17.17	17.10
FeO	9.16	9.32	9.13	9.15	9.33	9.74	9.26	9.59
MnO	0.20	0.19	0.17	0.20	0.20	0.22	0.18	0.18
MgO	3.86	3.86	4.20	3.35	3.73	3.82	4.16	4.36
CaO	9.33	9.18	9.66	9.17	9.20	9.69	9.98	10.60
Na ₂ O	4.21	4.25	3.97	4.52	4.11	3.57	3.33	3.19
K ₂ O	5.07	4.96	5.36	4.99	5.54	4.70	4.99	4.80
P ₂ O ₅	1.15	1.14	1.17	1.10	0.97	0.92	1.01	1.18
Cr ₂ O ₃	0.01	0.00	0.02	0.01	0.02	0.02	0.01	0.01
F	0.22	0.35	0.32	0.18	0.27	0.42	0.36	0.33
Cl	0.63	0.65	0.59	0.68	0.64	0.86	0.69	0.79
Total	100.00	100.00	100.00	100.00	100.00	100.00	100.00	100.00

Tab. 5.2: Chemical glass analyses.

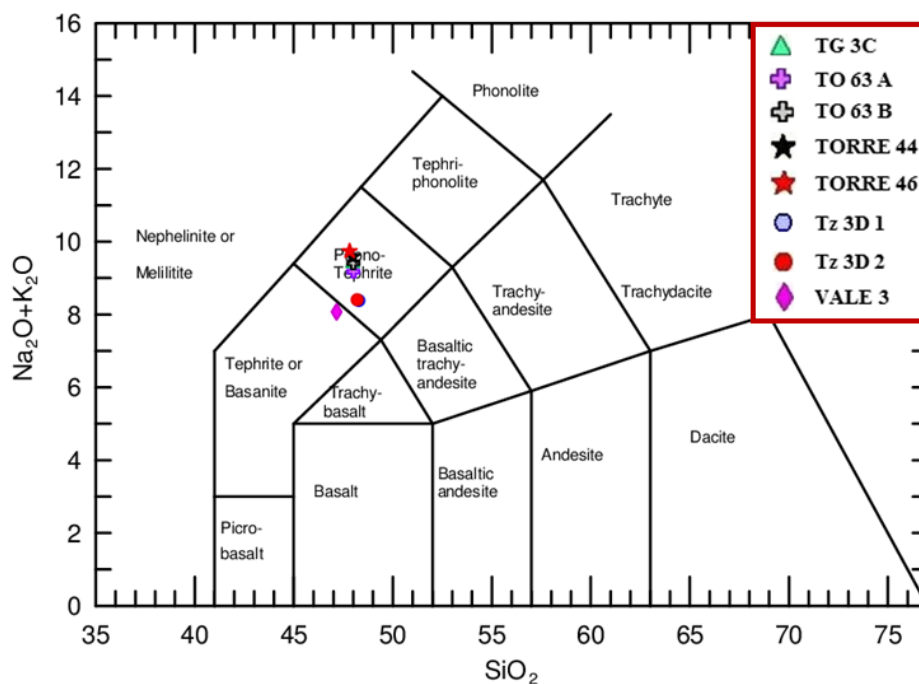


Fig. 5.2: Silica/Total alkali plot (TAS).

An exception is VALE 3. In fact, it belongs to the Tephrite or Basanite sector, with SiO₂ 46,64 wt% and Na₂O+K₂O 7.99 wt%.

Plots of MgO and CaO vs Al₂O₃ define a decreasing trend with increasing Al₂O₃. This is due to crystallization of pyroxene (Figure 5.3a).

Plots of SiO₂ and Al₂O₃ vs K₂O do not show any trend, suggesting no crystallization of K-Feldspar (Figure 5.3b).

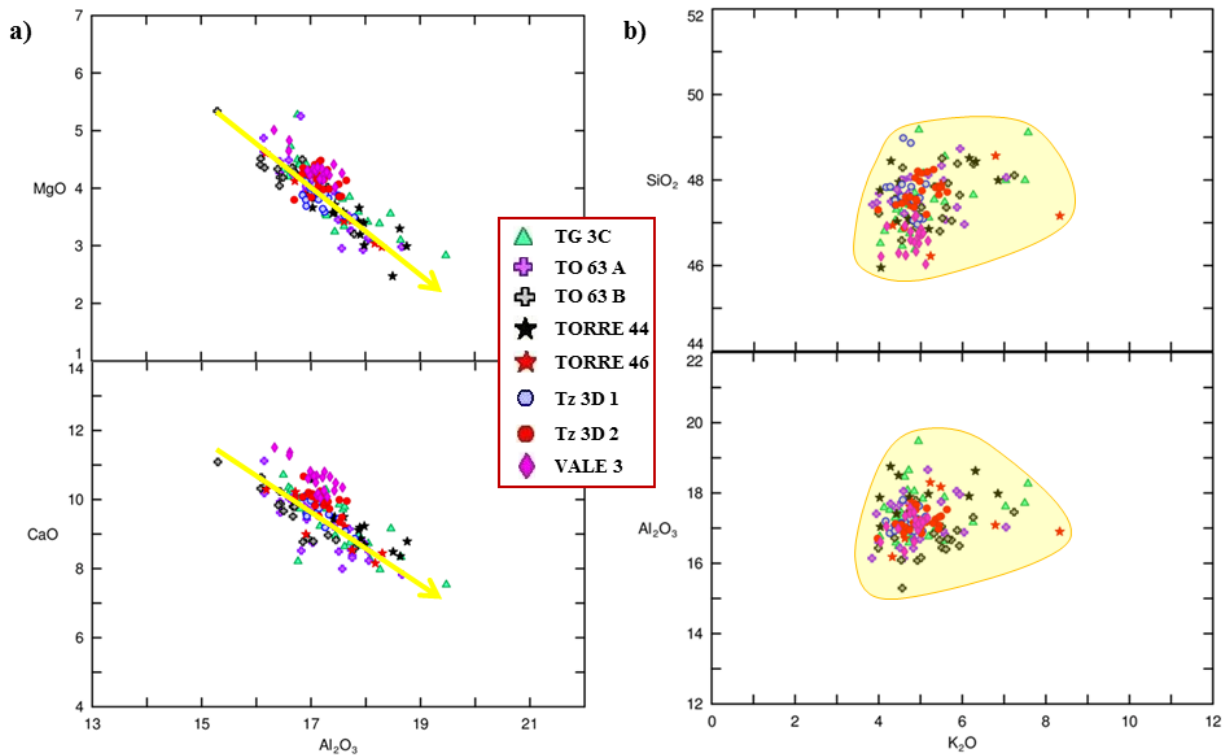


Fig. 5.3: Variation diagrams: (a) MgO and CaO vs Al₂O₃; (b) SiO₂ and Al₂O₃ vs K₂O.

5.4. Discussion and Conclusions

The chemical analyses on the AD 1139 medieval eruption samples show a less evolved tephritic composition compared to the two small-scale Plinian eruptions of AD 472 and AD 1631, which are considered as stratigraphic markers.

Periodic influxes of deep-seated tephritic magma (Belkin et al., 1985; Cortini et al., 1985; Cortini and Scandone, 1982; Hermes and Cornell, 1981), into a shallow magma system (Barberi and Leoni, 1980) tend to mix with differentiated magma causing the Plinian eruption (Sparks et al., 1977).

After the opening of the system, a new basaltic magma batch injected with appropriate frequency may stop differentiation and trigger an interplinian activity.

Due to the greater viscosity of phono-tephritic magma, the magmatic system will close, precluding the onset of interplinian eruptions. The periodic arrival of hot deep basic magma, followed by differentiation, continues during the repose period setting the stage for new interplinian eruptions.



CHAPTER 6

VOLCANICLASTIC FLOW HAZARD IN DENSELY POPULATED VOLCANIC AREAS: THE CASE OF *TORRE DEL GRECO* MUNICIPALITY (THE SOMMA-VESUVIUS VOLCANO, ITALY)

(Submitted to *Geoscience Journal*)

Abstract

The fieldwork allowed to collect useful data for the assessment of the hazard connected to the Volcaniclastic Flows events, documented by historical chronicles too.

This study uses a GIS-based methodological approach to integrate and combine information deriving from different sources: *i*) historical chronicles and local reports (20th century); *ii*) scientific literature about the recent activity of Somma-Vesuvius (AD 1631-1944); *iii*) rainfall data (20th century) and *iv*) morphological and morphometric analysis obtained by the Digital Elevation Model (DEM). The final result is the precise identification of the source areas of the volcaniclastic flows and of the physical and morphological parameters that control their triggering.

The historical analysis of the spatial and temporal distribution of the volcaniclastic flows recorded in the Vesuvian area during the 20th - 21st centuries (1906-2010) indicates that the most affected area is the south-western sector of Somma-Vesuvius and, in particular, the *Torre del Greco* municipality.

We also examined the relationships between the fallout deposits of the main recent eruptions of Somma-Vesuvius and the historical volcaniclastic flows of *Torre del Greco*. Results indicate that a funnel-shaped area, located immediately to south-west of the Somma-Vesuvius caldera boundary, could be the source for the volcaniclastic flows found in *Torre del Greco* municipality, probably remobilizing pyroclastic materials derived, mainly, from the 1822 eruption.

The methodology adopted can be applied in volcanic zones with morphological features similar to the Somma-Vesuvius area, in in sin-eruptive conditions and during a period of volcanic quiescence, when heavy and/or persistent rains are able to remobilize loose pyroclastic deposits.

While this approach represents only a starting point for studies aimed at the assessment and mitigation of volcaniclastic flow hazard, it proved to be a useful tool for the prevention of volcaniclastic flow hazard.

Keywords

Debris flow hazard, fallout deposit, Vesuvius, Torre del Greco municipality

6.1. Introduction

Volcanic edifices are the most common source of several different mass movements since loose sediments flows are easily triggered by prolonged rainfalls (*lahars*) (Thouret et al., 2007; Capra et al., 2004; Macías et al., 2004; Scott et al., 1995, 1989; Pareschi et al., 2000b; Newhall and Punongbayan, 1996; Pierson, 1995, 1985; Lowe et al., 1986).

These events are usually triggered by intense rains occurring either at the same time or shortly after an explosive eruption. Loose pyroclastic material is turned into volcaniclastic flows (containing about 60-80 vol. % sediment), hyper-concentrated flows (about 60-20 vol. %) or more diluted stream flooding (less than 20 vol. % sediment) (Smith, 1986).

The period of flooding hazard may outlast the eruption by years or even decades (Major, 2000; Nehwell and Punongbayan, 1996), depending on climate and the time needed to restore the original soil condition and vegetation cover (Sulpizio et al., 2006; Zanchetta et al., 2004b).

The main concern is the high destructive potential of volcaniclastic flows (Zanchetta et al., 2004a). In areas with recurrent volcanic activity, often characterized by mild to moderate explosive activity and by periods of quiescence of the order of years to decades, it is difficult to define the main factors driving the recurrence of volcaniclastic flows. An important factor influencing the initiation of volcaniclastic flows is surely the amount of rainfall, but the recurrence of volcanic activity and the morphology of drainage basins have relevance in producing favourable conditions for volcaniclastic flow generation.

The area at the foot of the Somma-Vesuvius volcano (Southern Italy) is affected by recurrent volcaniclastic flow events (Bisson et al., 2007b). It is a very vulnerable area due to its chaotic urban development after World War II. The rapid growth of municipalities (from 1400 inhabitants per km² in the 1944 to ~ 2500 inhabitants per km² in 2009; ISTAT, 2009), benefited from a long period of volcanic quiescence (the last eruption occurred in 1944). Volcaniclastic flows generation, however, did not cease during the period of volcanic rest, and still represents a high hazard in case of renewal of activity at Somma-Vesuvius.

Taking into account this possibility and with the aim of mitigating volcanic hazard, the scientific community, in collaboration with the Italian Civil Protection Agency, has hypothesized different volcanic

scenarios (Cioni et al., 2008) with different probabilities of occurrence (Neri et al., 2008). Three main different hazard zones have been distinguished: *i*) a Red Zone affected by invasions of Pyroclastic Density Currents (covering an area of roughly 10 km of radius from the present crater), *ii*) a Yellow Zone potentially affected by pyroclastic fallout deposits (located mostly toward the eastern areas of Somma-Vesuvius, i.e. those downwind of the present-day prevailing wind directions), and *iii*) a Blue Zone highly exposed to the flooding risk (coincident with the catchment's area of the *Acerra-Nola* Plain to the north and north-east of Somma-Vesuvius) (Figure 6.1).

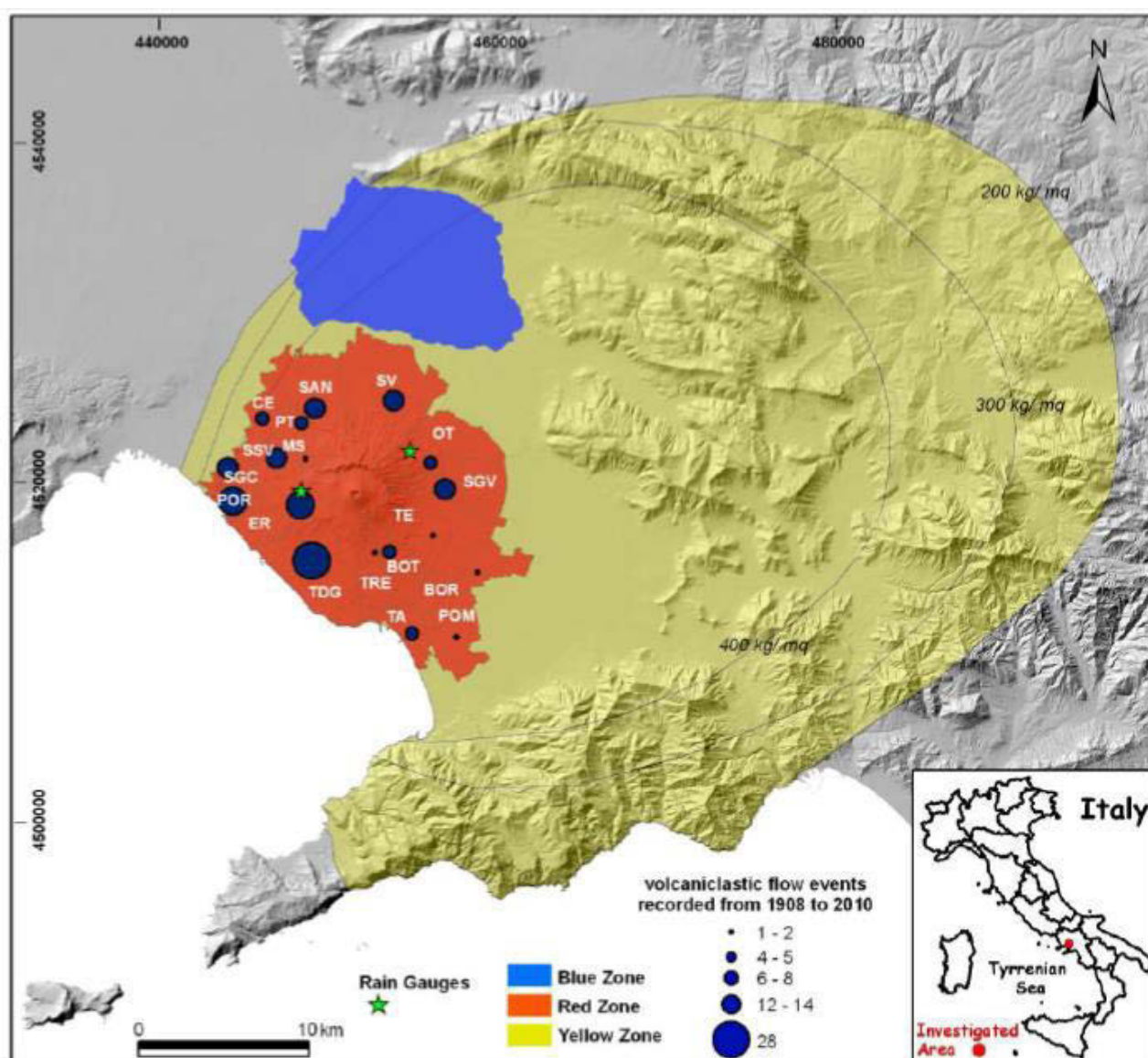


Fig. 6.1: Location Map of the study area. The x and y coordinates are expressed in meters (ED 50-652 UTM-Zone 33 Reference Cartographic System). The grey lines in the yellow zone indicate the load of fall out deposits (400, 300, 200 kg/m²) resulting from the simulated volcanic scenario (Cioni et al., 2002). Follow the acronyms used for municipalities of the Red Zone: *Somma Vesuviana* (SM), *Sant'Anastasia* (SAN), *Pollena Trocchia* (PT), *Cercola* (CE), *Ottaviano* (OT), *Massa di Somma* (MS), *San Giuseppe Vesuviano* (SGV). *San Sebastiano al Vesuvio* (SSV), *San Giorgio a Cremano* (SGC), *Ercolano* (ER), *Terzigno* (TE), *Portici* (POR), *Trecase* (TRE), *Torre del Greco* (TDG), *Boscotrecase* (BOT), *Boscoreale* (BOR), *Pompei* (POM), *Torre Annunziata* (TA).

All of these zones are characterized by a high degree of population density. In particular, the Red Zone hosts more than 600,000 inhabitants and presently comprises 25 municipalities (DPC, 2014) with

respect to the older version, which enclosed only the 18 circum-vesuvian municipalities (DPC, 1995). Due to availability and completeness of data, this work focuses on this latter group characterized by an average population density (ISTAT, 2011), which, systematically, increased from 1941 reaching a mean value of 2,500 inh/km² and peaks greater than 11,000 inh/km² in some municipalities as *Portici* and *San Giorgio a Cremano* (Figure 6.2).

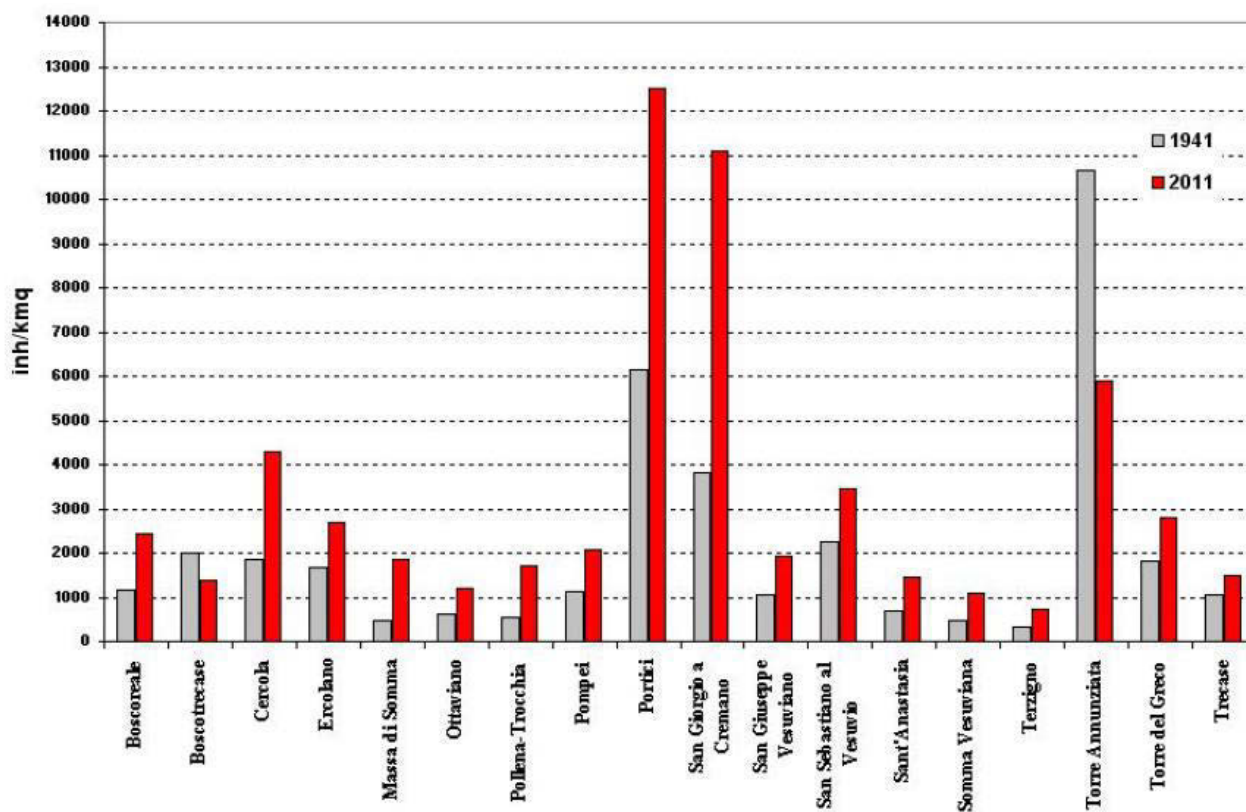


Fig. 6.2: Population density (inh/km²) from 1941 to 2009 for each municipality of the Red Zone.

6.2. Recent historical activity of Vesuvius

Due to the high risk for the population and its long historic record, Somma-Vesuvius is one of the world's most studied volcanoes. It is situated along the western side of the Campanian Plain and is bordered by Mesozoic platform carbonates forming the basement dissected by a Plio-Pleistocene NE-SW and NW-SE trending regional fault system, related to the opening of the Tyrrhenian basin (Patacca and Scandone, 1989). Somma-Vesuvius is a moderate size (1281 m a.s.l.) stratovolcano consisting of an older edifice with a summit caldera, Monte Somma, and a recent cone, Vesuvius, developed within the caldera after the AD 472 eruption (Rolandi et al., 1998).

The recent volcanic history of Vesuvius consists of about three century-long periods of semi-persistent activity, alternating effusive eruptions with mild to violent Strombolian explosions events. It began with the AD 1631 eruption and ended with the 1944 event.

The AD 1631 eruption is the strongest and most destructive of the 17th century and is classified as a small-scale Plinian eruption, characterized by a fallout dispersion axis towards east (Rosi et al., 1993). The different phases of this eruption are described by Rosi et al. (1993) and Rolandi et al. (1993c) on the basis of historical and stratigraphic data.

In the 18th century the main volcanic events are represented by the 1707, 1717, 1737, 1760, 1767, 1779, and 1794 eruptions. Except the first one characterized, mainly, by explosive activity (fall out deposit, volcanic ash and pyroclastic material), the others have been defined as mixed eruptions because emitted explosive products (Strombolian fountains) alternated to lava flows originated, often, from fractures opened on the southern flank of the volcano (Arrighi et al., 2001).

The municipalities more frequently involved by lava flows are located in the eastern sector of Vesuvius (*Boscotrecase* and *Ottaviano*, in particular), with the exception of *Torre del Greco* that was completely destroyed by the lava flow of 1794. In fact, a vent opened along the western fracture of *Montedoro*, between 320 and 480 meters of altitude, generated lava that flowed towards the centre of the city reaching and entering in the sea, for about 100 m (Nazzaro, 1997).

The strongest volcanic event of the 19th century is the sub-Plinian 1822 eruption, with a Phreatomagmatic phase and a south-east dispersion axis (Arrighi et al., 2001). After 12 years, the volcano activity started again in the western and eastern sectors, with ten effusive events (1834, 1855, 1861, 1868 and 1891-1894) alternated to mixed eruptions (1839, 1850, 1872, 1895), with the opening of several fractures and eruptive vents opened. A major eruptive mouth formed between 218 and 300 meters of altitude along the western fracture of *Montedoro*, in *Torre del Greco* municipality, during the 1861 eruption.

The 20th century is marked by two important eruptions (1906 and 1944) separated by weak Strombolian activity, dated 1929, 1932, 1938 and 1941 (Arrighi et al., 2001). The 1906 event, considered the most violent eruption of 20th century, is classified as violent Strombolian with north-east dispersion axis (Arrighi et al., 2001). It was described as polyphase strong eruption characterized by lava fountains, steady column phase, strong ash and lapilli emission (Arrighi et al., 2001). The municipalities more affected by pyroclastic deposits were *Ottaviano*, *Somma Vesuviana* and *San Giuseppe Vesuviano*, whereas the lava flows interested, mainly, *Boscotrecase* and *Torre Annunziata* localities. The volcanic activity in this century ended with the 1944 sub-Plinian eruption.

At present the Vesuvius is considered to be in a quiescent phase.

6.3. Material and Methods

In order to provide a useful contribution to mitigate and prevent volcaniclastic flow hazard in the Vesuvian area, the study has been divided in three steps: 1) a spatial and temporal analysis of volcaniclastic flows recorded during the last 100 years (from 1906 - to 2010), combined with the available precipitation data for the investigated temporal interval; 2) a detailed morphological study of the municipality most affected by historical flows; 3) the comparison of the spatial distribution of historical flows with that of fallout deposits deriving from the recent eruptions of Somma-Vesuvius (from AD 1631 to 1944), to investigate possible correlations between the age of fallout deposits and the occurrence of historical flows.

An accurate classification of all available information on historical volcaniclastic flows preceded these steps. First information was collected, recompiled and checked to avoid inconsistencies and repetition. Then we created a geo-referenced database of the volcaniclastic flows occurred in the 18 municipalities of the Red Zone during the last 100 years (from 1906 to 2010). In particular, on the basis of historical daily chronicles (newspapers and local historical reports) and previous works (Alessio et al., 2012; Vallario, 2004), 116 volcaniclastic flow events were identified and the related data were organized in a point vector layer. Since we do not know the exact location of all volcaniclastic flows occurred in the municipalities (more specific information about volcaniclastic flows only exist for *Torre del Greco*), each point in the vector layer identifies the barycentre of the polygon representing the administrative boundary of each municipality affected by historical flows and defines the number of events recorded in it.

116 volcaniclastic flow events were classified according to the municipality in which they occurred, the date of occurrence and, when available, the cumulative rainfall at the time of occurrence. This last information is available only for the events occurred from 1921 to 1985 (Table 6.1a). In addition, cumulative monthly rainfall for each year affected by volcaniclastic flow is organized in Table 6.1b. The rainfalls data come from Ricciardi et al. (2007) and the Servizio Idrografico e Mareografico Nazionale (SIMN, 2004).

Day	Years																			
	1921 October	1955 February	1956 January	1957 January	1959 September	1961 July	1961 November	1962 June	1963 May	1965 January	1966 April	1966 June	1969 September	1970 October	1971 January	1976 October	1979 October	1982 December	1985 October	1985 November
1	-	-	31,5	-	-	-	-	1,3	-	-	-	-	-	54,0	5,7	-	-	36,0	-	54,0
2	-	22,8	5,9	-	3,8	-	3,3	1,2	11,6	-	-	-	-	-	49	-	7,0	16,0	-	27,2
3	-	4,5	8,6	-	88,0	3,1	6,0	-	-	0,6	0,6	-	-	-	4,5	-	-	3,0	-	3,8
4	-	6,3	-	-	-	-	9,3	-	-	4,8	-	-	-	-	-	-	-	-	-	7,0
5	-	-	-	-	22,5	-	13,4	-	-	-	-	-	-	-	-	15,3	-	-	-	4,8
6	-	-	-	-	3,2	-	35,3	-	-	-	-	-	8,8	-	-	4,7	14,0	-	-	12,8
7	-	35,9	-	-	-	-	6,3	-	-	-	-	-	2,6	-	-	-	-	-	-	0,2
8	-	1,6	0,5	-	-	-	14,2	-	-	-	-	-	-	-	-	-	-	2,0	-	-
9	-	-	7,3	-	-	12,8	-	3,4	-	-	-	-	-	-	-	-	-	7,0	-	-
10	-	0,4	-	-	-	-	0,5	-	-	-	-	-	-	-	-	-	-	-	-	-
11	-	-	1,3	-	-	-	-	0,3	-	-	8,0	-	8,8	-	-	-	5,0	-	-	9,0
12	-	-	-	7,2	-	-	1,2	4,9	-	3,0	-	5,6	-	-	-	-	22,0	10,0	-	-
13	-	-	-	-	-	51,8	-	10,1	1,2	-	-	-	-	-	-	44,3	20,0	56,0	-	-
14	-	15,8	-	13,9	-	-	8,8	1,9	13,2	-	-	-	0,2	-	-	7,6	-	12,0	-	-
15	-	-	-	17,4	-	-	5	8,5	8,4	-	3,0	2,0	-	-	-	-	2,0	-	-	-
16	-	4,5	-	36,8	-	-	1,7	26,3	13,6	-	6,4	1,0	-	-	-	8,6	-	-	-	0,2
17	-	-	-	6,8	-	-	-	8,2	-	-	-	3,5	-	-	-	1,0	-	-	-	129,0
18	-	1,3	-	16,8	4,5	-	-	-	14,6	-	0,2	7,3	-	-	-	1,0	14,0	26,0	-	70,6
19	-	4,9	5,3	0,2	-	8,4	1,3	-	0,6	-	-	56,3	-	-	-	-	4,0	-	-	6,0
20	-	2,5	-	-	-	-	-	-	0,8	-	-	42,0	11,6	-	-	8,3	-	7,0	-	35,8
21	-	5,0	-	-	-	-	-	-	18,6	3,0	-	-	-	-	-	-	-	2,0	-	6,8
22	-	4,7	7,6	-	-	-	-	-	5,6	-	-	-	26,1	13,7	-	-	-	15,0	7,8	9,8
23	3,0	-	0,2	11,8	-	-	-	-	-	-	-	-	9,9	0,2	-	-	-	19,0	3,2	1,6
24	3,0	3,0	-	8,3	-	-	-	-	-	-	-	-	-	-	-	-	-	6,0	2,0	-
25	120,8	4,0	13,3	6,6	0,4	-	10,2	-	-	-	-	-	-	-	-	-	-	-	-	-
26	8,0	-	-	9,6	-	-	-	0,2	-	-	-	-	-	-	-	-	-	-	-	25,8
27	44,0	1,8	-	-	1,9	-	-	0,1	4,6	-	-	-	-	-	-	-	6,0	-	-	0,2
28	22,0	12,0	6,1	-	-	-	-	20,5	-	12,2	-	-	-	-	-	-	106,0	-	1,4	7,6
29	-	-	-	-	-	-	-	2,1	2,2	35,4	-	-	-	-	-	-	-	-	25,2	0,8
30	-	-	5,6	-	-	-	-	5,7	-	4,0	3,2	-	-	-	-	-	18,0	-	9,2	-
31	-	-	8,0	-	-	-	-	-	-	-	-	-	-	-	-	11,0	-	47,0	-	-

Tab. 6.1a: Daily cumulative precipitation (mm) according to the month affected by the events. The grey colour indicates the day of the event and the dash represents absence of rainfall (SIMN, 2004).

YEAR	Month													Oct + Nov
	January	February	March	April	May	June	July	August	September	October	November	December		
1906	83.7	108.0	56.2	n.p.	59.9	39.2	4.8	23.8	52	137.8	87.7	209.2	225.5	
1907	459.6	88.1	39.9	169.5	119.7	84.8	8.5	1.2	41.1	285.9	73.3	266.7	359.2	
1908	123.4	115.9	109	119.5	0.2	3.3	37.2	6.9	3.8	118.2	85.9	119.6	204.1	
1909	46.4	48.8	63.7	20.1	21	9.4	10.7	46.2	67.1	21.4	63.2	104.1	84.6	
1910	33.2	71.9	68.7	83.1	n.a.	n.a.	n.a.	n.a.	n.a.	n.a.	n.a.	n.a.	n.a.	
1911	n.a.	n.a.	n.a.	n.a.	n.a.	n.a.	6.6	22.5	168.7	35.0	61.2	92.1	96.2	
1921	67.2	48.7	53.5	49.0	45.4	87.9	17.8	36.9	48.4	175.1	114.6	28.4	289.7	
1948	118.2	35.4	5.9	80.3	83.3	19.9	50.3	8.9	116.5	128.8	19.5	18.1	148.3	
1950	78.2	105.1	29.0	90.7	23.3	8.2	n.a.	5.1	87.7	140.5	177.3	300.0	317.8	
1954	241.1	185.9	48.2	56.9	81.6	19.8	10.6	9.4	26.9	27.6	50.0	76.7	77.6	
1955	55.5	131.0	98.3	22.2	23.0	24.8	62.8	50.5	124.1	171.5	99.2	95.9	270.7	
1956	101.2	181.6	93.0	63.8	78.5	28.9	0.0	18.0	30.1	148.2	278.8	72.8	427	
1957	135.4	32.5	14.0	43.0	119.2	12.6	30.1	17.4	37.2	151.1	162.9	101.6	314	
1959	135.3	15.0	105.0	122.6	n.a.	30.4	32.9	30.1	124.3	67.5	135.0	293.6	202.5	
1960	155.5	149.2	216.0	81.8	39.0	3.2	25.7	n.a.	207.7	125.9	213.1	281.1	339	
1961	181.7	18.6	44.4	107.7	78.1	55.5	24.3	2.3	0.0	284.4	181.4	85.4	465.8	
1962	87.9	38.7	162.5	41.1	35.2	5.1	10.6	2.4	130.0	64.7	248.3	152.2	313	
1963	140.9	240.7	89.6	59.9	106.0	71.6	n.a.	21.2	67.0	118.5	54.0	134.1	172.5	
1965	103.6	81.4	43.4	141.0	41.0	29.2	1.8	45.6	119.6	9.8	207.4	102.0	217.2	
1966	211.2	88.8	16.8	66.2	71.4	13.4	30.2	42.2	55.4	155.4	216.4	139.6	371.8	
1969	65.3	115.0	208.5	39.7	27.1	38.3	15.6	59.4	175.6	6.1	109.5	282.8	115.6	
1970	222.7	81.6	138.9	39.1	55.5	38.7	3.5	38.2	48.6	82.2	64.6	107.7	146.8	
1971	60.5	72.7	25.0	30.1	64.4	31.0	16.7	3.6	82.4	110.0	201.3	109.0	311.3	
1973	240.6	166.0	78.6	33.6	n.a.	19.8	9.8	65.0	116.4	57.0	27.0	78.0	84	
1976	33.6	15.2	5.0	88.0	102.3	18.0	8.7	18.7	44.3	90.8	10.5	26.6	101.3	
1979	137.0	179.0	68.0	129.0	42.0	69.0	34.0	66.0	70.0	252.0	136.0	136.0	388	
1982	5.0	62.0	76.0	23.0	21.0	7.0	0.0	3.0	114.0	210.0	153.4	230.0	363.4	
1985	180.4	49.6	203.0	23.2	34.0	0.0	0.0	1.2	5.4	112.8	404.0	42.8	516.8	
1991	28.2	71.2	76.2	155.2	49.8	4.4	33.6	6.4	66.6	137.0	275.2	32.4	412.2	
1992	63.6	16.8	33.8	64.2	51.4	118.8	71.8	14.2	77.6	115.0	101.6	59.0	216.6	
1996	63.2	47.2	62.0	33.4	91.8	23.0	14.6	76.0	149.6	182.2	181.8	243.2	364	
1997	155.4	52.6	53.8	85.0	18.0	3.0	n.a.	72.8	12.0	115.4	262.6	165.0	378	
2000	44.2	55.2	68.4	168.6	28.0	17.0	17.4	n.a.	47.1	125.9	198.6	174.0	324.5	

n.a. = not available

Tab. 6.1b: Monthly cumulative precipitation (mm) according to the year affected by volcanoclastic flow events. In the grey cells the data deriving from Ricciardi et al. (2007); in the white cell the data deriving from SIMN (2004).

All this information has been imported into a geographical information system (GIS) of the circum-
vesuvian area (Bisson et al., 2002; Pareschi et al., 2000b). The GIS contains several thematic layers such
as a Digital Elevation Model (DEM) with a 10-meters step obtained by interpolating elevation points
and contour lines following a modified Delaunay approach (Favalli and Pareschi, 2004), IGM (Istituto
Geografico Militare) raster maps at nominal scales of 1:25,000, 1:50,000, 1:100,000 and 1:250,000
that visualize several cartographic information (orography, hydrography, viability, built-up areas) and, the

AIMA (Agency for Interventions on the Agricultural Market) high-resolution (1 meter) airborne images that permit the identification of detailed features such as roofs, bridges, road intersections, sidewalks, trees, etc. (Bisson et al., 2007b).

All vector and raster data presented in this paper are geocoded into the ED50-UTM-Zone33 reference cartographic system and have been processed in ESRI environment using the ARCGIS 9.3® software package.

6.4. Spatial and temporal analysis of historical events during the 20th century

The spatial distribution of historical events showed in Figure 6.1 reveals that the zones most affected by volcanoclastic flows are located in the south-western sector of Somma-Vesuvius, which includes the municipality of *Torre del Greco*, *Ercolano*, *Portici*, *San Giorgio a Cremano* and *San Sebastiano al Vesuvio*. 66 of 116 historical events (about 60 % of the total) occurred in this area and 28 events are recorded just in the Torre del Greco municipality (Figure 6.3). The north-western and north-eastern sectors are affected by roughly 16% of the total events, whereas the south-eastern sector is affected only by 12%.

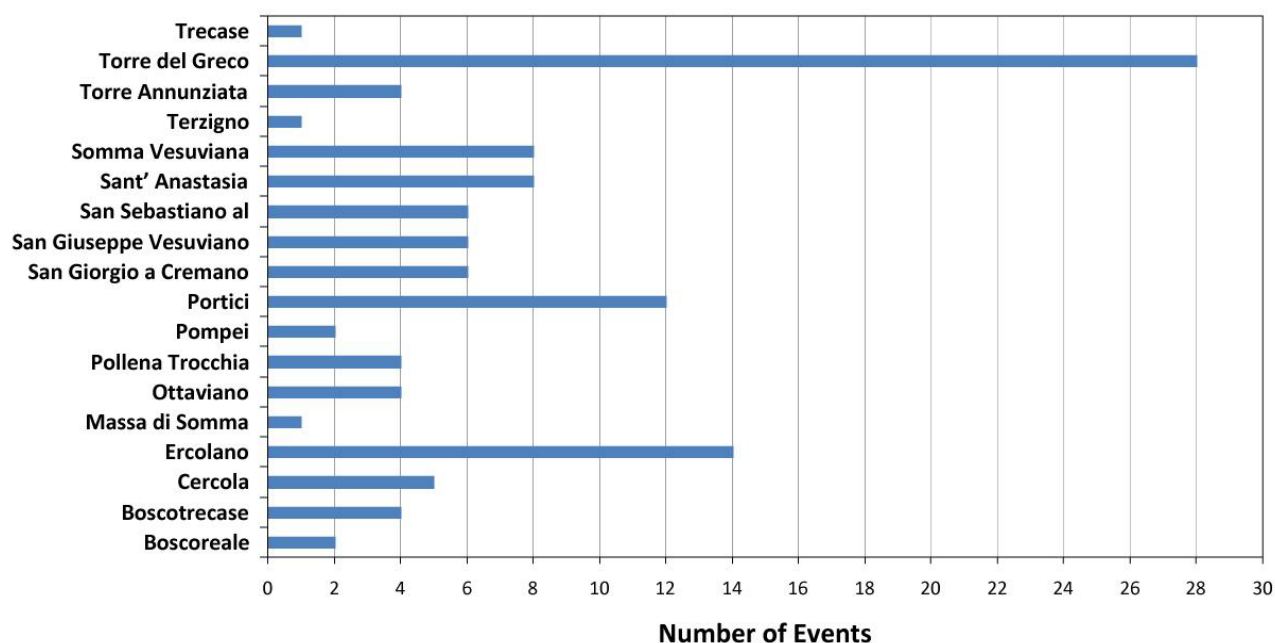


Fig. 6.3: Distribution of volcanoclastic flow events for municipality.

We formulated few hypotheses in the attempt to explain this peculiar distribution. One possible explanation could be found in the shadow effect that the Somma-Vesuvius has on precipitation. To confirm this hypothesis we collected the precipitation data recorded on the opposite flanks of Somma-Vesuvius. The only available data (provided by P. Madonia) are referred to autumn precipitation measures for the year 2002 on the basis of two rain gauges located at similar altitudes uphill of *Ercolano*

and *Ottaviano* villages (Figure 6.1). Despite the limitations, the data show that rainfalls in areas of the *Somma-Vesuvius* edifice facing the sea are indeed greater than in the opposite side (Table 6.2).

autumnal month	OVS (rainfall mm)	OTT (rainfall mm)
september	135.5	117.6
october	201.0	165.6
november	117.0	66.0
december	100.0	96.4
total	553.5	445.6

Tab. 6.2: Rainfall mm recorded by the pluviometric stations of *Ercolano* (OVS) and *Ottaviano* (OTT) during the 2002 autumnal season. See the location in Figure 6.1.

The hypothesis of a shadow effect is further corroborated by the observation that the summit of the volcano, whose height ranges from 1132 to 1281 m a.s.l., is a massive orographic barrier for clouds driven by marine winds. As a result the flanks of the volcano exposed to the sea receive higher amounts of precipitation. Everything else being equal, these areas have a higher probability to generate volcaniclastic flows.

Figures 6.4a and 6.4b respectively, report the annual and monthly distribution of events. The temporal distribution of events recorded between 1906 and 2010 shows the highest peak in 1985 and some lower but significant peaks during the 1906-1911 interval and the 1997 year. The peak of 1985 is in good agreement with the sum of the precipitation data recorded in the rainiest autumnal months (October and November) shown in Table 6.1b (see the red value). The sum corresponds to 516.8 mm of rainfall and represents the highest value of autumnal precipitations referred to years affected by events. Figure 6.4b shows the number of events according to the month of occurrence from 1906 to 2010 highlighting that more than 80% of events occurred in the autumnal period in which the mean precipitation values are higher as showed in Figure 6.4c. The monthly mean values of precipitation (expressed in mm) showed in Figure 4c have come from the daily measurements recorded at the pluviometric station of *Ercolano* (Ricciardi et al., 2007; SIMN, 2004).

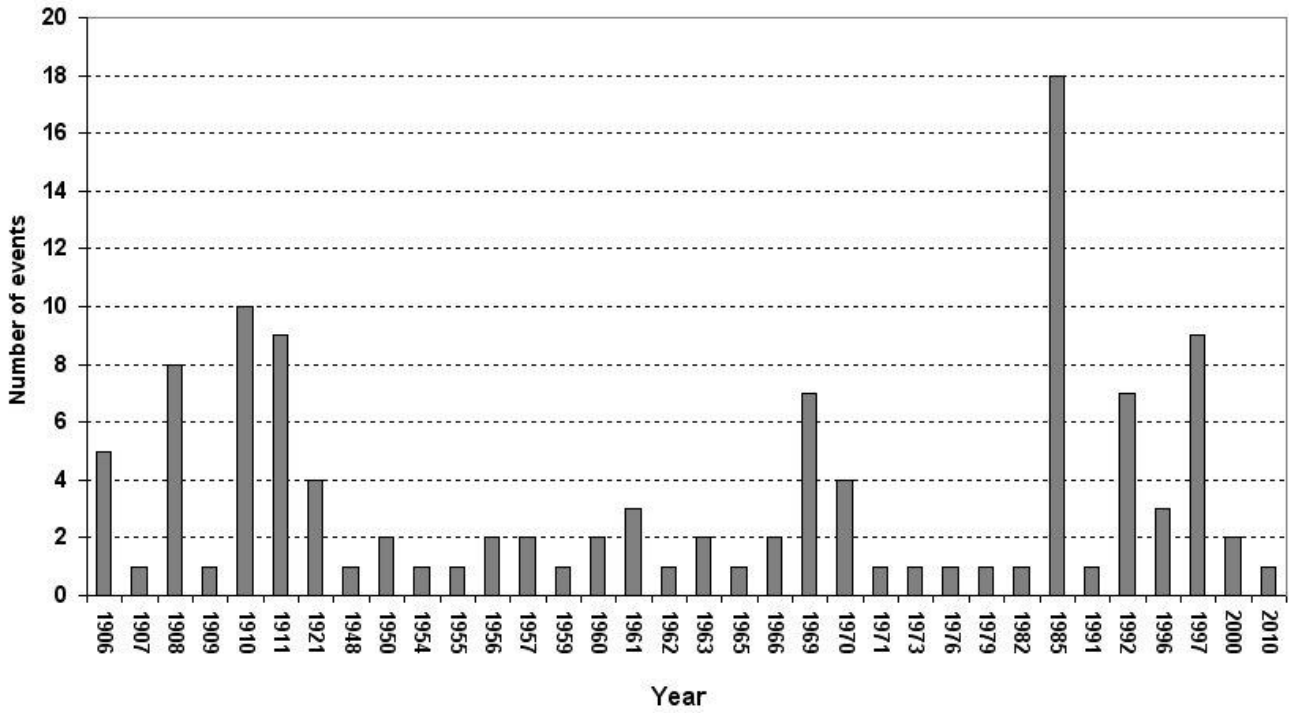


Fig. 6.4a: Number of volcanoclastic flow events recorded from 1906 to 2010.

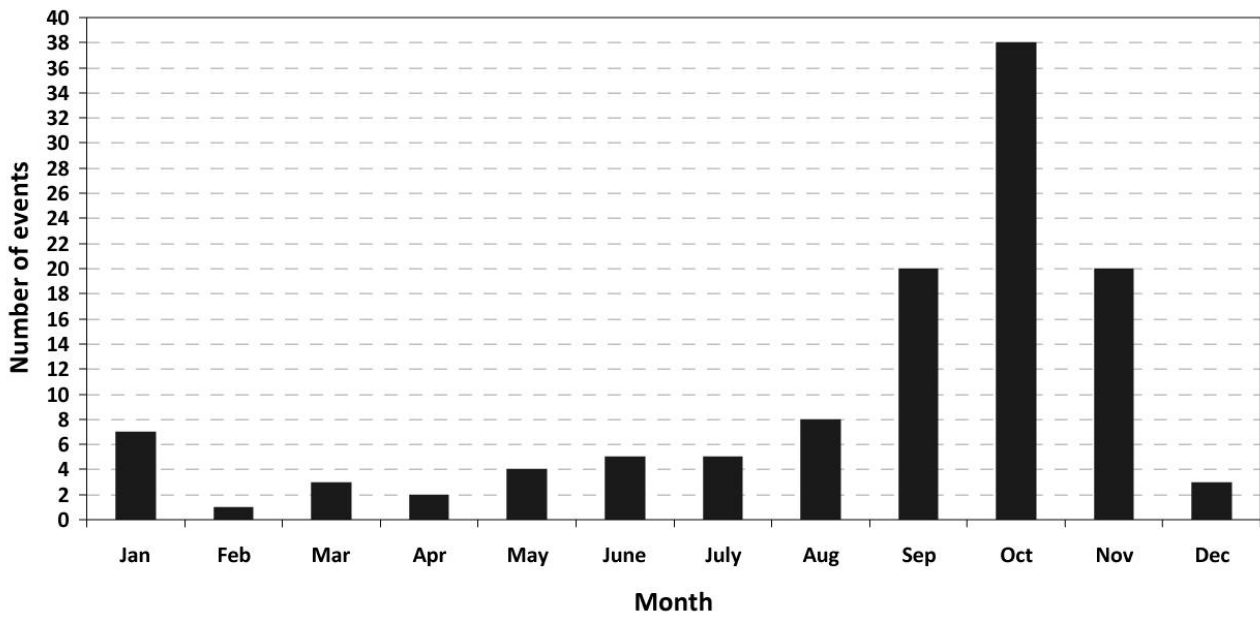


Fig. 6.4b: Distribution of volcanoclastic flow events according to the month of occurrence from 1906 to 2010.

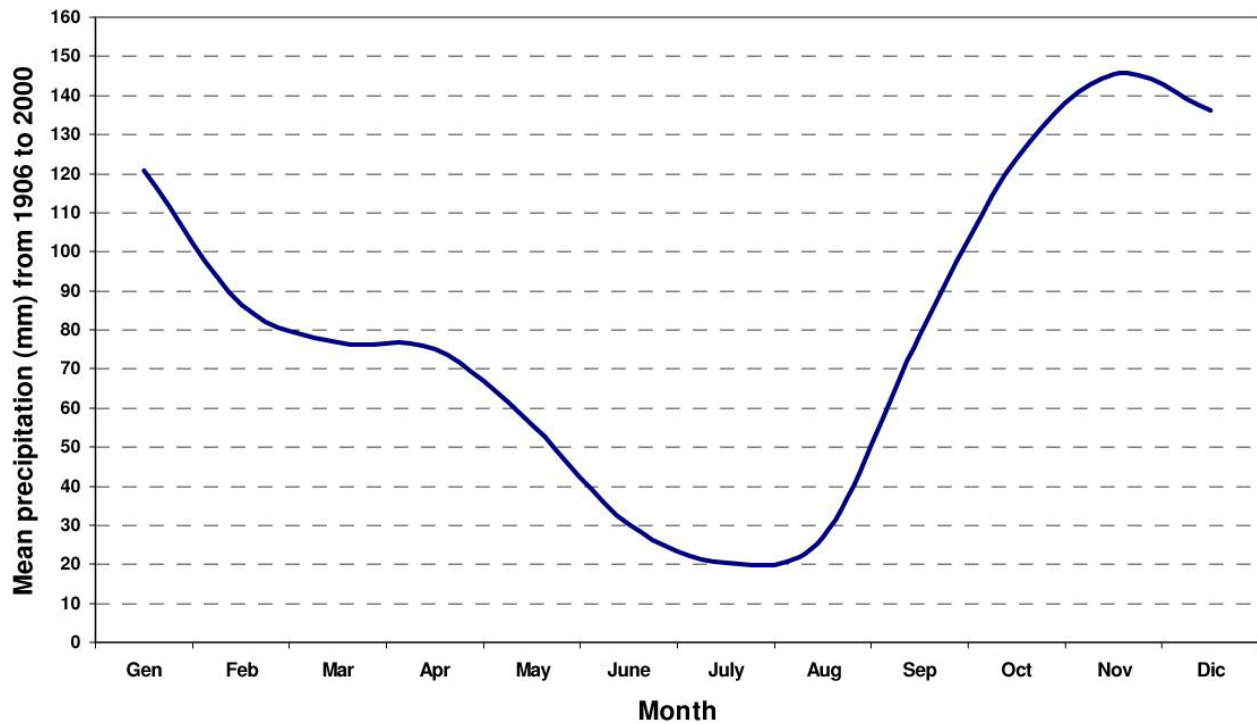


Fig. 6.4c: Distribution of mean monthly precipitation from 1906 to 2000 for the years affected by historical events.

6.5. Morphological considerations

Taking into account the spatial distribution of 116 historical events recorded in the Vesuvian area (Figure 6.1 and 6.2), we selected to present a specific topographic study of *Torre del Greco* municipality due to the higher number of events (28) recorded in the area. This study is based on morphological and morphometric analyses of the area combined with a detailed reconstruction of the paths of historical flows. The morphological and morphometric analyses have been obtained using different raster maps (matrices) derived from the previously mentioned DEM.

The morphology has been rendered with a shaded relief obtained applying the hillshade algorithm to the DEM. This algorithm uses a function that determines the illumination values for each cell in the DEM by setting the direction (azimuth) and angle (altitude) of a hypothetical light source. In the computation, the azimuth and the altitude were set to NW and to 45°, respectively. This information is processed along with calculations for slope and aspect to determine the final shadow values for each cell using the equation of Burrough and McDonell (1998):

$$\text{Hillshade} = 255 * ((\cos(\text{Zenith_rad}) * \cos(\text{Slope_rad})) + (\sin(\text{Zenith_rad}) * \sin(\text{Slope_rad}) * \cos(\text{Azimuth_rad} - \text{Aspect_rad})))$$

The maps of morphometric parameters analysed in this study (slope and curvature) have been obtained applying two different algorithms to DEM. The Slope map is calculated by processing the DEM according to the formula of Burrough and McDonell (1998):

$$S = \arctg[\sqrt{(dz / dx)^2 + (dz / dy)^2}] * 57.29578$$

where: S is the Slope expressed in angle and dz/dy and dz/dx are the elevation changes in directions x and y , respectively. For each cell the algorithm calculates the maximum rate of change in elevation in two directions (dz/dx , dz/dy) over the distance between the cell and its eight neighbours and identifies the steepest downhill descent from the cell. The result is a matrix where each cell memorizes an angle value between 0° and 90° .

The Curvature parameter is obtained combining the second derivatives calculated using DEM data along two different directions following the method of [Zeverbergen and Thorne \(1987\)](#). The curvature value is calculated subtracting the profile value (i.e. rate of change of slope measured along the slope direction) from the planform value (measured transverse to the slope direction). The first value governs flow acceleration and deceleration and sediment deposition and erosion, whereas the second value influences the flow concentration or dispersion. The result is a matrix where the cells with positive values indicate surfaces upwardly convex, whereas the cells with negative values indicate upwardly concave surfaces. The cells with values equal to zero represent flat or planar surfaces.

Under prolonged or heavy rainfalls, the Slope is the most important parameter governing the initiation of any type of landslide, because it directly controls the equilibrium between stabilizing and destabilizing forces. Previous studies carried out for the Vesuvian-Sub Apennine areas identified two different slope thresholds for triggering volcaniclastic flows. These thresholds are usually between 25° and 28° ([Zanchetta et al., 2004b](#); [Pareschi et al., 2002, 2000b](#); [Calcaterra et al., 2000, 1999](#); [De Riso et al., 1999](#)), but in the presence of funnel-shaped drainage basins some authors suggest thresholds between 15° and 18° ([Bisson et al., 2010](#); [Ferrucci et al., 2005](#); [Zanchetta et al., 2004b](#); [Pareschi et al., 2002](#)).

The Curvature plays a significant role in the initiation of a volcaniclastic flow because it identifies areas that preferentially collect water and volcaniclastic colluvium, promoting soil saturation and sliding ([Zanchetta et al., 2003](#)). The triggering of these flows seems favoured by a negative value (concave topography) rather than by a positive one (convex topography).

For these reasons, the Slope and Curvature maps ([Figure 6.5a](#) and [6.5b](#)) can provide a useful contribution to identify areas potentially prone to disruption and consequently to triggering of volcaniclastic flows.

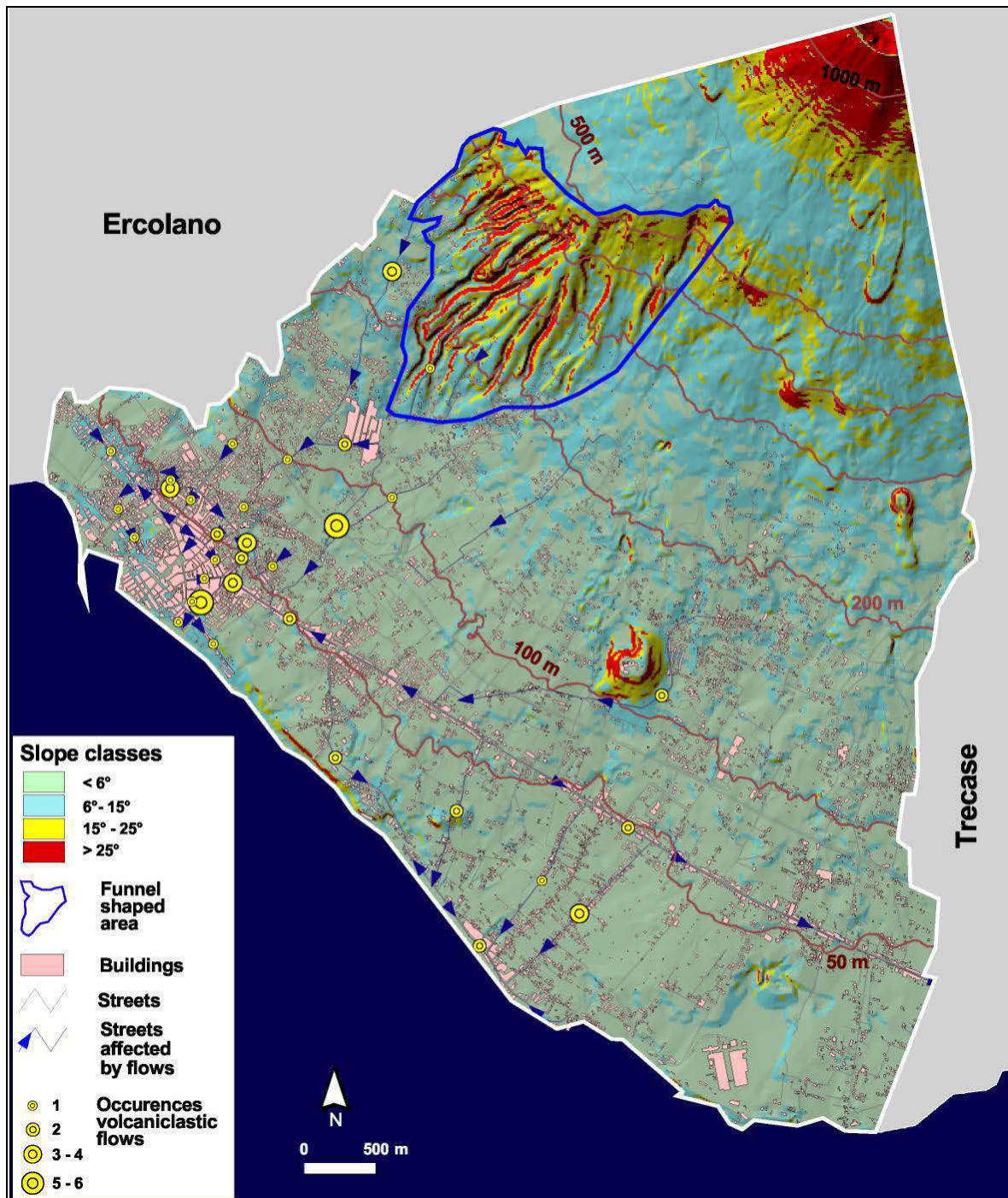


Fig. 6.5a: The slope map and urban element draped on shaded relief image in *Torre del Greco* municipality. The paths of the flows are drawn by blue thin lines with directional arrows, the size of the yellow circles indicates the number of events recorded in the streets.

Figure 6.5a shows the Slope map draped on the shaded relief and visualized using 3 thresholds (25° , 15° and 6°) defined in previous works (Bisson et al., 2013, 2010; Mazzarini et al., 2007; Pareschi et al., 2004, 2002) to distinguish areas with high (slope $\geq 25^\circ$), moderate ($15^\circ \leq \text{slope} < 25^\circ$) and very low ($6^\circ \leq \text{slope} < 15^\circ$) proneness to flows initiation from areas more exposed to inundation (slope $< 6^\circ$). This shows a series of urban elements of *Torre del Greco* town derived from a more detailed GIS (1:5.000 scale) of the Vesuvian area (Pareschi et al., 2000c).

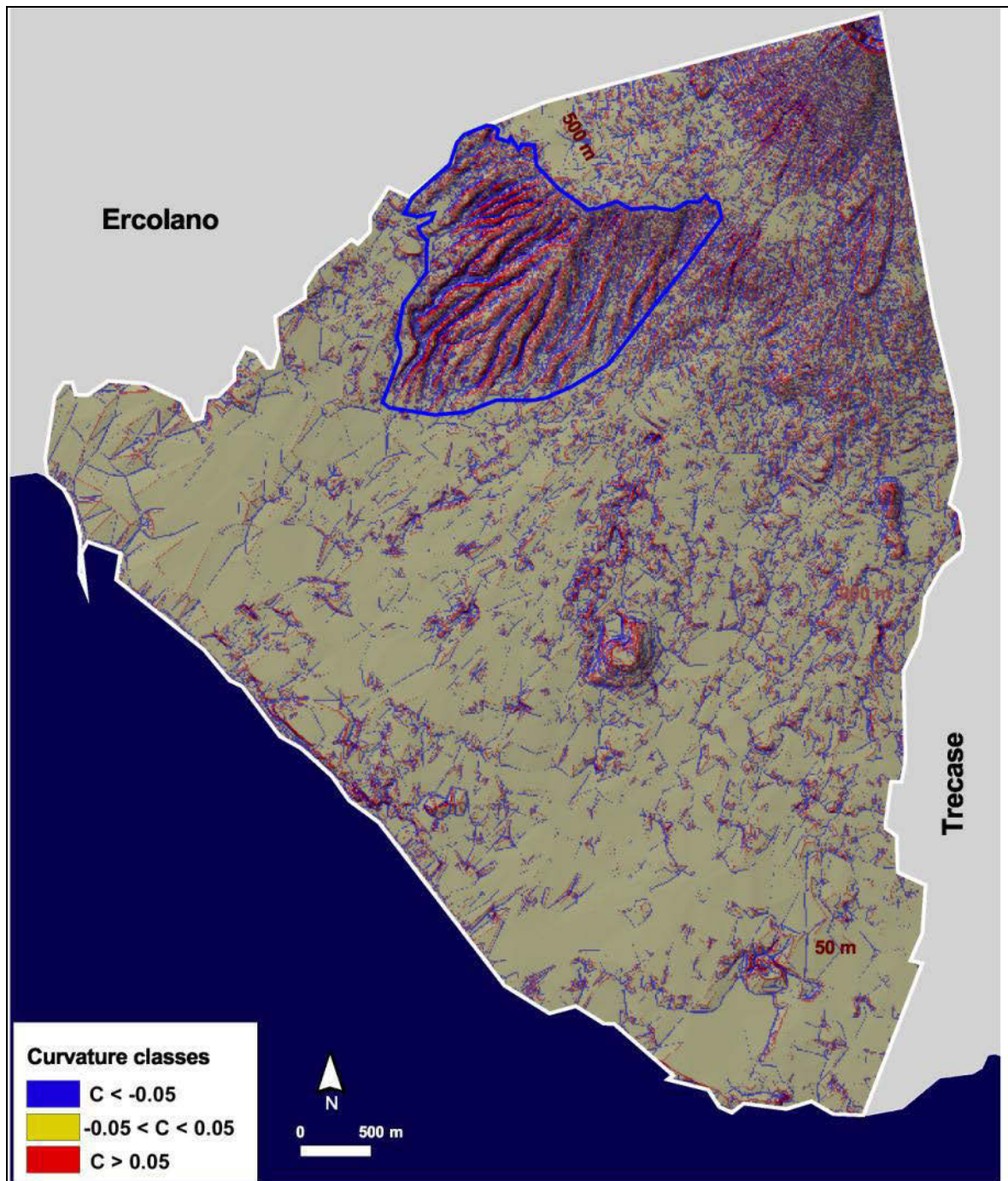


Fig. 6.5b: The curvature map draped on shaded relief image in *Torre del Greco* municipality.

Figure 6.5b shows the Curvature map, always draped on the shaded relief, and visualized according to 3 classes ($Curv < -0.05$; $-0.05 \leq Curv \leq 0.05$; $Curv > 0.05$) that identify concave, flat and convex areas, respectively.

Using this as reference cartographic base, and adding the reports gathered from local newspapers, we located the paths of the 28 historical volcanoclastic flows which affected the town and created a database that includes, for each event, the date of occurrence (day, month, year), the affected roads (street names), the number of deaths and some additional detail about the typology of the event itself (Table 6.3).

TORRE DEL GRECO EVENTS

Day	Month	Year	Involved Streets and Localities	Deaths	Event typology
24	October	1908	Contrada Lava Fiorillo (between Ercolano e Torre del Greco), Circonvallazione, Cavallerizzi, Di Donna Vincenzo (toward Ercolano), San Giuseppe alle Paludi, Lava Troia	1	rapid debris flow
24	October	1910	XX Settembre, Contrada Montedoro, G. De Bottis, Cappuccini, Contrada Camaldoli, Vico Menarca	4	landslide; rapid debris flow
22	September	1911	Nazionale, XX Settembre, Fiorillo, Umberto I, Luigi Palomba square, Purgatorio, Montedoro, Circonvallazione, Capo Torre locality		rapid debris flow
27	October	1921			rapid debris flow
28	September	1959	Stone quarry in Camaldoli locality	1	rapid debris flow, multiple landslides
7	July	1961	Contrada Ponte Rivieccio (Grotta)	1	rapid debris flow
12	November	1961	Cavallo	2	rapid debris flow, landslide
30	May	1963	Nazionale Santa Maria La Bruna		rapid debris flow, landslide
13	January	1965	Via Circonvallazione	1	rapid debris flow
20	September	1969	A. De Gasperi (near the railways bridge), Santa Maria La Bruna		rapid debris flow
1	October	1970	Cappuccini, G. Beneduce, Piscopia, XX Settembre (blocked sewers), Luigi Palomba Square, Agostinella, Lava Troia, Vittorio Veneto, Litoranea, G. De Bottis where a chasm opened, G. Marconi		rapid debris flow
19	January	1971	Cappella Bianchini locality, Lagni Rivieccio zone		rapid debris flow
19	October	1976	Monsignor Felice Romano	1	rapid debris flow, landslide
28	October	1979	Cavallo	1 (lost)	rapid debris flow
18	December	1982	Cavallo	2	rapid debris flow
Night between 30 and 31	October	1985	XX Settembre, Ponte della Gatta, Nazionale, Scappi, Litoranea, Cavallo, Purgatorio, A. De Gasperi, Santa Maria La Bruna, Curtoli (disruption of road surface), C. Battisti		rapid debris flow, landslide
2	November	1985	Vittorio Emanuele, Scappi, Cavallo, Nazionale Santa Maria La Bruna, Circonvallazione, Montedoro		rapid debris flow, landslide
17	November	1985	Cavallo, Maresca, Sant'Elena		rapid debris flow, landslide
15	July	1991	n.a.		debris flow
26	March	1992	n.a.		debris flow
5	August	1992	n.a.		debris flow
3-4	October	1992	Luigi Palomba Square		rapid debris flow
22	August	1996	Harbour zone, XX Settembre		debris flow
13	November	1997	n.a.		debris flow
19	November	2000	n.a.		debris flow

n.a.= not available

Tab. 6.3: Rainfall mm recorded by the pluviometric stations of *Ercolano* (OVS) and *Ottaviano* (OTT) during the 2002 autumnal season. See the location in [Figure 6.1](#).

According to our database, the streets most often affected by the flows are via *Circonvallazione* and via *Santa Maria La Bruna* with 4 events, via *XX Settembre* with 5 events and *Alveo Cavallo* with 6 events ([Table 6.3](#) and [Figure 6.5a](#)). It is worth noting that the term „*alveo*“ means old riverbed, suggesting that the street was originally an old channel. This is not an unique example in the Vesuvian area, which was subjected to intense urbanisation in the last 60 years. The growth of the road network progressively transformed many old fluvial riverbeds and several “*Regi Lagni*” channels into roads ([Alessio et al., 2013](#)).

In [Figure 6.5a](#) the traces of the paths and the directions of flows are visualized as thin blue lines and arrows, respectively. The occurrences of the flows in the street is represented by a circle, the greater the circle, the greater the number of events recorded in that street. According to this data, the streets most frequently affected by flows are located in the south-western sector of the town, the most urbanized and

populated zone of *Torre del Greco* according to Pareschi et al. (2000a) and Alessio et al. (2012). Both Figure 6.5a and 6.5b highlight an area just above the town (between 130 and 600 m a.s.l.) consisting of evident gullies and channels characterized by lengths ranging from 400 to 1250 m and widths of about 30 m.

On the basis of these morphological evidences the boundary of this area has been delineated with a funnel-shaped polygon feature having an extension of about 2.8 km² where more than 60% is characterized by slope > 15° (Figure 6.6a) and the convex, concave and flat morphology cover the 51%, 44%, 4% of the total areas, respectively (Figure 6.6b).

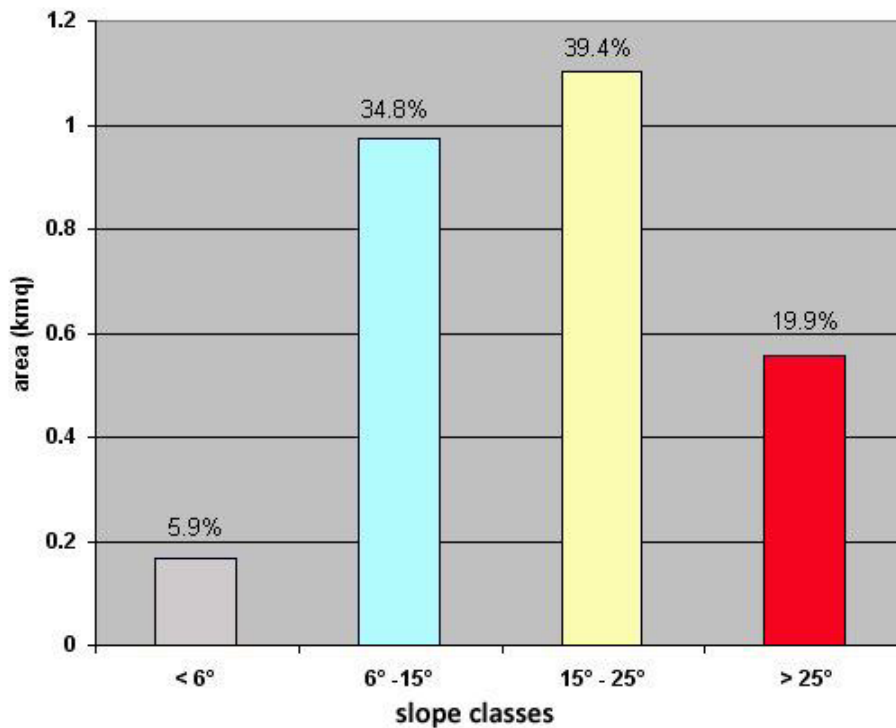


Fig. 6.6a: Distribution of slope classes in the funnel shaped area.

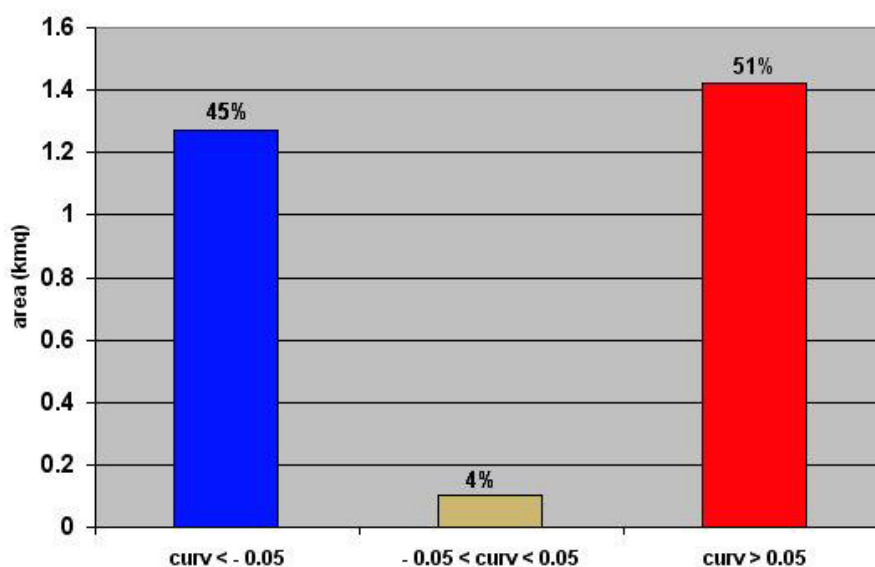


Fig. 6.6b: Distribution of curvature classes in the funnel shaped area.

These morphometric characteristics combined with the traces of flows paths individuated in *Torre del Greco* town (Figure 6.5a) suggest that the funnel-shaped area is most likely the preferential zone of passage for the 28 historical volcanoclastic flows. Generation of these flows is likely linked to the remobilisation of pyroclastic material located in higher portions of the volcanic edifice and represented by fallout deposits of recent Vesuvian eruptions (Figure 6.7).

However in case of renewal of volcanic explosive activity, we cannot exclude the possibility that this funnel-shaped area might first become a zone of deposit for the fall-out material and, after a progressive accumulation, a source of volcanoclastic flows triggered and controlled by the morphological and morphometric characteristics described above.

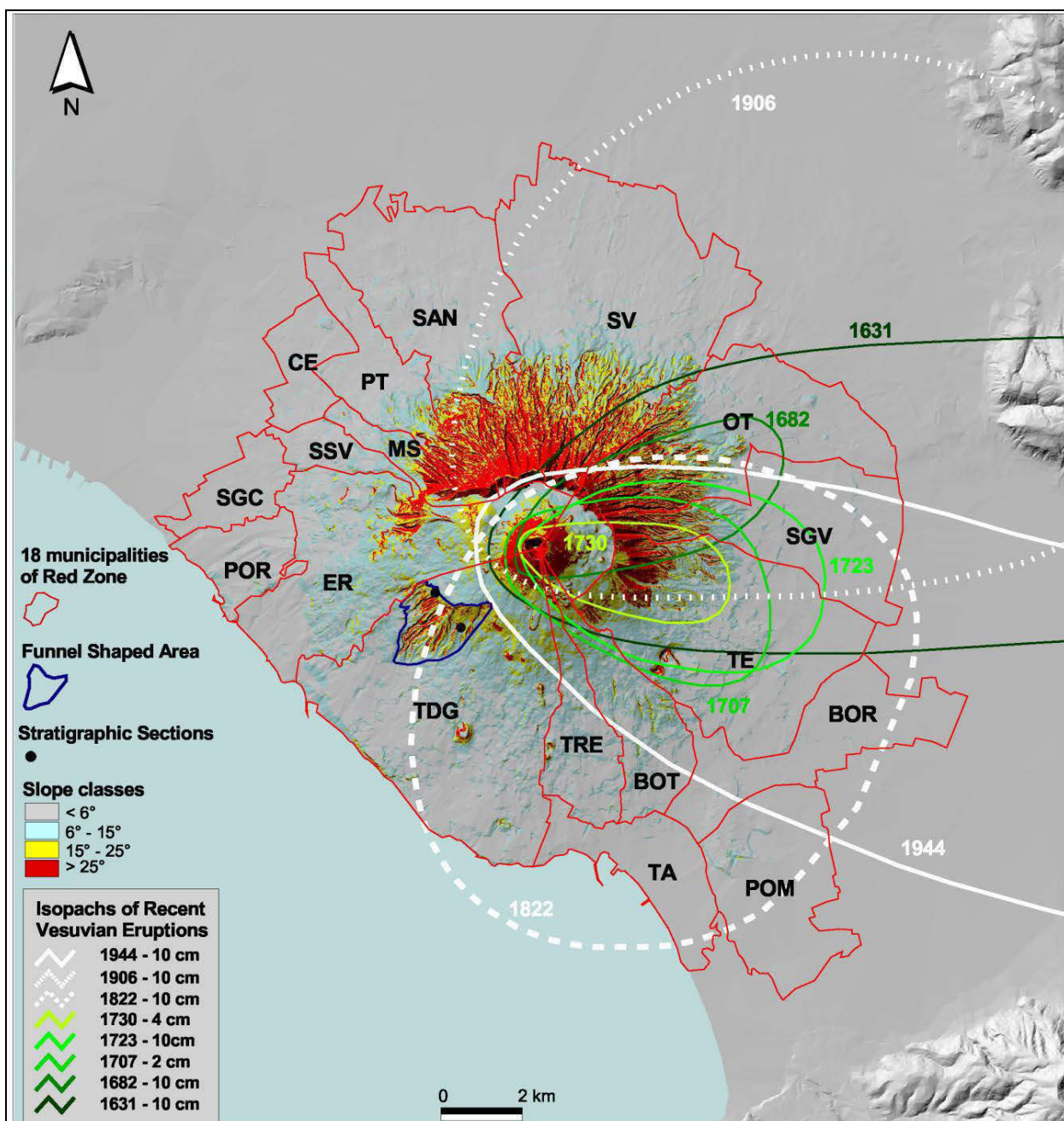


Fig. 6.7: The isopachs of the thinnest isopachs of fall-out deposits for the main recent volcanic eruptions (from AD 1631 to 1944). The red line defines the boundary of the 18 municipalities of the Red Zone. The black circles in the funnel shaped area indicate the locations of some 1906 lahars deposits recognized during a recent field survey (personal communication from C. Principe).

6.6. Volcaniclastic Historical flows recorded in *Torre del Greco* municipality

To understand which fallout deposits could be linked to the 20th century volcaniclastic flow events triggering, the spatial distribution of events has been correlated with the dispersion maps of fall-out deposits related to recent volcanic eruptions (AD 1631-1944).

For the major eruptions of this period, data on the thickness of fallout deposits (isopachs and measuring points) derived from the literature and from key georeferenced geological sections (Table 6.4) were transformed into a digital vector format (line and point layers) storing thickness values in cm. Data were processed choosing a linear spatial interpolation (Bisson and Del Carlo, 2013) and then memorized in a matrix where each 10-m cell represents the thickness of the fallout deposit. The most significant fallout isopachs have been derived from each grid by reconstructing the thinnest one on the basis of the available literature data (Table 6.4).

All processing was performed in a GIS platform. The derived isopachs are showed in Figure 6.7 and highlight that the zone immediately above the funnel shape area is characterized by the presence of pyroclastic deposits belonging mainly to 1822, 1906 and 1944 eruptions. In the case of heavy and persistent rainfall, these deposits could have been eroded and remobilized, originating some of the historical volcaniclastic flows. Considering the thicknesses of fallout deposits related to these 3 eruptions, those of 1822, ranging from 15-20 cm (dashed lines, Figure 6.7) could indicate the pyroclastic material that with mayor probability, would have originated the historical flows after a remobilization caused by an intense rainfall.

By analysing the other recent eruptions according to the direction of the dispersal axis and to the minimum thickness of the fallout deposits, we can observe that also the pyroclastic products of the 1906 eruption (dotted white lines in Figure 6.7) could to be linked to the triggering of some historical volcaniclastic flows. In this case the initiation of flows occurred through the remobilisation of some 1906 lahars originally located in the funnel shape area. A recent field survey has identified, in the upper part of two stratigraphic sections located in this area (black points in Figure 6.7), thick levels of volcaniclastic deposits that have been attributed to the lahars of the 1906 eruption on the basis of their depositional and chemical characteristics (Arrighi et al., 2001). Note that the occurrence of these lahars could be reasonably correlated with the secondary peaks in the number of events between 1908 and 1911 (Figure 6.4a). In the case of the more recent 1944 eruption we cannot come to similar conclusion because no evidence of fallout deposits or lahars has been observed in funnel shape area.

6.7. Discussion and Conclusions

This work presents an historical analysis of the 20th century volcanoclastic flows occurred in a very densely populated area of the Somma-Vesuvius region.

The study is based on the collection of data from historical reports and local newspapers, which were organized in a georeferenced database that individuates 116 volcanoclastic flow events recorded between 1906 and 2010. This database has been integrated with a detailed GIS at a scale 1:5,000 relative to the main urban features of *Torre del Greco* municipality. A series of different information (historical records, precipitation data, morphological and morphometric studies, fall-out deposits dispersion maps) were analysed to define the spatial distribution of these 116 historical events and the possible relations with the pyroclastic deposits of the main recent eruptions of Vesuvius.

The spatial analysis reveals that the area most exposed to volcanoclastic flow hazard is the south-western sector of Vesuvius, affected by the 60% of historical volcanoclastic flows, while the remaining 40% is shared among the others three sectors. This peculiar distribution can be likely explained by the shadow effect of the Somma-Vesuvius on precipitation. The summit of the volcano represents an orographic barrier for clouds carried by marine winds, and as consequence the south-western sector of the volcano receives greater amounts of precipitation which make more likely the triggering of volcanoclastic flows.

The spatial distribution of historical events recorded in the south-western sector also reveals that the municipality most affected by volcanoclastic flows is *Torre del Greco*. For this reason we developed a detailed morphological and morphometric analysis of this municipality combined with a specific study of the paths of historical flows. This allowed us to identify a funnel shaped area located just above the town, between 130 and 600 m a.s.l., characterized by several channels and gullies that probably directed the transit of historical flows towards the town. The source of these flows could be the remobilisation of fall-out deposits located in the higher portion of the volcanic edifice. This conclusion seems to be supported by the fallout deposits dispersion maps related to some recent eruptions of Vesuvius, which indicate that a part of pyroclastic deposits linked to volcanic activity of 1822 and 1906 is located above the funnel shaped area and, therefore, could have been involved in the triggering of 20th volcanoclastic flow events.

Although this work represents only a starting point for studies on the prevention of volcanoclastic flow hazard in densely populated volcanic areas, its findings provide useful indications for the assessment and mitigation of the risk of volcanoclastic flow in the Somma-Vesuvius area. It seems worthwhile to point out that the more populated municipalities are located exactly in the sector of the volcano most exposed to volcanoclastic flows (south-western sector); for this reason particular attention should be paid to *Portici* and *San Giorgio a Cremano* territories where population density reaches 11,000 person per km².



CHAPTER 7

7. Summary and Conclusions

The fieldwork carried out in the territory, was instrumental to reconstruct the paths of some medieval lava flows and to determine the location of possible eruptive centre, which were buried either partially or completely, or obliterated by building constructions.

[Principe et al. \(2004\)](#) identified a few medieval eruptions with eccentric vents close to the coastline. Here, it has been possible to recognize other eccentric medieval vents very close to the coastline.

Using the detailed cartography it was possible to observe that the medieval tephra fallout, in particular that of the AD 1139 eruption, was found to occur in the south-western sector of Vesuvius, in addition to the finding of [Rolandi et al. \(1998\)](#), which studied twenty sections from outcrops around the eastern sector of the volcano, from *Sant'Anastasia* to *Torre del Greco*.

The present level of medieval tephra of the AD 1139 eruption in both eastern and south-western sectors of Vesuvius, allowed to identify a different dispersion pattern and, consequently, a new horizon that is relevant in terms of fallout hazard.

From the study and analysis of the sampled medieval tephra fallout, it was found that modern tephra are characterized by a predominant distribution to east ([Arrighi et al., 2001](#)). However, in the south-western area, the tephra were found in the higher slopes (*Piano delle Ginestre* and *Cappella Bianchini*), where they caused remobilization and development of lahars.

The AD 472 eruption deposits do not outcrop in the south-western sector, but they can be observed in other sectors of the volcano and in *Pollena*. Along the coast they can be traced only in *Torre Annunziata*. In the south-western sector the only major medieval level that can be located is the AD 1139 tephra eruption.

The fieldwork carried out on the territory allowed to identify and map the historically known deposits of lahars, which caused a large number of victims and considerable damages to the territory. One of these outcrops is near the vents of the 1794 eruption.

GIS processing of historical and field data of epiclastic deposits in the south-western sector of Vesuvius showed that the modern lahars were the result of remobilization of modern tephra which outcrop only in the *Piano delle Ginestre*, were triggered by rainfalls and then funnelled along the waterways of *Cappella Bianchini*.

Using the DEM it was possible to determine the morphometric parameters (slope, curvature) and delimit the hydrographic basins, with their respective areas of confluence (source area) and accumulation

(expansion area), and the possible channels of water-flow, currently modified by human interventions (riverbeds-road).

Hydrologic Annals were important to study the amount, intensity, and duration of daily rainfalls in relation to years, months and, consequently, seasons.

For the AD 79 eruption of *Pompei*, the lahars deposits are impressive and more important than modern ones, because they affected the entire coast producing a flat morphology.

In conclusion, the work done in the south-western sector of the Somma-Vesuvius volcano allowed to: *i*) to significantly, improve the mapping of medieval eruptions; *ii*) improve the awareness of risk connected to the opening of eccentric effusive vents; *iii*) increase the knowledge of the AD 1139 medieval explosive eruption; *iv*) confirm the mechanisms and the distribution of epiclastic deposits.

Based on data available in the literature, the prevailing direction of the Vesuvian tephra is eastward. The data obtained in this work identified an eruption classified like a violent Strombolian, which has southward direction. The other eruptions are the AD 79 Plinian eruption, with a very high column, and 1822 sub-Plinian eruption.

References

- Alessio, G., De Falco, M., Di Crescenzo, G., Nappi, R., Santo, A. (2012). Landslide and alluvial hazard high-resolution mapping of the Somma-Vesuvius volcano by means of DTM, remote sensing, geophysical and geomorphological data GIS-based approach. 7^a Riunione Annuale del Gruppo GIT “Geology and Information Technology”.
- Alessio, G., De Falco, M., Di Crescenzo, G., Nappi, R., Santo, A. (2013). Flood hazard of the Somma-Vesuvius region based on historical (19-20th century) and geomorphological data. *Annals of Geophysics*, 56(4): S0434.
- Alfano, G.B. (1923). Le eruzioni del Vesuvio tra il 79 e il 1631. Comunicazione letta nella seduta sezionale dell'associazione del 13 settembre 1923.
- Alfano, G.B. (1924). Le eruzioni del Vesuvio tra il 79 e il 1631 (studio bibliografico). Napoli: Scuola tipografica Pontificia per i figli dei carcerati. Valle di Pompei.
- Allen, M.E., Sibahi, Z., Sohm, E.D. (1980). Evaluation of the Office of the United Nations Disaster Relief Coordinator. JIU/REP/80/11.
- Andronico, D., Calderoni, G., Cioni, R., Sbrana, A., Sulpizio, R., Santacroce, R. (1995). Geological map of Somma-Vesuvius. *Periodico di Mineralogia*, 64: 77-78.
- Andronico, D., Cioni, R. (2002). Contrasting styles of Mount Vesuvius activity in the period between the Avellino and Pompeii Plinian eruptions, and some implications for assessment of future hazards. *Bullettin of Volcanology*, 6: 372-391. doi:10.1007/s00445-002-0215-4
- Andronico, D., Cioni, R., Marianelli, P., Santacroce, R., Sbrana, A., Sulpizio, R. (1996a). Introduction to Somma-Vesuvius. In: Vesuvius Decade Volcano. Workshop Handbook. Napoli. September 17-22.
- Andronico, D., Cioni, R., Sulpizio, R. (1996b). General stratigraphy of the past 19,000 yrs at Somma-Vesuvius. In: Vesuvius Decade Volcano. Workshop Handbook. Napoli. September 17-22.
- Arnò, V., Principe, C., Rosi, M., Santacroce, R., Sbrana, A., Sheridan, M.F. (1987). Chapter 2. Eruptive history. In: Santacroce, R. (Ed.). Somma-Vesuvius. *Quaderni de 'La Ricerca Scientifica' CNR*, 114(8): 53-103.
- Arrighi, S., Principe, C., Rosi, M. (2001). Violent strombolian and subplinian eruptions at Vesuvius during post-1631 activity. *Bullettin of Volcanology*, 63: 126-150. doi:10.1007/s004450100130
- Barberi, F., Bizouard, H., Clocchiatti, R., Métrich, N., Santacroce, R., Sbrana, A. (1981). The Somma-Vesuvio magma chambre: a petrological and volcanological approach. *Bull Volcanol*, 44: 295-315.
- Barberi, F., Leoni, L. (1980). Metamorphic carbonate ejecta from Vesuvius plinian eruptions: evidence of occurrence of shallow magma chambers. *Bull. Volcanol.*, 43(1): 107-120.
- Bates, R.L., Jackson, J.A. (1987). *Glossary of Geology* (3rd Edition). Alexandria, VA: American Geological Institute.
- Belkin, H.E., De Vivo, B., Roedder, E. (1985). Fluid inclusion geobarometry from ejected Mt. Somma-Vesuvius nodules. *Amer. Miner.*, 70: 288-303.
- Belkin, H.E., De Vivo, B., Torok, K., Webster, J.D. (1998). Pre-eruptive volatile content, melt-inclusion chemistry, and microthermometry of interplinian Vesuvius lavas (pre-A.D. 1631). *Journal of Volcanology and Geothermal Research*, 82: 79-95.
- Belkin, H.E., Kilburn, C.R.J., De Vivo, B. (1993). Sampling and major element chemistry of the recent (AD 1631-1944) Vesuvius activity. *Journal of Volcanology and Geothermal Research*, 58: 273-290.
- Bertagnini, A., Landi, P., Rosi, M., Vigliargio, A. (1998). The Pomici di Base plinian eruption of Somma-Vesuvius. *Journal of Volcanology and Geothermal Research*, 83: 219-239.
- Bianco, F., Castellano, M., Milano, G., Ventura, G., Vilardo, G. (1998). The Somma-Vesuvius stress field induced by regional tectonics: evidences from seismological and mesostructural data. *Journal of Volcanology and Geothermal Research*, 82: 199-218.
- Bigi, G., Castellarin, A., Catalano, R., Coli, M., Cosentino, D., Dal Piaz, G.V., Lentini, F., Parotto, M., Patacca, E., Praturlon, A., Salvini, F., Sartori, R., Scandone, P., Vai, G.B. (1990). Synthetic structural-kinematic map of Italy. Time of main alpidic deformations and of related sedimentary metamorphic and magmatic processes. Scale 1:2,000,000. In: Bigi, G., Cosentino, D., Parotto, M., Sartori, R., Scandone, P. (Eds.). Structural Model of Italy. *Quaderni de 'La Ricerca Scientifica' CNR*, 114(3): Sheet 5.

- Bisson, M., Cosimi, G., Favalli, M., Leoni, F.M., Mazzarini, F., Pareschi, M.T., Santacroce, R., Sgro, S., Sulpizio, R., Zanchetta, G. (2002). GIS database for the assessment of debris flow hazard in two areas of the Campania region (southern Italy). *Il Nuovo Cimento C*, 25(4): 433-447.
- Bisson, M., Del Carlo, P. (2013). A GIS-based application for volume estimation and spatial distribution analysis of tephra fallout: a case study of the 122 BC Etna eruption. *Annals of Geophysics*, 56(1): R0105. 1-12.
- Bisson, M., Fornaciai, A., Mazzarini, F. (2007a). SITOGE0: A geographic database used for GIS applications. *Il Nuovo Cimento C*, 30(3): 325-335. doi:10.1393/ncc/i2007-10243-9
- Bisson, M., Fubelli, G., Sulpizio, R., Zanchetta, G. (2013). A GIS-based approach for estimating volcanoclastic flow susceptibility: a case study from Sorrentina Peninsula (Campania Region). *Italian Journal of Geosciences*, 132(3): 394-404.
- Bisson, M., Pareschi, M.T., Zanchetta, G., Sulpizio, R., Santacroce, R. (2007b). Volcanoclastic debris-flow occurrences in the Campania region (Southern Italy) and their relation to Holocene-Late Pleistocene pyroclastic fall deposits: implications for large-scale hazard mapping. *Bulletin of Volcanology*, 70(2): 157-167.
- Bisson, M., Sulpizio, R., Zanchetta, G., Demi, F., Santacroce, R. (2010). Rapid terrain-based mapping of some volcanoclastic flow hazard using Gis-based automated methods: a case study from southern Campania, Italy. *Natural Hazards*, 55: 371-387.
- Bonomo, R., & Ricci, V. (2010). Application of the unconformity bounded stratigraphic units (UBSU) to the geological survey of the volcanic island Ustica (Italy). *Geological Society of America Special Paper*, 464: 51-61. doi:10.1130/2010.2464(03)
- Brocchini, D., Principe, C., Castradori, D., Laurenzi, M.A., Gorla, L. (2001). Quaternary evolution of the southern sector of the Campania Plain and early Somma-Vesuvius activity: insights from the Trecase 1 well. *Mineralogy and Petrology*, 73: 67-91.
- Bruno, P.P.G., Cippitelli, G., Rapolla, A. (1998). Seismic study of the Mesozoic carbonate basement around Mt. Somma-Vesuvius, Italy. *Journal of Volcanology and Geothermal Research*, 84: 311-322.
- Bruno, P.P.G., Rapolla, A. (1999). Study of the sub-surface structure of Somma-Vesuvius (Italy) by seismic reflection data. *Journal of Volcanology and Geothermal Research*, 92: 373-387.
- Burrough, P.A., McDonnell, R.A. (1998). *Principles of geographical information systems*. Oxford: Oxford University Press.
- Calcaterra, D., Parise, M., Palma, B., Pelella, L. (1999). The May 5th 1998, landsliding event in Campania (southern Italy): inventory of slope movements in the Quindici area. In: Yagi, N., Yamagami, T., Jiang, J. (Eds.). *Proceedings of International Symposium on Slope Stability Engineering*. Shikoku. Matsuyama. Japan. November 8-11. Rotterdam. Balkema. Pp. 1361-1366.
- Calcaterra, D., Parise, M., Palma, B., Pelella, L. (2000). Multiple debris flows in volcanoclastic materials mantling carbonate slopes. In: Wieczorek, G.F., Naeser, N.D. (Eds.). *Debris-Flow Hazards Mitigation: Mechanics, Prediction, and Assessment*. Rotterdam. Balkema. Pp. 99-107.
- Capra, L., Poblete, M.A., Alvarado, R. (2004). The 1997 and 2001 lahars of Popocatepetl volcano (Central Mexico): textural and sedimentological constraints on their origin and hazards. *Journal of Volcanology and Geothermal Research*, 131: 351-369.
- Carafa, G. Duca di Noja (1775). *Mappa topografica della città di Napoli e de' suoi contorni*, stampata a Napoli nel 1775. Napoli.
- Cassano, E., La Torre, P. (1987). Chapter 4. Geophysics. In: Santacroce, R. (Ed.). *Somma-Vesuvius. Quaderni de 'La Ricerca Scientifica' CNR*, 114(8): 175-195.
- Cerbai, I., Principe, C. (1996). *Bibliography of Historic Activity on Italian Volcanoes*. Institute of Geochronology and Isotope Geology. Italian National Research Council (IGGI). Internal report n.° 6/96.
- Chang, K.H. (1975). Unconformity bounded stratigraphic units. *Geological Society of America Bulletin*, 86(11): 1544-1552. doi:10.1130/0016-7606(1975)86<1544:USU>2.0.CO;2
- Chevallier, L. (1986). Tectonics of Marion and Prince Edward volcanoes (Indian Ocean): result of regional control and edifice dynamics. *Tectonophysics*, 124: 155-175.
- Cioni, R., A. Longo, G. Macedonio, R. Santacroce, A. Sbrana, R. Sulpizio and D. Andronico (2002). Assessing pyroclastic fall hazard through field data and numerical simulations: the example from Vesuvius. *Journal of*

- Geophysical Research*, 108(B2): 1-11.
- Cioni, R., Bertagnini, A., Santacroce, R., Andronico, D. (2008). Explosive activity and eruption scenarios at Somma-Vesuvius (Italy): Towards a new classification scheme. *Journal of Volcanology and Geothermal Research*, 178: 331-346.
- Cioni, R., Civetta, L., Marianelli, P., Metrich, N., Santacroce, R., Sbrana, A. (1995). Compositional layering and syn-eruptive mixing of a periodically refilled shallow magma chamber: the AD 79 Plinian eruption of Vesuvius. *Journal of Petrology*, 36(3): 739-776. doi:10.1093/petrology/36.3.739
- Cioni, R., D’Oriano, C., Bertagnini, A., Andronico, D. (2013). The 2nd to 4th century explosive activity of Vesuvius: new data on the timing of the upward migration of the post-AD 79 magma chamber. *Annals of Geophysics*, 56(4): S0438-17. doi:10.4401/ag-6444
- Cioni, R., Santacroce, R., Sbrana, A. (1999). Pyroclastic deposits as a guide for reconstructing the multi-stage evolution of the Somma-Vesuvius caldera. *Bullettin of Volcanology*, 60: 207-222. doi:10.1007/s004450050272
- Civetta, L., Santacroce, R. (1992). Steady state magma supply in the last 3400 years of Vesuvius activity. *Acta Vulcanologica*, 2: 147-159.
- Cortini, M., Lima, A., De Vivo, B. (1985). Trapping temperatures of melt inclusions from ejected Vesuvian mafic xenoliths. *Journal of Volcanology and Geothermal Research*, 26: 167-172.
- Cortini, M., Scandone, R. (1982). The feeding system of Vesuvius between 1754 and 1944. *Journal of Volcanology and Geothermal Research*, 12: 393-400.
- D’Oriano, C., Cioni, R., Bertagnini, A., Andronico, D., Cole, P.D. (2011). Dynamics of ash-dominated eruptions at Vesuvius: the post-512 AD AS1a event. *Bullettin of Volcanology*, 73: 699-715. doi:10.1007/s00445-010-0432-1
- De Riso, R., Budetta, P., Calcaterra, D., Santo, A. (1999). Le colate rapide in terreni piroclastici del territorio campano. *Atti Convegno Previsione e prevenzione di movimenti franosi rapidi*, Trento: 17-19.
- De Seta, C., Di Mauro, L., Perone, M. (1980). *Ville Vesuviane*. Milano: Rusconi Immagini.
- De Vivo, B., Rolandi, G., Gans, P.B., Calvert, A., Bohrsen, W.A., Spera, F.J., Belkin, H.E. (2001). New constraints on the pyroclastic eruptive history of the Campanian volcanic Plain (Italy). *Mineralogy and Petrology*, 73(1): 47-65. doi:10.1007/s007100170010
- Delibrias, G., Di Paola, G.M., Rosi, M., Santacroce, R. (1979). La storia eruttiva del complesso vulcanico Somma Vesuvio ricostruita dalle successioni piroclastiche del Monte Somma. *Rendiconti della Società Italiana Mineralogia e Petrologia*, 35: 411-438.
- Di Renzo, V., Di Vito, M.A., Arienzo, I., Carandente, A., Civetta, L., D’Antonio, M., Giordano, F., Orsi, G., Tonarini, S. (2007). Magmatic history of Somma-Vesuvius on the basis of new geo-chemical data from a deep bore-hole (Camaldoli della Torre). *Journal of Petrology*, 48(4): 753-784. doi:10.1093/petrology/egl081
- Di Vito, M.A., Sulpizio, R., Zanchetta, G., Calderoni, G. (1998). The geology of the South Western Slopes of Somma-Vesuvius, Italy, as inferred by borehole stratigraphies and cores. *Acta Vulcanologica*, 10(2): 383-393.
- Doglioni, C., Gueguen, E., Harabaglia, P., Mongelli, F. (1998). On the origin of W-directed subduction zones and applications to the western Mediterranean. In: Durand, B., Jolivet, L., Horvath, F., Séranne, M. (Eds.). (1999). The Mediterranean Basins: Tertiary Extension within the Alpine Orogen. *Geological Society London*. Special Publication.
- DPC (1995). Pianificazione Nazionale d’Emergenza dell’Area Vesuviana. Presidenza del Consiglio dei Ministri-Dipartimento della Protezione Civile. Roma.
- DPC (2014). Disposizioni per l’aggiornamento della pianificazione di emergenza per il rischio vulcanico del Vesuvio. Presidenza del Consiglio dei Ministri-Dipartimento della Protezione Civile. Roma.
- Ellis, M., King, G. (1991). Structural control of Flank Volcanism in Continental Rift. *Science*, 254: 839-843.
- Favalli, M., Pareschi, M.T. (2004). Digital elevation model construction from structured topographic data: the DEST algorithm. *Journal of Geophysical Research*, 109(F04004): 1-17. doi:10.1029/2004JF000150
- Ferrucci, F., Gaudiosi, G., Pino, N.A., Luongo, G., Hirn, A., Mirabile, L. (1989). Seismic detection of a major Moho upheaval beneath the Campania volcanic area (Naples, Southern Italy). *Geophys. Res. Lett.*, 6(11): 1317-1320. doi:10.1029/GL016i011p01317
- Ferrucci, M., Pertusati, S., Sulpizio, R., Zanchetta, G., Pareschi, M.T., Santacroce, R. (2005). Volcaniclastic debris flows at La Fossa Volcano (Vulcano Island, southern Italy): insights for erosion behaviour of loose pyroclastic

- material on steep slopes. *Journal of Volcanology and Geothermal Research*, 145(3): 173-191.
- Finetti, I., Morelli, C. (1974). Esplorazione sismica a riflessione dei Golfi di Napoli e Pozzuoli. *Bollettino di Geofisica Teorica e Applicata*, XVI(62-63): 175-221.
- Groppelli, G., Viereck-Goette, L. (Eds.). (2010). *Stratigraphy and geology of volcanic areas* (Special Paper, 464). Boulder, CO: The Geological Society of America.
- Guiraud, M., Laborde, O., Philip, H. (1989). Characterization of various types of deformation and their corresponding deviatoric stress tensors using microfault analysis. *Tectonophysics*, 170: 289-316. doi:10.1016/0040-1951(89)90277-1
- Hermes, O.D., Cornell, W.C. (1981). Quenched crystal mush and associated magma composition as indicated by intercumulus glasses. *Journal of Volcanology and Geothermal Research*, 9: 133-149.
- Hyppolite, J., Angelier, J., Roure, F. (1994). A major change revealed by Quaternary stress patterns in the Southern Apennines. *Tectonophysics*, 230: 199-210.
- ISTAT (2009). www.istat.it
- ISTAT (2011). Censimento popolazione 2011. Accessed March 2015.
- Johnston-Lavis, H.J. (1891). Geological map of Monte Somma and Vesuvius, 1:10.000, constructed during the years 1880-1888. London: George Philip & Son.
- La Torre, P., Nannini, R., Sbrana, A. (1983). Geothermal Exploration in Southern Italy: Geophysical interpretation of the Vesuvian area. *Bollettino di geofisica teorica ed applicata*, 26(130 suppl.): 197-208.
- La Vega, F., La Vega, P. (1797). Topografia dei Villaggi di Portici, Resina e Torre del Greco e di porzione de' loro territori per quanto serve a rischiarare altra Carta dell'antico stato dell'agro ercolanese 1:8200. In: Rosini C.M. *Dissertatio Isagogica ad Herculaneum Voluminum Explanationem, pars prima*. Napoli: Ex Regia Typographia.
- Lavecchia, G. (1988). The Tyrrhenian-Apennines system: structural setting and seismotectogenesis. *Tectonophysics*, 147: 263-296.
- Le Bas, M. J., Le Maitre, R. W., Streckeisen, A., Zanettin, B. (1986). A chemical classification of volcanic rocks based on the total alkali-silica diagram. *Journal of Petrology*, 27: 745-750.
- Le Hon, H.S. (1866). Carte Topographique des laves du Vesuve, a l'échelle de 1/25.000, 1631-1861, avec la coupe geologique du Rivage Napolitan. Bruxelles et Leipzig, C. Muquardt; Naples, A. Detken.
- Le Maitre, R.W. (2002). *Igneous Rocks: A Classification and Glossary of Terms* (2nd ed.). Cambridge: Cambridge University press.
- Lirer, L., Munno, R., Postiglione, I., Vinci, A., Vitelli, L. (1997). The A.D. 79 eruption as a future explosive scenario in the Vesuvian area: evaluation of associated risk. *Bull Volcanol*, 59: 112-124.
- Lirer, L., Pescatore, T.S., Booth, B., Walker, G.P.L. (1973). Two Plinian pumice-fall deposits from Somma-Vesuvius, Italy. *Geological Society of America Bulletin*, 84: 759-772.
- Locardi, E., Nicolich, R. (1988). Geodinamica del Tirreno e dell'Appennino Centromeridionale: la nuova carta della Moho. *Mem. Soc. Geol. Ital.*, 41: 121-140.
- Lowe, D.R., Williams, S.N., Leigh, H., Connort, C.B., Gemmell, J.B., Stoiber, R.E. (1986). Lahars initiated by the 13 November 1985 eruption of Nevado del Ruiz, Colombia. *Nature*, 324: 51-53.
- Luongo, G. (1988). Tettonica globale dell'Italia Meridionale: subduzione o bending?. In: L'Appennino Campano-Lucano nel quadro geologico dell'Italia meridionale. *Atti 74° Congr. Nazionale Soc. Geol. Ital.*, Sorrento: 157-161.
- Luongo, G., Cubellis, E., Obrizzo, F., Petrazzuoli, S.M. (1991). A physical model for the origin of volcanism of the Tyrrhenian margin: the case of the Neapolitan area. *Journal of Volcanology and Geothermal Research*, 48: 173-185.
- Macías, J., Capra, L., Scott, K.M., Espíndola, J.M., García-Palomo, A., Costam, J.E. (2004). The 26 May 1982 breakout flows derived from failure of a volcanic dam at El Chichón, Chiapas, Mexico. *Geological Society of America Bulletin*, 116: 233-246.
- Major, J.J. (2000). Gravity-driven consolidation of granular slurries-implications for debris-flow deposition and deposit characteristics. *Journal of Sedimentary Research*, 70(1): 64-83.
- Marani, M., Trua, T. (2002). Thermal constriction and slab tearing at the origin of a superinflated spreading ridge:

- Marsili volcano (Tyrrhenian sea). *J Geophys Res*, 107(B9): EPM 3 1-15.
- Martí, J., Ablay, G.J., Redshaw, L.T., Sparks, R.S.J. (1994). Experimental studies of collapse calderas. *Journal of the Geological Society*, 151: 919-929.
- Mazzarini, F., Bisson, M., Pareschi, M.T. (2007). Zonazione dei bacini e delle aree esposte a colate di fango per l'Apron del Vesuvio. Progetto Speed - Prodotto D2.4.2. INGV.
- Milia, A., Raspini, A., Torrente, M.M. (2007). The dark nature of Somma-Vesuvius volcano: Evidence from the 3.5 ka BP Avellino eruption. *Quaternary International*, 173-174: 57-66. doi:10.1016/j.quaint.2007.03.001
- Milia, A., Raspini, A., Torrente, M.M. (2008). The dark nature of Somma-Vesuvius volcano: Evidence from the 3.5 ka BP Avellino eruption - Reply. *Quaternary International*, 192: 110-115. doi:10.1016/j.quaint.2008.04.007
- Milia, A., Raspini, A., Torrente, M.M. (2009). Evidence of slope instabilities and tsunamis associated with the 3.5 ka Avellino eruption of Somma-Vesuvius volcano, Italy. *Geological Society, London, Special Publications*, 322: 105-119. doi:10.1144/SP322.4
- Morghen, G., R.o Inc.re (1794). Pianta della Città di Torre del Greco distrutta in parte dalla Lava corsa nella notte del 15 Giugno de"1794.
- Moscarella, E. (1973). Le eruzioni vesuviane dell'alto Medio Evo storicamente accertate. *Rievocatore XXIV* 3-5: 11-13.
- Murphy, M.A., Salvador, A. (1999). International Stratigraphic Guide-An Abridged Edition. *Episodes*, 22(4): 255-271.
- NACSN (1983). North American stratigraphic code. *American Association of Petroleum Geologists Bulletin*, 67: 841-875.
- Nazzaro, A. (1997). *Il Vesuvio. Storia eruttiva e teorie vulcanologiche*. Biblioteca scientifica. Volume 3 di Geofisica dell'ambiente e del territorio. Napoli: Liguori Editore.
- Neri, A., Aspinall, W.P., Cioni, R., Bertagnini, A., Baxter, P.J., Zuccaro, G., Andronico, D., Barsotti, S., Cole, P.D., Esposti Ongaro, T. (2008). Developing an event tree for probabilistic hazard and risk assessment at Vesuvius. *Journal of Volcanology and Geothermal Research*, 178(3): 397-415.
- Newhall, G., Punongbayan, R.S. (1996). Fire and mud: eruptions and lahars of Mount Pinatubo, Philippines. PHIVOLCS. Seattle: Quezon City and University of Washington Press.
- Nunziata, C., Natale, M., Luongo, G., Panza, G.F. (2006). Magma reservoir at Mt. Vesuvius: Size of the hot, partially molten, crust material detected deeper than 8 km. *Earth and Planetary Science Letters*, 242: 51-57.
- Oldow, J.S., D'Argenio, B., Ferranti, L., Pappone, G., Marsella, E., Sacchi, M. (1993). Large-scale longitudinal extension in the southern Apennines contractional belt, Italy. *Geology*, 21: 1123-1126.
- Palmieri, L. (1862). Intorno all'incendio del Vesuvio cominciato il dì 8 dicembre 1861. *Rendiconto delle Tornate dell'Accademia Pontiniana, Anno Decimo, 40-61*: 72-83. Napoli.
- Palmieri, L. (1887). Il Vesuvio e la sua storia. In: Furcheim, F. (Ed.). Lo spettatore del Vesuvio e dei Campi Flegrei.
- Pareschi, M.T., Cavarra, L., Favalli, M., Giannini, F., Meriggi, A. (2000a). GIS and volcanic risk management. In: Natural Hazards. Springer.
- Pareschi, M.T., Favalli, M., Giannini, F., Sulpizio, R., Zanchetta, G., Santacroce, R. (2000b). May 5, 1998, debris flows in circum-Vesuvian areas (southern Italy): Insights for hazard assessment. *Geology*, 28(7): 639-642.
- Pareschi, M.T., Santacroce, R., Favalli, M., Giannini, F., Bisson, M., Meriggi, A., Cavarra, L. (2000c). Un GIS per il Vesuvio. Pisa: Felici Editori.
- Pareschi, M.T., Santacroce, R., Sulpizio, R., Zanchetta, G. (2002). Volcaniclastic debris flows in the Clanio Valley (Campania, Italy): insights for the assessment of hazard potential. *Geomorphology*, 43(3): 219-231.
- Pareschi, M.T., Zanchetta, G., Favalli, M., Sulpizio, R., Santacroce, R., Bisson, M., Demi, F. (2004). La pericolosità vulcanica in aree medio-distali al Vesuvio legata alle colate di fango e alluvionamenti. INGV.
- Pasquarè, G., Abbate, E., Bosi, C., Castiglioni, G.B., Merenda, L., Mutti, E., Orombelli, G., Ortolani, F., Parotto, M., Pignone, R., Polino, R., Premoli, Silva, I., Sassi, F.P. (1992). Carta Geologica d'Italia, scala 1:50.000: Guida al Rilevamento. Roma, Servizio Geologico Nazionale (Ed.). *Quaderni, serie III, v. 1*.
- Patacca, E., Scandone, P. (1989). Post-Tortonian mountain building in the Apennines. The role of the passive sinking of a relic lithospheric slab. In: Boriani, A., Bonafede, M., Piccardo, G.B., Vai, G.B (Eds.). The

- lithosphere in Italy. *Atti Conv. Lincei*, 80: 157-176.
- Pierson, T.C. (1985). Initiation and flow behaviour of the 1980 Pine Creek and Muddy River lahars, Mt. St. Helens, Washington. *Geo Soc Am Bull*, 96: 1056-1069.
- Pierson, T.C. (1995). Flow characteristic of large eruption-triggered debris flows at snow-clad volcanoes: constraints for debris-flow models. *Journal of Volcanology and Geothermal Research*, 66: 283-294.
- Pouchou, J.-L., Pichoir, F. (1984). A new model for quantitative X-ray microanalysis. Part I: application to the analysis of homogeneous samples. *La Recherche Aerospatiale*, 3: 13-38.
- Principe, C. (1979). *Le eruzioni storiche del Vesuvio: riesame critico, studio petrologico dei prodotti e implicazioni vulcanologiche* (Unpublished master's thesis). University of Pisa, Pisa.
- Principe, C. (1997). *BIBV: Bibliography of Historic Activity on Italian Volcanoes* (GGI Internal Report). CNR-Istituto di Geocronologia e Geochimica Isotopica.
- Principe, C. (1998). The 1631 eruption of Vesuvius: Volcanological concepts in Italy at the beginning of the XVII century. In: Morello, N. (Ed.). *Volcanoes and History*. International Commission on the History of Geological Sciences: 525-542.
- Principe, C. (2003). Cronologia dell'attività del Vesuvio fra il 79 A.D. ed il 1631. Submitted to Archivio Storico delle Province Napoletane.
- Principe, C., Brocchini, D., Arrighi, S., Luongo, G., Giordano, D., Perillo, M., Di Muro, A., Marti, J.M., Bisson, M., Paolillo, A. (2010). Vesuvius volcano-tectonic history - a new perspective. IAVCEI Collapse Caldera Commission Workshop: 51-53.
- Principe, C., Brocchini, D., Perillo, M. (1999). The Cognoli di Trocchia volcano and Monte Somma Growth. *Plinius*, 22: 316-17.
- Principe, C., Giannandrea, P. (2008). UBSU e cartografia geologica. Problemi e potenzialità di utilizzo delle unità a limiti inconformi (UBSU) nell'interpretazione e nella rappresentazione cartografica dei depositi vulcanici quaternari. L'èempio dei fogli n.ro 451 "MELFI" e n.ro 452 "RIONERO IN VULTURE". *Il Quaternario*, 21(1a): 61-68.
- Principe, C., Marini, L. (2008). Evolution of the Vesuvius magmatic-hydrothermal system before the 16 December 1631 eruption. *Journal of Volcanology and Geothermal Research*, 171(3): 301-306.
doi:10.1016/j.jvolgeores.2007.12.004
- Principe, C., Rosi, M., Santacroce, R., Sbrana, A. (1987). Chapter 1. Explanatory notes to the geological map. In: Santacroce, R. (Ed.). *Somma-Vesuvius. Quaderni de 'La Ricerca Scientifica' CNR*, 114(8): 11-52.
- Principe, C., Tanguy, J.C. (2009). Vesuve, le plus „fameux“ volcan du monde. Eruption, Objectif Volcans. Revue trimestrielle. *PYROS*, 21: 31-39.
- Principe, C., Tanguy, J.C., Arrighi, S., Paiotti, A., Le Goff, M., Zoppi, U. (2004). Chronology of Vesuvius" activity from AD 79 to 1631 based on archeomagnetism of lava flows and historical sources. *Bulletin of Volcanology*, 66: 703-724. doi:10.1007/s00445-004-0348-8
- Recupito, G.C. (1633). *De Vesuviano incendio nuntius*. Neapoli: Ex Regia Typographia Egidii Longhi, MDCXXXII.
- Ricciardi, G.P., Siniscalchi, V., Cecere, G., Macedonio, G. (2007). Meteorologia Vesuviana dal 1864 al 2001.
- Rolandi, G., Maraffi, S., Petrosino, P., Lirer, L. (1993a). The Ottaviano eruption of Somma-Vesuvio (8000 y B.P.): a magmatic alternating fall and flow-forming eruption. *Journal of Volcanology and Geothermal Research*, 58: 43-65.
- Rolandi, G., Mastrolorenzo, G., Barrella, A.M., Borrelli, A. (1993b). The Avellino plinian eruption of Somma-Vesuvius (3760 y. B.P.): the progressive evolution from magmatic to hydromagmatic style. *Journal of Volcanology and Geothermal Research*, 58: 67-88. doi:10.1016/0377-0273(93)90102-W
- Rolandi, G., Barrella, A.M., Borrelli, A. (1993c). The 1631 eruption of Vesuvius. *Journal of Volcanology and Geothermal Research*, 58: 183-201.
- Rolandi, G., Munno, R., Postiglione, I. (2004). The AD 472 eruption of the Somma volcano. *Journal of Volcanology and Geothermal Research*, 129: 291-319. doi:10.1007/s00445-004-0348-8
- Rolandi, G., Petrosino, P., Mc Geehin, J. (1998). The interplinian activity at Somma-Vesuvius in the last 3500 years. *Journal of Volcanology and Geothermal Research*, 82: 19-52. doi:10.1016/S0377-0273(97)00056-5

- Rosi, M., Principe, C., Vecci, R. (1993). The 1631 Vesuvius eruption. A reconstruction based on historical and stratigraphical data. *Journal of Volcanology and Geothermal Research*, 58(1-4): 151-182. doi:10.1016/0377-0273(93)90106-2
- Rosi, M., Santacroce, R. (1983). The AD 472 “Pollena” eruption: volcanological and petrological data for this poorly-known, plinian-type event at Vesuvius. *Journal of Volcanology and Geothermal Research*, 17(1-4): 249-271. doi:10.1016/0377-0273(83)90071-9
- Rosi, M., Santacroce, R., Sbrana, A. (1986). Geological map of Somma-Vesuvius volcanic complex (scale 1:25,000). In: Santacroce, R. (Ed.). Somma-Vesuvius. *Quaderni de ‘La Ricerca Scientifica’ CNR*, 114(8).
- Salvador, A. (Chairman). International Subcommittee on Stratigraphic Classification (1987). Unconformity-bounded stratigraphic units. *Geological Society of America Bulletin*, 98(2): 232-237. doi:10.1130/0016-7606(1987)98<232:USU>2.0.CO;2
- Salvador, A. (Ed.). (1994). *International Stratigraphic Guide: A Guide to Stratigraphic Classification, Terminology, and Procedure* (No 30). Geological Society of America.
- Santacroce, R. (Ed.). (1987). *Somma-Vesuvius*. Quaderni de „La Ricerca Scientifica“CNR, 114(8).
- Santacroce, R., Cioni, R., Marianelli, P., Sbrana, A., Sulpizio, R., Zanchetta, G., Donahue, D.J., Joron, J.L. (2008). Age and whole rock-glass compositions of proximal pyroclastics from the major explosive eruptions of Somma-Vesuvius: A review as a tool for distal tephrostratigraphy. *Journal of Volcanology and Geothermal Research*, 177: 1-18.
- Santacroce, R., Sbrana, A. (2003). Carta geologica del Vesuvio. Scala 1:15,000. Progetto CARG. Servizio Geologico Nazionale - Consiglio Nazionale delle Ricerche. Firenze: S.E.L.C.A.
- Scott, K.M. (1989). Magnitude and frequency of lahars and lahar-runout flows in the Toutle-Cowlitz River system. *US Geol Surv Prof Pap*, 1447(B): 33.
- Scott, K.M., Vallance, J.W., Pringle, P.T. (1995). Sedimentology, behavior, and hazard of debris flows at Mount Rainer, Washington. *US Geol Surv Prof Pap*, 1547: 56.
- Sevink, J., van Bergen, M.J., van der Plich, J., Feiken, H., Anastasia, C., Huizinga, A. (2011). Robust date for the Bronze Age Avellino eruption (Somma-Vesuvius): 3945 ± 10 calBP (1995 ± 10 calBC). *Quaternary Science Review*, 30: 1035-1046. doi:10.1016/j.quascirev.2011.02.001
- Sigurdsson, H., Carey, S., Cornell, W., Pescatore, T. (1985). The eruption of Vesuvius in A.D. 79. *National Geographic Research*, 1(3): 332-387.
- SIMN - Servizio Idrografico e Mareografico Nazionale (2004). Regione Campania, Settore Programmazione Interventi di Protezione Civile sul Territorio: Annali Idrologici e altre pubblicazioni del Compartimento di Napoli del SIMN. A cura del Centro Funzionale per la Previsione Meteorologica e il Monitoraggio Meteoro-Idro-Pluviometrico e delle Frane. Napoli. Dicembre - CDRom.
- Smith, G.A. (1986). Coarse-grained nonmarine volcanoclastic sediment: terminology and depositional process. *Geological Society of America Bulletin*, 97: 1-10.
- Somma, R., Ayuso, R.A., De Vivo, B., Rolandi, G. (2001). Major, trace element and isotope geochemistry (Sr-Nd-Pb) of interplinian magmas from Mt. Somma-Vesuvius (Southern Italy). *Mineralogy and Petrology*, 73: 121-143.
- Spadini, G., Wezel, F.C. (1995). Structural evolution of the “41st parallel zone”: Tyrrhenian Sea. *Terra Nova*, 6: 552-562.
- Sparks, R.S.J., Sigurdsson, H., Wilson, L. (1977). Magma mixing: a mechanism for triggering acid explosive eruptions. *Nature*, 267: 315-318.
- Stothers, B.R., Rampino, R.M. (1983). Volcanic Eruptions in the Mediterranean before A.D. 630 from written and archaeological sources. *Journal of Geophysical Research*, 88: 6357-6371.
- Sulpizio, R., Bonasia, R., Dellino, P., Mele, D., Di Vito, M.A., La Volpe, L. (2010b). The Pomici di Avellino eruption of Somma-Vesuvius (3.9 ka BP). Part II: sedimentology and physical volcanology of pyroclastic density current deposits. *Bullettin of Volcanology*, 72: 559-577. doi:10.1007/s00445-009-0340-4
- Sulpizio, R., Cioni, R., Di Vito, M.A., Mele, D., Bonasia, R., Dellino, P. (2010a). The Pomici di Avellino eruption of Somma-Vesuvius (3.9 ka BP). Part I: stratigraphy, compositional variability and eruptive dynamics. *Bullettin of Volcanology*, 72: 539-558. doi:10.1007/s00445-009-0339-x

- Sulpizio, R., Mele, D., Dellino, P., La Volpe, L. (2005). A complex, Subplinian-type eruption from low-viscosity, phonolitic to tephri-phonolitic magma: the AD 472 (Pollena) eruption of Somma-Vesuvius, Italy. *Bulletin of Volcanology*, 67: 743-767. doi:10.1007/s00445-005-0414-x
- Sulpizio, R., Mele, D., Dellino, P., La Volpe, L. (2007). Deposits and physical properties of pyroclastic density currents during complex Subplinian eruptions: the AD 472 (Pollena) eruption of Somma-Vesuvius, Italy. *Sedimentology*, 54: 607-635. doi:10.1111/j.1365-3091.2006.00852.x
- Sulpizio, R., Zanchetta, G., Demi, F., Di Vito, M.A., Pareschi, M.T., Santacroce, R. (2006). The Holocene syneruptive volcanoclastic debris flows in the Vesuvian area: Geological data as a guide for hazard assessment. *Geological Society of America Special Papers*, 402: 217-235.
- Tarquini, S., Isola, I., Favalli, M., Mazzarini, F., Bisson, M., Pareschi, M.T., Boschi, E. (2007). TINITALY/01: a new Triangular Irregular Network of Italy. *Annals of Geophysics*, 50(3): 407-425. doi:10.4401/ag-4424
- Thorarinsson, S. (1974). The terms tephra and tephrochronology. In: Westgate, J.A., Gold, C.M. (Eds.). World bibliography and index of Quaternary tephrochronology. Edmonton, CA: University of Alberta.
- Thouret, J.C., Lavigne, F., Suwa, H., Sukatja, H., Surono, B. (2007). Volcanic hazards at Mount Semeru, East Java (Indonesia), with emphasis on lahars. *Bull Volcanol*, 70: 221-244.
- Vallario, A. (2004). *Sarno. Sei anni dalla catastrofe*. Napoli: Alfredo Guida Editori.
- Vilardo, G., De Natale, G., Milano, G., Coppa, U. (1996). The seismicity of Mt. Vesuvius. *Tectonophysics*, 261: 127-138.
- Zanchetta, G., Bini, M., Cremaschi, M., Magny, M., Sadori, L. (2013). The transition from natural to anthropogenic-dominated environmental change in Italy and the surrounding regions since the Neolithic: An introduction. In: Zanchetta, G., Bini, M., Cremaschi, M., Magny, M., Sadori, L. (Eds.). The transition from natural to anthropogenic-dominated environmental change in Italy and the surrounding regions since the Neolithic. *Quaternary International*, 303: 1-9.
- Zanchetta, G., Sulpizio, R., Di Vito, M.A. (2004a). The role of volcanic activity and climate in alluvial fan growth at volcanic areas: an example from southern Campania (Italy). *Sedimentary Geology*, 168: 249-280.
- Zanchetta, G., Sulpizio, R., Pareschi, M.T., Leoni, F.M., Santacroce, R. (2004b). Characteristics of May 5-6, 1998 volcanoclastic debris flows in the Sarno area (Campania, southern Italy): relationships to structural damage and hazard zonation. *Journal of Volcanology and Geothermal Research*, 133: 377-393.
- Zanchetta, G., Sulpizio, R., Santacroce, R., Cosimi, G., Sgrò, S., Pareschi, M.T., Bisson, M., Favalli, M. (2003). Volcanoclastic debris flows in the Clanio valley (Campania, Italy). Fast slope movements prediction and prevention for risk mitigation. Naples. May: 11-13.
- Zeuberger, L.W., Thorne, C.R. (1987). Quantitative analysis of land surface topography. *Earth surface processes and landforms*, 12: 47-56.